NTNU – Trondheim
Norwegian University of
Science and Technology

Slender Well Design

Kristian Hoff

Subsea Technology
Submission date: June 2012
Supervisor: Sigbjørn Sangesland, IPT

Norwegian University of Science and Technology
Department of Petroleum Engineering and Applied Geophysics

NTNU
Norges teknisk-naturvitenskapelige universitet
Fakultet for ingeniørvitenskap og teknologi
Faculty of Engineering and Technology
Studieprogram i Undervannsteknologi – Drift og Vedlikehold
Study Programme in Subsea Technology – Operations and Maintenance

Institutt for Produksjons- og Kvaltitetsteknikk
Department of Production and Quality Engineering

HOVEDOPPGAVE/DIPLOMA THESIS/MASTER OF SCIENCE THESIS

Kandidatens navn/The candidate's name: *Kristian Hoff*
Oppgavens tittel, norsk/Title of Thesis, Norwegian: *Slank brønnkonstruksjon*
Oppgavens tittel, engelsk/Title of Thesis, English *Slender Well Design*

Utfyllende tekst/Extended text:

Background:
Offshore wells being constructed today have a large well volume and are being drilled with large, high cost drilling units. There is an important potential for cost reduction through starting the well with a substantially smaller diameter, which imply reduced casing dimensions and cost, reduced mud volumes and cost, reduced BOP size and cost, and the possibility to use lower cost drilling units. The cost reduction potential is highest for subsea wells. The project objective is to develop a 15000 psi (1000 bar) Slender Subsea Well (SSW) concept based on enabling technologies. One key element in the slender well design is a liner hanger system for close clearance casings and high pressure rating.

Task:
1) Present and evaluate an alternative slender well design for exploration drilling.
2) Evaluate alternative liner hanger systems and the pre-installed liner (PIL) concept.
3) Propose a final design of a slender well.
4) Perform finite element analysis of expandable liner hanger suitable for slender wells

Supervisor: *Sigbjørn Sangesland*
Studieretning/Area of specialization: *Subsea Technology – Operations and maintenance*
Fagområde/Combination of subject: *Drilling*
Tidsrom/Time interval: *January 15 – June 10, 2012*

……
Sigbjørn Sangesland

Preface

This master thesis is carried out in the 4th semester of the Master of Science in Subsea Technology, Department of Production and Quality Engineering, at the Norwegian University of Science and Technology (NTNU). The thesis constitutes 30 out of 30 European Credit Transfer System (ECTS) credits for the spring term of 2012.

The project title is “Slender Well Design” and is given by the Department of Petroleum Engineering and Applied Geophysics. The project work has been carried out in the period January to June in 2012.

I would like to thank my supervisor Professor Sigbjørn Sangesland at NTNU for guidance and constructive conversations. I would also like to thank PhD candidate Jesus Alberto de Andrade Correia at NTNU for his good help.

……..

Kristian Hoff, June 10, 2012

Summary

This thesis has proposed a slender well concept for exploration drilling with 15000 psi pressure rating based on enabling technologies. The main findings relates to the use of expandable liner hangers to reduce the required radial clearance between consecutive casing sections. Finite element analysis of the liner hanger expansion is performed in Ansys Workbench, a platform for advanced engineering simulations.

The background for the thesis relates to the high cost of constructing offshore wells. There is a potential for considerable cost reduction by starting the well with a substantially smaller diameter, without compromising the final pipe size across the zone of interest. The topic builds on ongoing research in SBBU – Centre for drilling and wells for improved recovery, a joint project between NTNU, Sintef, University in Stavanger and IRIS.

The slender well concept renders the possibility to use modified 3rd or 4th generation semi-submersible rigs. These rigs have significantly lower day-rates compared to new 5th and 6th generation rigs. Cost reduction is also expected with respect to consumption of steel for casing, drilling fluids and cement. Additional savings in steel is obtained by basing the casing program mainly on liners.

The expandable liner hanger of choice is based on the XPak liner hanger developed by TIW. Finite element analysis indicated that a pressure rating of 15000 psi is feasible with the proposed liner hanger system. To avoid reduction in burst and collapse rating, the expansion mandrel is retained in the liner hanger after expansion. The mandrel is designed such that it creates an internal flush design with the liner string. It is recommended to use metal-to-metal sealing to avoid communication around the liner top. The slender well is constructed with limited radial clearance between consecutive casing sections. The problem of high surge pressures during running in hole is overcome by introducing a surge protection system with an artificial inner annulus to displace drilling fluids.

The concept of pre-installing a liner string in the surface casing is introduced to render the possibility of an additional casing section and reduction in riser ID. The concept is untested and further evaluation is recommended.

For further work on the topic proper field testing is recommended to validate the reliability of the concept. An assessment of slender well production drilling is also recommended to fully exploit the potential in slender well design. More detailed analysis and testing is necessary to qualify the expandable liner hanger for 15000 psi.

Table of Contents

Table of Figures

Table of Tables

Abbreviations

APDL	Ansys Programming Design Language
API	American Petroleum Institute
BHA	Bottom Hole Assembly
BOP	Blow Out Preventer
C	Celsius
DHM	Downhole Motor
ECD	Equivalent Circulating Density
EDP	Emergency Disconnect Package
F	Fahrenheit
FEA	Finite Element Analysis
HP	High Pressure
HSE	Health Safety Environment
ID	Inner Diameter
IRIS	International Research Institute of Stavanger
ISO	International Standard Organization
LMRP	Lower Marine Riser Package
LPTJ	Low Pressure Telescopic Joint
LWD	Logging While Drilling
MD	Measured Depth
ML	Mud Line
MODU	Mobile Offshore Drilling Unit
MPa	Mega Pascal (= 10^6 Pascal)
MWD	Measurements While Drilling
NCS	Norwegian Continental Shelf
NRV	Non-Return Valve
NTNU	Norwegian University of Science and Technology
OCTG	Oil Country Tubular Goods
OD	Outer Diameter
OH	Open Hole
PBR	Polished Bore Receptacle
PDC	Polycrystalline Diamond Compact
PIL	Pre-Installed Liner
PSI	Pounds per Square Inch
RKB	Rotary Kelly Bushing
RMS	Root Mean Square
ROP	Rate Out Penetration
RPM	Rounds Per Minute
SSC	Sulfide Stress Cracking
SSW	Slender Subsea Well
TRIP	Transformation Induced Plasticity
UTS	Ultimate Tensile Strength
WOB	Weight On Bit

1 Introduction

Offshore wells being constructed today have a large well volume and are being drilled with large, high cost drilling units. There is a potential for considerable cost reduction through starting the well with a substantially smaller diameter without compromising the size of the pipe across the zone of interest. This will in turn result in reduced casing dimensions and cost, reduced mud volumes and cost, reduced BOP size and cost, and the possibility to use lower cost drilling units. The cost reduction potential is highest for subsea wells.

Previous attempts to slim down wells have been characterized by smaller hole and casing sizes whilst maintaining standard clearances between casing and liner strings. This often resulted in a small hole across the reservoir with associated problems of specialized equipment requirements, reduced drilling rates, complicated well evaluation and reduced flow path [1]. As a consequence operators have often concluded that the economic or technical benefits do not outweigh the additional work or that well functionality is compromised. A key aspect in the development of the slender well concept has therefore been to enable greater flexibility in the well design, while maintaining optimum final pipe size. Flexibility is obtained by reducing the annular clearance between consecutive cased sections. This reduces the telescoping effect and means that a wider variety of well architecture options exist [2].

A key cost reduction enabler is liner strings. Considerable material savings is associated with replacing casing strings suspended in the well head with liner hanger-suspended liner strings. To make the liner hanger compatible with the slender well concept, evaluation of expandable liner hangers are undertaken. These hangers require less radial clearance to be set and are not prone to failures often associated with conventional mechanical liner hangers. A formal study among operators in the Gulf of Mexico in 1999 identified several problems with mechanical liner tops [3]:

- Liner top integrity, lap squeeze
- Packer, hanger and centralization issues such as preset, failure to set and failure to seal

The development of expandable liner hangers was initiated to eliminate these failure modes. In retrospect the technology has demonstrated several advantages over conventional systems, e.g. its capability to successfully deploy, cement and isolate the liner top [4].

1.1 Background and Objectives

The topic for the thesis builds on ongoing research in SBBU – Centre for Drilling and Wells for improved recovery, which is a joint project between NTNU, Sintef, University in Stavanger and IRIS. The project group is studying the contingency for slender wells as an alternative for both exploration and production drilling. A feasibility study for 15ksi pressure rating is the main goal of the pre-project in SBBU. Other focus areas in the pre – project phase are well integrity, well construction requiring smaller rig, metal to metal sealed liner hangers, qualification and standardization. Several of these topics will also be pursued in this thesis, together with the main objective to develop a 15000 psi (1000 bar) Slender Subsea Well (SSW) concept based on enabling technologies. One key element in slender well design is the expandable liner hanger system for high pressure.

The main objectives of this thesis are:

5) Present and evaluate an alternative slender well design for exploration drilling.

6) Evaluate alternative liner hanger systems and the pre-installed liner (PIL) concept.

7) Propose a final design of a slender well.

8) Perform finite element analysis of expandable liner hanger suitable for slender wells.

1.2 Market Situation

It has been suggested that most of the “easy oil” and new large oil fields are history. More exploration wells in proportion to found hydrocarbons are needed to locate new fields on the Norwegian Continental Shelf (NCS) [5]. Hence the drilling cost needs to be cut, assuming the exploration budgets are held constant. This is the main argument for introducing slender well drilling. The most considerable cost driver related to drilling is the rig day-rates. With the exception of a decrease during the financial crises in 2008/2009, the day-rates for ultra deepwater (over 1500m) rigs have steadily increased since 1996, see Figure 1. Reasons are ever larger rigs with high construction costs, together with a scarcity of rigs on the market.

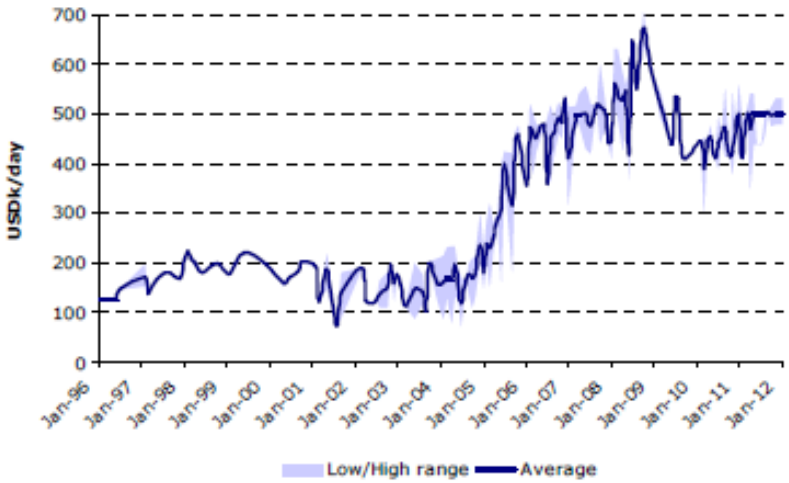

Figure 1: Historical day-rates for ultra deepwater rigs [6]

One way to avoid the high day-rates of the 5th and 6th generation semi-submersible rigs is to employ older, rebuilt 3rd or 4th generation rigs. Use of these rigs is made possible because the BOP, wellhead and riser is smaller and lighter than in conventional drilling. Resulting in less required riser tensioner capacity, deck storage space and variable deck loads. This report will not go into further detail on how rigs can be modified to conduct slender well drilling. For more information, see reference from Saga Petroleum [5].

2 Slender Well Design; Conformance with State-Of-The-Art Technology

2.1 Background and Basis

The objective of a slender well is to deliver the largest possible final casing or liner size while reducing the size of the intermediate casings and surface casing as compared to a traditional well plan. This is obtained by reducing the radial clearance between consecutive casing sections, and in addition scaling down the conductor casing. The industry has long relied on general rules-of-thumb when it comes to radial clearance between casings. Detailed engineering may find that these rules are conservative or out of date. Generally, at least 3/5-4/5" of radial clearance is recommended between casing coupling and the design ID of the next larger casing string [7]. The clearance between the OD of the casing and the drilled hole depends on the hole and the mud condition. 1 1/2" in total diameter difference is acceptable when formations are competent and lightweight mud is used. For more general-purpose well completions, 2-3" is preferred. At the same time excessive clearance must be avoided due to the risk of poor displacement of drilling fluids [8]. New developments within slender well design allow for clearances between consecutive cased liners to be as low as 1/8" radially in the lower reaches and as much as 1/4" in the upper reaches of the well [2]. Other benefits with the slender well design are [2]:

- **Economic:** Less consumable's related to drilling, such as steel for casing, drilling fluids and cement. This result in easier logistics and may result in faster overall drilling. Several wells may be drilled for the same price as one conventional well, increasing earnings from the field.
- **Environmental:** Less cuttings and drilling fluids to handle and dispose.
- **Safety:** Smaller casing dimensions reduce the risk related to handling and transportation.
- **Contingency:** Additional casings may be run and liners set over troublesome zones without compromising the final hole size.
- **Bottom-up design:** Especially beneficial for production wells where the production rate is determined by the size of the completion/production tubing. One also avoids excessively large top-hole sizes.
- **Abandonment:** If the well design is based on liners without tieback, well abandonment is simplified due to the lack of overlapping casing strings and potential leak paths at the top of the well

2.2 Technology Enablers

A key element in the slender well design is to reduce the size of the surface casing. This renders the possibility to reduce the wellhead system size and BOP size from the conventional 18 3/4" to an 11" or a 13 5/8". Other important technological drivers that will influence the development of the slender well concept have been identified in a report by Saga Petroleum [5]. A brief summary of their findings is cited below:

- **Muds**
  Drilling performance in wells with narrow annuli has greatly improved due the introduction of pseudo oil muds. Improved formation control, drill string lubrication, hole cleaning and hydraulics are some of these fluids main advantages. This is important as slender drilling aims at longer open hole sections and narrower hole clearances.
- **Bits**
  Use of polycrystalline diamond compact (PDC) bits has enabled higher weight on bit (WOB) and increased rate of penetration (ROP). These new bits in combination with downhole motors (DHM) have also increased the ROP in smaller holes as the bit revolutions per minute (RPM) have increased.
- **DHM**
  Continuous developments have improved the efficiency and lifetime of DHMs. They, together with measurements while drilling (MWD), have provided the basis for the steerable bottom hole assembly (BHA) technology. As an example, National Oilwell Varco can deliver DHM-sizes down to 1 11/16" [9], enabling efficient drilling also through smaller casings.
- **MWD**
  MWD has improved the drilling process both with respect to directional control accuracy and in facilitating improved drilling process. It is vital for accurate horizontal drilling in a steerable BHA.
- **Logging while drilling (LWD)**
  LWD enables collection of the most common formation and reservoir parameters in real time whilst drilling. As of 1994, when the report was published, the LWD technology concentrated on 8 1/2" or larger hole application. It is not known where the industry stands today, but it is recognized that complexity increases when building smaller tools. This is due to space requirements and structural integrity. For most exploration wells there is a need for side-wall-sampling and formation fluid sampling (RFT). Hence, there will be a need for wireline-operations, and the net additional time consumption for other logging runs might therefore be less significant.
- **Heave compensation (active/passive)**
  Constant WOB is essential to obtain good penetration rates. Thus active heave compensation in addition to passive compensation is recommended and necessary for floating drilling operations.

All technology enablers mentioned above are known to the industry and should not represent any insuperable problems. Besides the pre-installed liner system presented in

Chapter 2.3.1, the slender well concept is mainly based on existing and field-tested equipment.

2.3 Slender Well Design

A slender exploration well with appurtenant drilling equipment is proposed, see Figure 2. As seen from the figure a surface BOP is mounted below the moon pool. The BOP is required because the riser will not be equipped with a kill and choke line to the subsea arrangement. The top of the riser have a telescopic joint and riser tensioners to take the vertical displacements (heave motion) of the mobile offshore drilling unit (MODU). A question concerning the assembly of the top-arrangement arises, should the surface BOP be placed above or below the telescopic joint? If the BOP is located below the telescopic joint, the BOP will hang in the splash zone below the moon pool. Well pressure and flow may then be routed to a choke on the deck over high pressure flexible hoses. Should the BOP be placed above the telescopic joint, the BOP can be permanently fixed to a skid frame in the moon pool. An advantage with the second alternative is that the BOP no longer is subjected to the loads from rig heave and wave forces. In addition riser tension requirements are reduced roughly with the weight of the BOP [10].

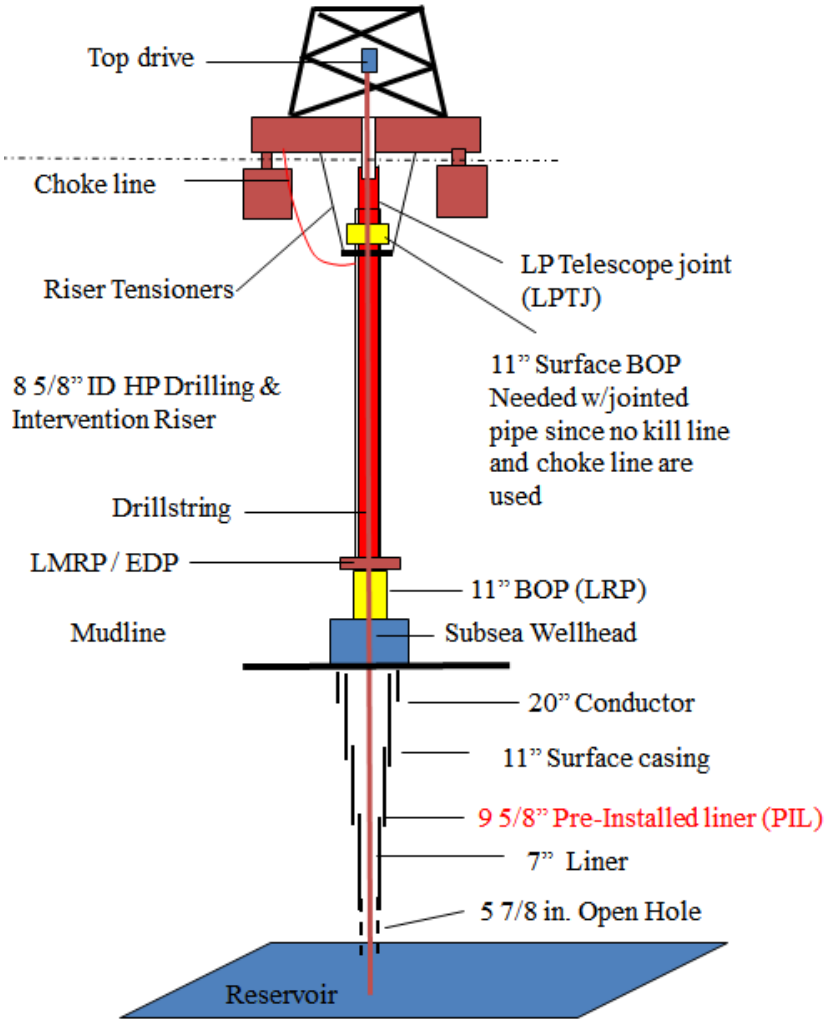

Figure 2: Suggested slender exploration well

Another advantage with having the BOP fixed in the moon pool is that it easily and safely can be accessed for maintenance and repair. However, the telescopic joint will be subjected to the annulus pressure, or circulating back pressure of the system. Such a system require advanced sealing to contain the pressure [10]. It needs to cope with the displacement of the telescopic joint and be of acceptable durability.

It is suggested to use an 8 5/8" ID high pressure drilling riser. The dimension of the riser will depend on the size of the drill string, together with the casing program, and might have to be scaled up. To render the use of an 8 5/8" ID riser it is made reservations to a 3 1/2" drill string and a pre-installed liner (PIL) in the surface casing. A 3 1/2" drill string is chosen to ensure proper space for cuttings and mud return through the riser. Drilling with a 3 1/2" drill string has some disadvantages though. The drill string might not have sufficient strength to drill the larger top hole sections. In this case it is necessary with a second larger drill string. The cuttings are normally dumped on the seabed when drilling the top hole sections, so the riser ID is of no concern. Drawbacks with having a second drill string is less space on the rig deck and time to change and make up a new string in the derrick. Another factor influencing the choice of riser size is the running tool for the PIL. The ID of the chosen liner equals 8 3/8". Hence, the running tool will be slightly smaller than 8 3/8", thus possible to pass through the riser.

2.3.1 Casing Program

The casing program with grades and properties is cited in Table 1. They are all picked from the API casing list [11]. From the table it is evident that not all casing sections are rated for 15000 psi (100 MPa). The pressure will vary with depth, so a detailed formation evaluation is required to approve the program.

Table 1: Properties of casings [11]

Casing/liner [in]	Grade	Wall thickness [in]	Weight [lb./ft.]	Burst [MPa]	Collapse [MPa]
20	Q-125	0.635	133	47.9	11.1
11 3/4	Q-125	0.582	71.0	74.7	39.7
9 5/8	Q-125	0.625	61.1	97.9	81.4
7	Q-125	0.453	32.0	97.6	80.7
5	Q-125	0.362	18.0	109.2	102.2

2.3.1.1 Pressure Rating

A pressure rating of 15000 psi is desirable, but it is recognized that with most of the wells drilled on the Norwegian Continental Shelf (NCS) it is sufficient with a 10000 psi rating[1]. The pressure rating is defined by the pressure of fluids within the pores of a reservoir. This is usually hydrostatic pressure, or the pressure exerted by a column of water from the formation's depth to sea level. The well structure needs to handle the differential pressure between the formation and the hydrostatic pressure in the wellbore. An essential part of mud engineering is to control the hydrostatic pressure of the mud column during drilling.

[1] Conversation with supervisor

The weight of the mud must be controlled so that the hydrostatic pressure stays within the pore pressure and fracture pressure of the formation. Too low pressure can result in influx of fluids downhole. Excessive pressure can fracture the formation and cause lost circulation.

From a design-point of view the biggest concern with the proposed well design may be that the intermediate string or the last full string becomes the top part of the liner. Thus it must handle the burst pressure generated by the zones crossed by the liner. It is crucial to check the strength of the top part of the last full string against the new maximum expected surface pressure.

2.3.2 Pre-Installed Liner (PIL)

Preinstalling a liner in the surface casing is a patented idea assigned by Ocean Riser Systems AS. The idea is based on suspending a subsequent liner section in the surface casing. The conductor and surface casing is normally installed before running the riser, but as the risk of encountering high pressure pockets increases with depth, a riser and a BOP is installed before drilling the following hole sections. Consequently, the riser ID has to be larger than the OD of the casing sections below the surface casing. However, by pre-installing the next section in the surface casing, the riser ID can be reduced. The concept is illustrated in Figure 3.

The hanging mechanism to suspend the liner before running in hole can be a J-slot, which is unhooked by lifting and rotating, see Figure 4. This is a fairly simple system where a J-shaped slot is fixed to the internal surface of the host-casing. Externally the top of the liner is fitted with a knob which slides into the J-slot. The liner is lifted up by the running tool and rotated some degrees to pass the slot when running in hole.

As discussed the hole needs to have a 1-1 1/2” larger diameter than the liner OD. This means that the bit is larger than the ID of the PIL. If the drill bit is to be run through the PIL it has to be collapsed. Thus drilling out the section below the surface casing relies on the use of expandable drill bits and under-reamers. There is no obvious alternative regarding setting of the PIL after running. It will, among other things, depend on the ID of the surface casing. An 11” surface casing with a subsequent 9 5/8” liner, as suggested in Figure 3, does not allow for any of the investigated mechanical liner hangers. As an example, Baker Hughes’ Flex-Lock III hydraulically set 9 5/8” liner hanger needs an 11 3/4” host-casing[2]. The alternative is to use an expandable liner hanger, as will be discussed more thoroughly in Chapter 3. If for any reason a mechanical liner hanger is preferred, the size of the surface casing could be increased to e.g. 11 3/4”.

[2] Information found on www.bakerhughes.com

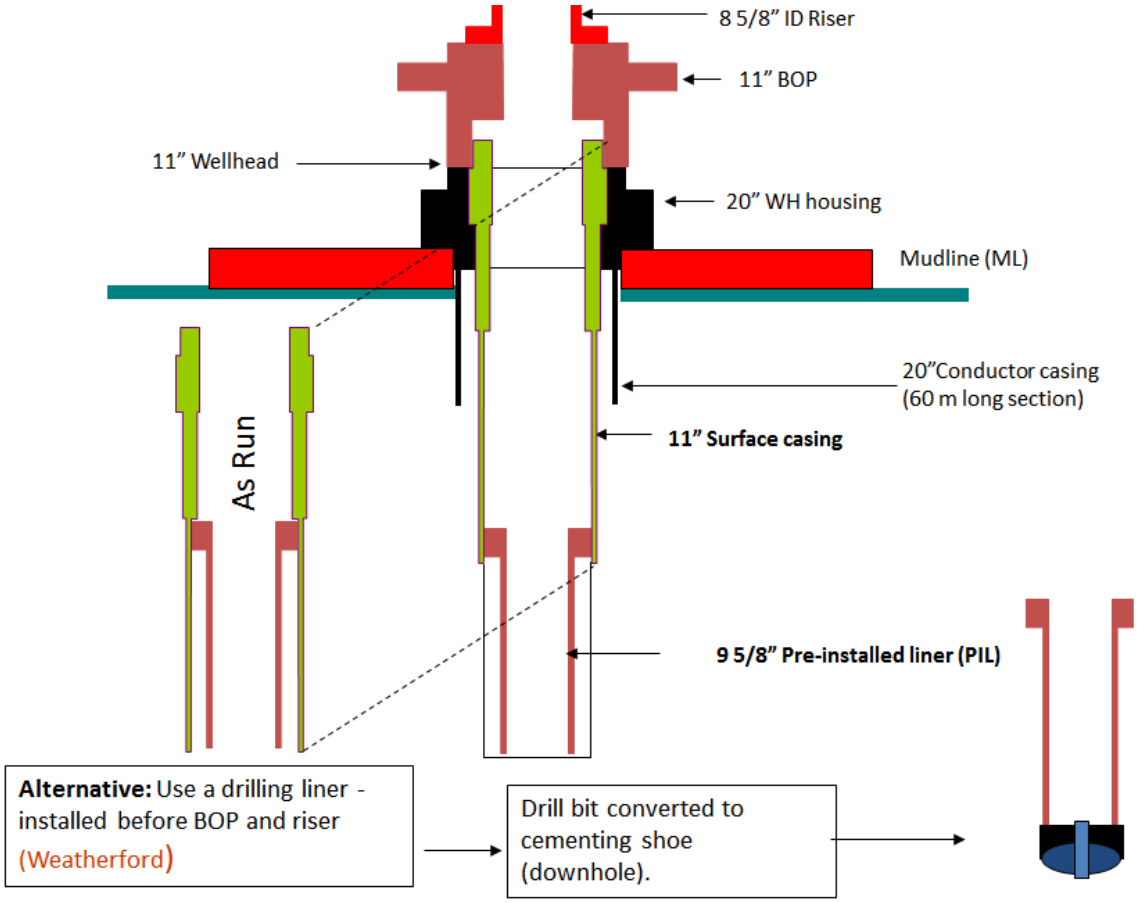

Figure 3: Pre-installed liner concept (SBBU)

It is believed that successful implementation of the PIL concept will be advantageous in slender well drilling. Technological development is required before testing can commence. During the work on this thesis no major show stoppers were identified, but it is a well-known fact that the petroleum industry is conservative towards new technology. In this respect proper engineering and field testing, with appurtenant successful results are required before implementation is pertinent.

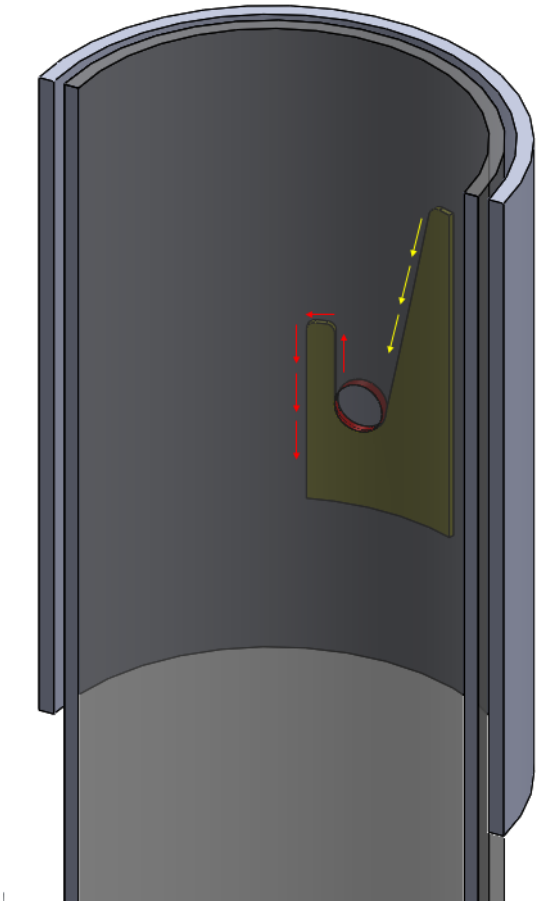

Figure 4: Example of a J-slot mechanism

2.3.3 Risk Evaluation

As with all petroleum related operations, HSE is a constant concern. Reducing the size of the wellhead and surface casing can affect the integrity of the well foundation. Dynamic loads from the BOP and riser system are transferred to the upper parts of the well. Rig drift-off and strong sea currents will transfer loads from the riser to the BOP and wellhead, creating a bending moment. If the conductor casing cannot provide sufficient support and column stiffness, the well can be damaged. Especially on poorly consolidated top soil locations. The issue is mitigated to a certain degree by down-scaling the BOP and riser dimensions, but a case-to-case evaluation of the well foundation strength is recommended. It might be required to replace the 20”conductor by a larger size pipe.

Another risk with the proposed well design is leakage over the liner top is. The liners are initially installed without tieback to the wellhead. Thus it is a risk of communication between the annulus and the cased wellbore. Attention should therefore be given to the sealing integrity of the liner hanger. It might be necessary with a tieback on the 7” liner to maintain well integrity in case of abnormal pressures.

2.4 Economical Merits

It is hard to conclude on the economical merits of the slender well concept. Among other factors, it depends on the present value of the MODU to be modified and the required modification investments. Disregarding the rig costs, it is evident that the economic benefits of the slender well concept are significant, and improving with increasing water depth. It includes casing steel, drilling fluids and handling of cuttings. The potential savings by going from a conventional 18 3/4" to an 11" WH based casing program for a 4590 m deep well (from RKB) are presented in Table 2. A synopsis of the setting depths and casing dimensions can be found in Appendix A.

Table 2: Calculated mud, casing and cutting savings

Well design	Slender	Conventional	Reduction [%]
Total volume in riser [m³]	13.9	69.1	79.8
Total volume cuttings [m³]	227.8	584.1	61.0
Total mud volume [m³]	130.9	164.7	20.5
Total casing/liner length [m]	4280	10145	57.8

Reducing the volume of cuttings significantly decrease cleaning and disposal costs. The mud cost is directly related to the mud volume used. So one can expect direct cost savings, but further savings can be attained through other mud related cost. Reduced requirements to mud pumps and mud cleaning equipment are expected as smaller holes require less mud circulation volume and rate. This can further improve hole cleaning as mud maintenance improves with less volume to handle. The savings in casing length is based on the use of liners without tieback to the wellhead. The casing dimensions are disregarded.

3 Liner Hanger Selection

The suggested slender exploration well is based on using mainly liners rather than full length casings. In a conventional well the casing sections are hung from a casing hanger in the wellhead, with each new casing overlapping the previous. This system requires a lot of steel. By replacing the full length casings with liners, considerable material savings could be obtained.

To render such a system one has to make use of liner hangers. A liner hanger anchors the liner string to the inside of the previous casing. The conventional liner hanger is a mechanical cone and slips system, see left picture in Figure 5. The biggest problem with such liner hangers is the required radial space to set, not making them ideal for use in slender wells. The alternative is an expandable liner hanger, see right picture in Figure 5.

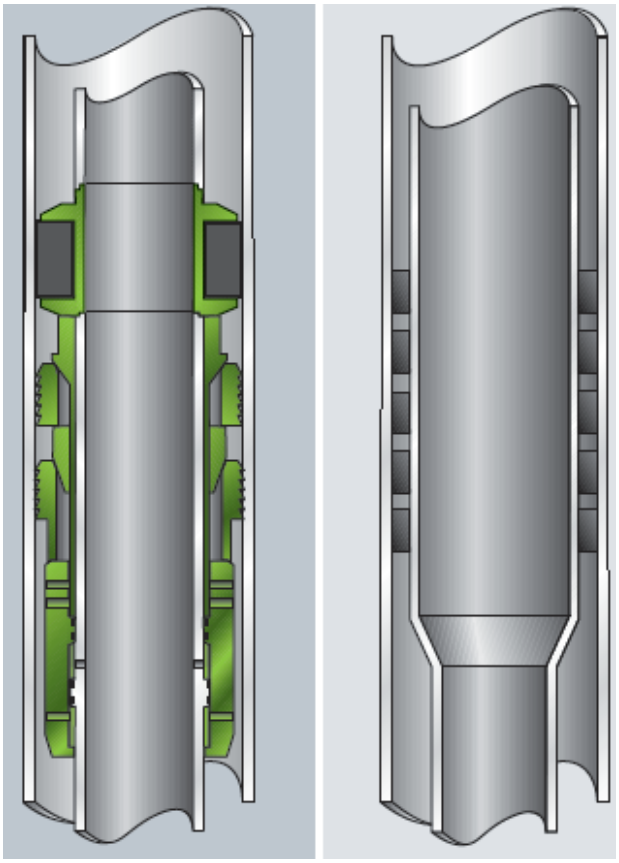

Figure 5: Comparison between mechanical (left) and expandable liner hanger [12]

An expandable liner hanger is basically a pipe that is expanded and pressed against the host casing. Expansion is obtained by means of an expansion cone/mandrel or direct hydraulic pressure. The contact pressure between the liner hanger and host casing maintain hanging capacity and sealing. Externally the hanger can be fitted with slips or inserts to increase the hanging capacity. Sealing is achieved by using elastomeric bands, metal-to-metal, or a combination of the two. An expandable liner hanger does not have any movable parts externally, making it less susceptible to premature setting or other failures often associated with mechanical liner hangers. In recent years several companies have developed

expandable liner hangers. A selection of providers and a short description of their product follow below. Figures of each liner hanger system can be found in Appendix B.

TruForm – Weatherford[3]

Weatherford have developed the TruForm expandable liner hanger, see Figure 39. TruForm is qualified to ISO 14310 V0 standards at 12000 psi. ISO 14310 is a standard that provide requirements and guidelines for packers and bridge plugs as defined herein for use in the petroleum and natural gas industry [13]. V0 is a design validation requirement including gas test, axial loads, temperature cycling and a zero bubble acceptance criterion. Sealing is obtained by elastomeric packers with anti-extrusion barriers. Seal rating is the same above and below the elements. Hanging capacity is created from tungsten carbide inserts. These are recessed in the pre-expanded hanger to avoid damage to the casing. The TruForm hanger is also run with a polished-bore receptacle that is equipped for second-run packer or tieback-packer applications, providing operational flexibility.

The first field trial was conducted in an Algerian well for Sonatrach. A 7” liner was set in a 9 5/8” casing at 3303 m MD to provide a double barrier against salt flows and maintain isolation throughout the drilling and completion process. In addition to the 7 x 9 5/8” system, Weatherford can deliver 9 5/8 x 11 3/4” and 11 3/4 x 13 3/8” systems with the same pressure rating.

TORXS – BakerHughes[4]

BakerHughes delivers the TORXS expandable liner hanger system, see Figure 40. TORXS makes use of metal-to-metal sealing that is proven in more than 35000 installations. The expansion cone has an adjustable diameter to compensate for any variations in casing diameter. To reduce the risk of the pipe getting stuck in cement the hanger is partly set before displacing the cement. The hanger is expanded so that the slips are set, but the packer is set independently after the cement is in place. TORXS needs a pressure in the range of 3000 – 4000 psi to displace the cone and expand the hanger. For close-clearance applications the system can be fitted with a diverter valve to avoid damage to the formation from high surge pressure. The diverter valve increases the flow area by displacing fluid inside the liner. A more thoroughgoing description of the the diverter system follows in Chapter 4.3.1.

Versaflex – Halliburton

Halliburton delivers the Versaflex expandable liner hanger, see Figure 41. This hanger is somewhat simpler than the two previous with respect to design. Externally it only consists of five one-foot elastomeric bands that provide both hanging and sealing capacity. On the 7 5/8” x 9 5/8” system a single band can take 450000 lbf (204 116 kg) of hanging weight [14].

The Versaflex liner hanger is manufactured in a variety of sizes, ranging from 5” x 7” to 11 7/8” x 13 5/8”. In the course of the literature survey no information on pressure rating was found.

[3] Information and picture found on www.weatherford.com
[4] Information and picture found on www.bakerhughes.com

XPAK – TIW Tools[5]

TIW is a Texas based company making tools for the oil and gas industry, one being the XPAK expandable liner hanger, see Figure 42.

The XPAK liner hanger is designed with an expansion section of 16”-24” in length, depending on the liner size. Hanging capacity is obtained by hardened slips. Sealing is maintained by a combination of metal-to-metal contact, and elastomeric bands as backup. After expansion the mandrel is left in place to support the expanded tube and eliminate the low collapse rating associated with expandable tubulars. The XPAK system has no pre-defined dimensions, but is manufactured upon demand and specification from the costumer. A selection of the sizes built is presented in the table below [15]:

Table 3: Compatible liner hanger and casing sizes

Liner hanger [in.]	Host-casing [in.]
3 1/2	4 1/2
4	5 1/2
4 1/2	5 1/2 and 5 3/4
5	7 and 7 3/4
5 1/2	7, 7 5/8, 7 3/4 and 8 5/8
7	9 5/8
7 5/8	9 3/8, 9 5/8, 9 7/8 and 10 3/4
9 5/8	11 3/4 and 11 7/8
11 3/4	13 5/8
14	16
17	20
18	22

HETS – Read Well Services[6]

HETS is the only liner hanger among the ones presented that utilizes direct hydraulic pressure for expansion, see Figure 43. The internal volume of the liner hanger is sealed off by two expandable seals (Downhole Hydraulics Module). Pressure is applied from the surface to expand the hanger. Metal encapsulated elastomers seals of the annulus and is ISO 14310 V0 tested to 5000 psi.

[5] Information and picture found on www.tiwtools.com
[6] Information and picture found on www.readwellservices.com

3.1 Discussion

Based on the literature survey and the target of a 15000 psi pressure rating, it has been chosen to pursue the XPak expandable liner hanger from TIW. From initial evaluations of the system it seems fit for use in the proposed slender well. The main argument for choosing the XPak is the retained expansion mandrel. The pressure rating of expanded tubular decreases as a function of expansion ratio, as will be examined more thoroughly in Chapter 5.5. Retaining the mandrel after expansion prevents this phenomenon. Another advantage is persistent seal integrity between liner hanger and host-casing, as the mandrel prevents separation of the two under external pressure.

4 Liner System Design

4.1 Annular Seal

It is decisive that the liner top seal off any gas or fluid from leaking into the wellbore. Standard practice in liner installation procedures recommends at least 300 ft. of overlap from the host-casing seat to the top of the liner [16]. With that the liner top is positioned above any bottom joints of the casing which might have been damaged by drilling out after cementing the casing. If the whole length of the liner is cemented the overlap also forms a cement plug in the annulus between the casing and the liner. In most cases the cement plug prevents communication around the top of the liner, but abnormal pressure and even pressure gradient reversals can cause leakage. One reason being the poor conditions in the overlap. Non-centralized pipe and movement of pipe can prevent complete mud removal, leading to communication. Other conditions in the overlap that are not ideal include [16]:

- No fluid loss to formation to dispose the slurry of excess water.
- The cement may be over-retarded for the setting temperature at the liner top.
- Creation of micro-annulus on the liner OD when internal pressure is reduced during later phases of drilling, completion or production.
- Creation of permeability in the overlap plug when the hydrostatic pressure in the cement column regresses to that of the mix water, allowing gas to invade and cause fluid movement through the setting column.

An advantage with expandable liner hangers is that they can be both rotated and drifted during cementing to improve the cement job. Whether the whole length of the liner is cemented or not, the main sealing between the liner hanger OD and the host casing is obtained by metal-to-metal seals, see Figure 6.

The seal design adapted to the liner hanger is often found in subsea wellheads. Milberger and Radi [17] and Boehm and Hosie [18] have studied the function of metal seals for use in oil field drilling and production equipment. Both reports found that a metal seal based on the principle of wickers bite contact is a robust and reliable design. This type of seal is fabricated by cutting a series of separate triangular grooves in the sealing surface. The triangular lands are called wickers. When expanding the liner hanger the casing material is impressed on these wickers. The indentation process results in a normal force and a shear force on the surface of the seal material. As a result the casing deforms plastically and the wickers bite deep, increasing the ability to seal across sections with rough surface topology or defects. The normal stress to perform this process is approximately 2.6 times the casing materials yield stress [19].

Buchter [20] found that line contact is not an effective seal. Finite bands, like wickers, are more effective, but must be of minimal width to reduce the force required to energize the seal. From experiments he also found that an average pressure of at least twice the softer materials yield strength was required to observe leakage. Above this point, the contact pressure required for sealing is linearly proportional to the internal pressure to be sealed.

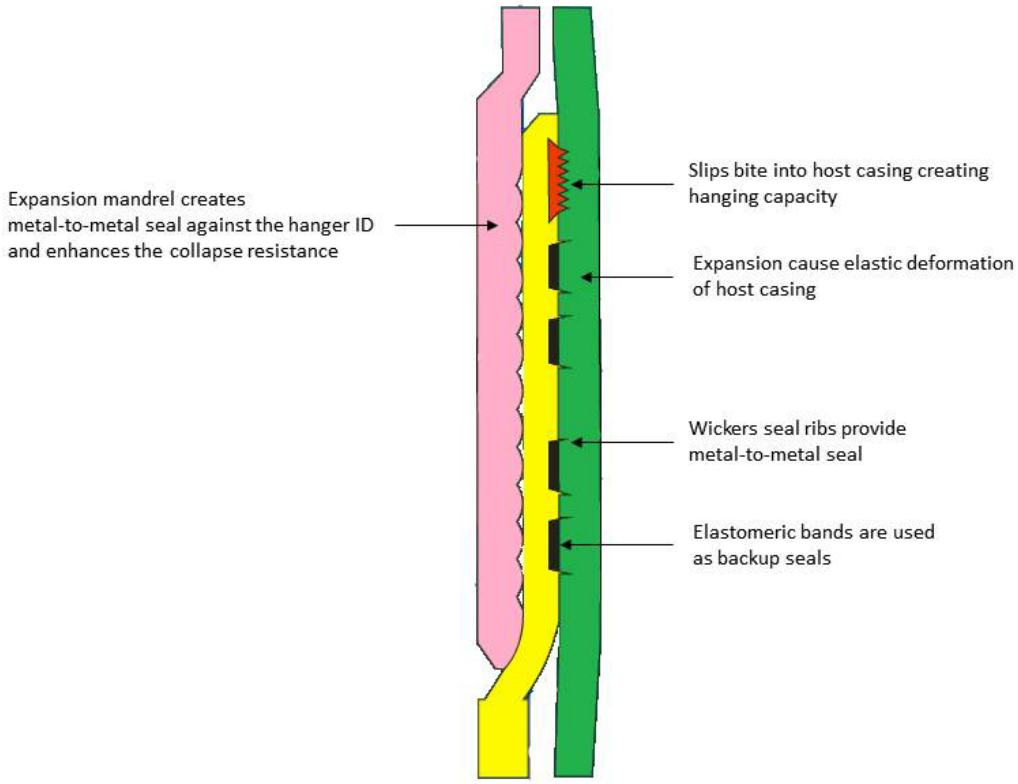

Figure 6: Principle of liner hanger seal and slips [21].

In addition to, or alternatively to metal-to-metal sealing, elastomers can be used. Elastomers have been the conventional sealing material for the most common oil and gas industry wellbore isolation/intervention devices [22]. However, it is perceived that metal-to-metal seals have a clear advantage over elastomeric seals in hostile, high pressure and high temperature environments. Common failure modes related to elastomers include [22]:

- Gasification/explosive decompression
- Temperature degradation
- Shearing across extrusion gap
- Dynamic fatigue under pressure cycles
- Compression load catastrophic failures
- Chemical degradation

The following description of the above points is referred from Mackenzie and Garfield [22]. Gasification is a threat to elastomers because of their low elastic strength. Conditions with high differential pressure can lead to serious damage in the elastomer after just one single decompression cycle. Fluids in contact with an elastomeric surface are absorbed into the material and gas diffuses into the bulk of the elastomer until fully saturated. If the external pressure suddenly drops the compressed gas nucleates at the voids expands, leading to high tensile stresses in the void wall. If higher than the strength of the elastomer, the stress may lead to cracking of the elastomer. Metal will not experience this phenomenon since gas cannot penetrate the metal components of the seal itself.

Elastomeric seals are highly temperature sensitive and break down mechanically at temperatures as low as 150-200 degrees F (65.5-93.3˚C). Studies have shown that metal-to-metal seals have the potential to operate successfully in temperatures up to 700 degrees F (371.1˚C).

Anti-extrusion rings are normally used to avoid shear failure across extrusion gaps, but at high loads the inherent lack of strength in the elastomer may cause failure.

Both seal types are sensitive to chemical degradation. Constructing the metal seal from nickel based alloy improves the resistance to chemical attack, including corrosion resistance.

4.1.1 Design Principles of Metal Seals

There are only a few principles governing the design of a reliable metal seal [17]:

- Metal surface finish
- Differential hardness between the contacting parts
- Surface contact stress
- Plastic deformation of the sealing element

Metal surface finish

The surface finish of the contacting parts is considered the most important principle. Better surface finish requires less contact stress and, thus, less plastic deformation. API 6A [23] defines a set of requirements for surface finishes depending on seal type, including ring gaskets and gaskets. For the more common oil field metal seals the basic requirement is 32 µin. root mean square (RMS). RMS is a number describing the surface roughness and is calculated from [24]:

$$RMS = \sqrt{\frac{1}{L}\int_0^L z(x)^2 dx}$$

Where z(x) is the vertical deviation from the profile's center line and L is the length of the center line, see Figure 7.

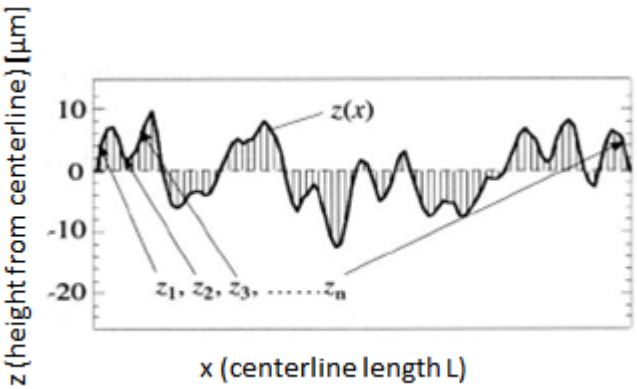

Figure 7: Detailed view of surface roughness [24]

Differential hardness between the contacting parts
Obtaining a good metal seal relies on difference in the hardness of the base material and the seal material, mainly because it reduces galling of the casing material. No good data is found on the topic, but based on experience Milberger and Radi [17] states that the metal seal should be of a differential hardness of 10 points on the Rockwell C scale. Rockwell is a dimensionless number describing the hardness of a material.

Surface contact stress
Yielding of the casing material is necessary to obtain a good seal, but contact stress higher than necessary should be limited to avoid plastic deformation of the seal metal. The required contact stress is related to the surface finish, so a smoother surface allows for lower contact stress.

Plastic deformation of the sealing element
Large plastic deformation is used to permit rougher sealing surfaces and/or reduce the leak flow rate. Differential hardness is important where plastic deformation of the seal is expected. Required plastic deformation should be determined on the basis of maintaining the seal and its structural integrity.

4.1.2 Contact and Seal Deformation

A two-dimensional illustration of the contact between wedge seal and casing without deformation of the seal is shown in Figure 8.

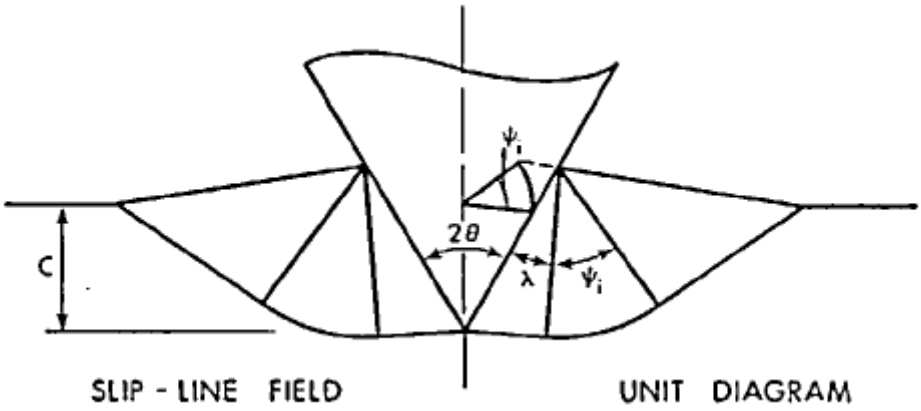

Figure 8: Deformation of casing from seal indentation [25].

From Johnson et.al. [25] it is shown that the pressure *P* on the wedge seal is given by:

$$P = k_i(1 + 2\psi_i + sin2\lambda) \quad \textbf{(1)}$$

Where k_i is the yield stress of the casing in pure shear. The shear stress is:

$$\tau = k_i sin2\theta \quad \textbf{(2)}$$

A wedge seal loaded symmetrically by a normal pressure *P* and a shear stress τ is shown in Figure 9.

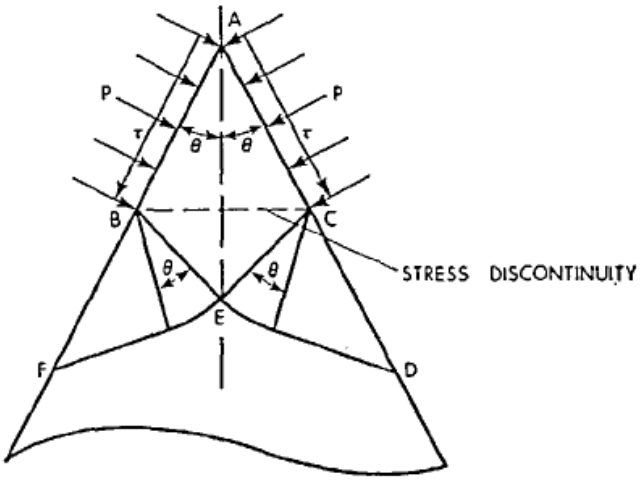

Figure 9: Symmetrically loaded seal [25]

For the seal to remain rigid the following condition has to be satisfied:

$$k_w > \frac{P + \tau cot\theta}{2(1 + \theta)} \quad \textbf{(3)}$$

Where k_w is the yield stress of the wedge seal in pure shear. From Equation (1) (with $\lambda = \pi/4$) and (3) the necessary condition for indentation without deformation of the seal is obtained:

$$\frac{k_w}{k_i} > \frac{1 + \psi_i}{1 + \theta} \quad \textbf{(4)}$$

It follows that the left-hand side of Equation (4) has to be above curve 2 in Figure 10 to avoid deformation of the seal.

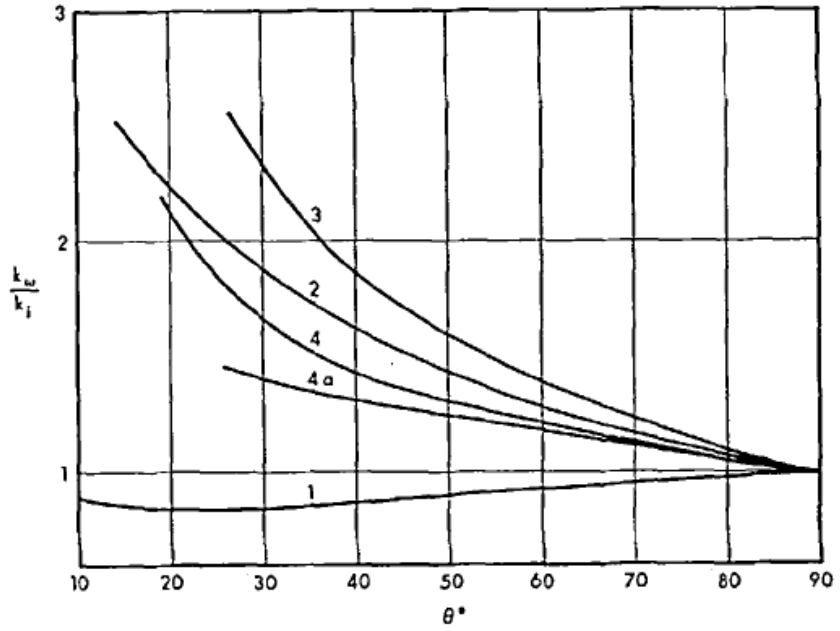

Figure 10: Relationship between the seal half-angle and yield shear stress ratio of seal and casing [25]

4.2 Liner Hanger Body and Expansion Mandrel

For the purpose of this thesis the liner hanger is made from standard OCTG material. The internal surface of the liner hanger is polished to reduce the friction between hanger and expansion mandrel. The expansion mandrel will be coated with a hard, low friction coating, typically a ceramic. Externally the mandrel is designed with a multiple ball profile to further reduce the friction, see Figure 11.

Figure 11: Design of expansion mandrel.

The ball profiles also create a series of metal-to-metal seals against the inside of the liner. In the upper end the mandrel is fitted with an integrated packer bore receptacle (PBR) which provides a dynamic sealing option in case of thermal variations. The PBR also works as a liner tie-back receptacle with a ball type expansion joint. The opening angle at the bottom of the mandrel should not be too small relative to the longitudinal axis. This will increase the expansion pressure due to increased frictional force and the hanger body can rupture. To ease the initiation of expansion the top part of the liner hanger body is designed with an angle, see Figure 12. This guides the mandrel smoothly into the hanger and reduces the contact pressure compared to a sharp edge contact.

Accurate machining of the liner hanger body is required to avoid variations in wall thickness. Imperfections in the wall thickness may cause localization of plastic deformation in areas of minimum wall thickness during expansion [26]. Consequently, necking and ductile failure can occur.

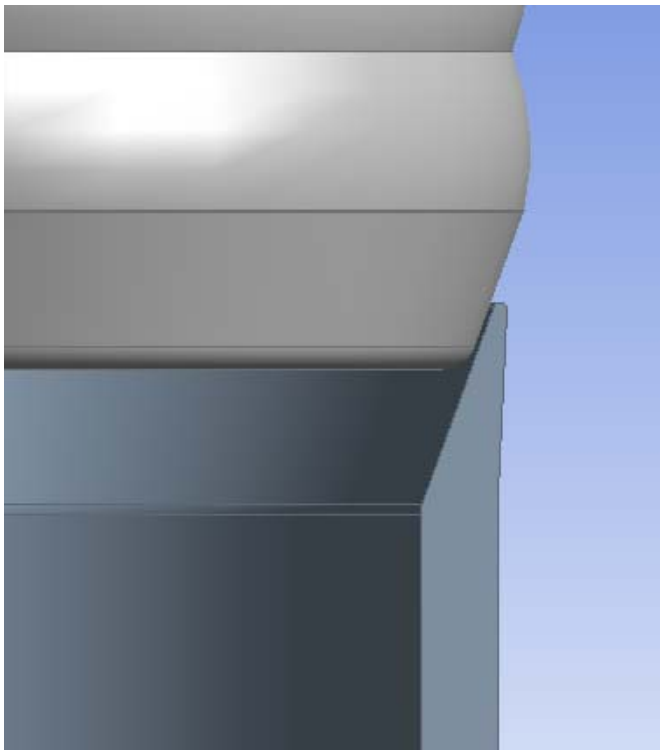

Figure 12: Cross-section of the liner hanger body

4.2.1 Radial Clearance

As a consequence of retaining the mandrel after expansion there will be a required minimum radial clearance between the host-casing and the pre-expanded liner hanger. This is an effect of the internal flush design and the required wall thickness of the mandrel. Flush is defined as a design which does not compromise the internal diameter, and thereby offering no restriction to fluid flow. This means that the ID of the mandrel equals the ID of the liner string. In addition the mandrel is restricted to have a minimum wall thickness so that it does not undergo large deformation during expansion.

No data has been found on required wall thickness of the expanded liner hanger, but as an assumption it is set to the same as the liner string. The assumption is based on the hanging capacity of the hanger. If the initial wall thickness of the hanger body equals the liner string, it will have a smaller thickness after expansion. That in turn can comprise a reduction in axial strength of the hanger. If the pre-expanded hanger body thickness is proportionally larger than the liner string, they will be equal after expansion. Calculation of required wall thickness is found in Chapter 5.6.

Based on the above one can conclude that the minimum required radial clearance must be approximately the expanded wall thickness of the liner hanger. To obtain some elastic deformation of the host-casing, and with that the required contact pressure to maintain sealing and hanging capacity, the post-expanded OD of the liner hanger should be 0.2” larger than the ID of the host-casing.

4.3 Running Tool

During running in hole or drill-down the liner hanger and the liner is connected to a conveyance pipe through the setting tool. Connection is obtained by use of a collet on the running tool, see Figure 13. The collet grips a worked profile on the inside of the liner, below the liner hanger. Rotating dogs are paired with a profile sub in the hanger to enable rotation of the liner. As the hydraulic pressure to release the collet is large, there is little to no chance of accidental release of the liner.

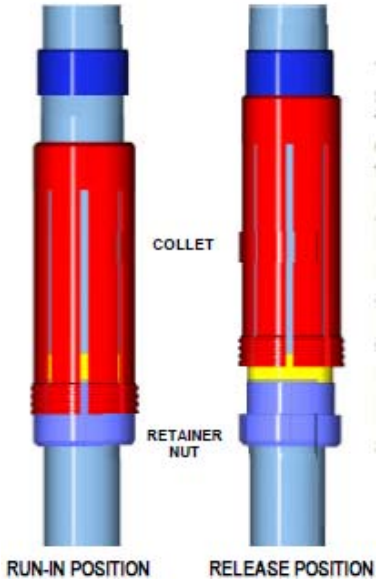

Figure 13: Collet on the running tool [27]

One of the drawbacks with the XPak-system is the lack of a surge protection system. All the drilling fluid has to be displaced in the annulus. This could result in fracture of the formation if the running speed is not properly controlled, which in turn increases the trip time. A solution would be to use a flow diversion shoe at the bottom of the liner, see Figure 14.

Figure 14: Floe diversion shoe [2]

The diversion shoe has holes to an inner flow area for fluid to travel inside the liner in an artificial annulus. The system is originally design for a slender well concept developed by

Caledus ltd. [2]. Thus it is not compatible with the XPak running tool as-is, but adaptation should make it fit for use.

4.3.1 Details on Surge Protection System and Cementing

In wells with conventional casing dimensions, standard float equipment is used when running the casing strings. With standard equipment all of the fluid in the well is displaced in the annulus between the running casing and previously set casing. Slender wells have tight radial clearances that may cause high surge pressures against the formation. The casing or liner acts as a piston because the fluid cannot be displaced at a sufficient rate. This increases trip time and may result in loss of drilling fluids to the formation. The solution is to install a surge protection system.

A surge protection system increases the flow area by creating an artificial annulus inside the running liner. Above the setting tool the fluid is diverted from inside the liner to the annulus between the casing and the setting tool. The increased flow area allows for higher trip speed as the surge pressure is reduced. When the liner is in place a ball is dropped and pressure applied to close a non-return valve (NRV). The NRV closes off the ports to the inner annulus. This turns the float shoe to normal bottoms-up circulation and the hole is ready for cementing, see Figure 46 in Appendix C for various circulation modes.

A challenge during cementing operations is to avoid high pressure and associated ECD [2]. The problem can be avoided by enlarging the hole while drilling to create an annular space around the liner equivalent to that for conventional casing cementing operations. As mentioned before, this can be obtained by using bi-center PDC bits and/or under-reamers. A successful cement job depends on complete displacement of the drilling fluids. In this conjunction, recommended casing hardware is a U-tubing control tool. The cement slurry has a density which is greater than the density of the mud which it displaces. This can result in the phenomenon of U-tubing. The forces resisting the flow of cement are insufficient to allow the pumping pressure to be maintained. The cement slurry falls in the casing under the effect of gravity faster than the pumping rate. Accordingly, when U-tubing occurs, the cement slurry is no longer under the control of the pump. This is undesirable because the increased flow rates in U-tubing can cause a strong turbulent flow which can erode seriously any weak formations around the casing and cause laminar flow and undesirable flow regime while equilibrium is being sought. Further, it can result in a vacuum being formed behind the U-tubing cement slurry and the slurry may then halt while the pump slurry fills the vacuum. It can also cause surging in the rate at which the mud is forced to the surface. This can be difficult to control at surface without causing unfavorable pressure increases downhole [28].

4.3.2 Setting Sequence

After the cement job is successfully completed, hydraulic pressure at the surface is increased until a shear ring is broken and the setting tool activated. The required pressure depends on the dimension and thickness of the liner hanger together with expansion ratio. Usually 3000-4000 psi is sufficient to force the mandrel through the liner hanger [29]. Force is created by the hydraulically loaded pistons in the setting tool. The force is transferred to an inner mandrel which moves downwards and pulls the setting sleeve along. The sleeve then pushes

the expander through the liner hanger. The various components constituting the setting tool are illustrated in Figure 45, Appendix C. According to TIW the hanger provides sufficient tension capacity to support a liner string of whatever length the connections allow. More on connections follow in Chapter 4.4.1.

Setting tool release happens in one of the two following ways. The primary alternative is by letting the liner mandrel move down as the drill string is slacked off. This pushes the retainer nut, which has been situated underneath the collet and locked it in place, out and releases the collet from the groove profile in the liner. Disconnection is maintained by a ratchet system. The setting tool can now be retrieved and hoisted to surface. The secondary alternative should this mechanism fail, is right hand rotation to free-up the tool. The integrated combined packer bore and tie-back receptacle eliminates the need for a separate expansion joint above the hanger.

4.4 Liner String

The liner string will be made of standard OCTG material. The options are limited due to the target pressure rating of 15000 psi. The various casing grades specified by API Spec. 5CT [30] are presented in Table 4. For the relevant casing program presented earlier, see Table 1, all casings was of grade Q125.

When selecting casings an evaluation between wall thicknesses and casing grades must be done. Choosing a higher grade casing means a smaller wall thickness can be used to obtain the same pressure rating, and vice versa. For the relevant casing program presented earlier, see Table 1, all casings was of grade Q125.

Table 4: API Spec 5CT casing grades [30]

Grade	**Min. yield strength** [MPa]	**Min. ultimate tensile strength** [MPa]
H40	276	414
J55/K55	379	517
M65	448	586
L80	552	655
N80	552	689
C90/T95	621	689
P110	758	862
Q125	862	931

4.4.1 Connections

Casing and liner strings have connections designed after strength and sealing considerations. The connections are isolated pressure vessels that contain threads, seals and stop shoulders [31]. The three basic types of connections are: Weld-on, coupling and integral, see Figure 15. The two primary methods used to seal the threads are interference and metal-to-metal. The

typical sealing method for V-shaped and wedge-shaped threads is interference. Interference relies on the compression of the individual threads against each other. Despite high make-up torque the interference seal alone is not enough, because there has to be some tolerance in the thread dimensions for the connection to be made. The solution is to use a lubricant to fill the gaps. Metal-to-metal seal relies on metal contact other than the threads. This can be a tapered surface in the box and pin, a shoulder contact, or a combination of the two [32].

The most common connections in use today is the API 8-rd, where 8-rd means eight threads per inch and rounded profile. It is either short thread and coupling (ST&C) or long thread and coupling (LT&C), and has an interference seal. The threads are wedge-shaped and susceptible to jump-out, meaning the threads override each other, when subjected to high tension or compression. Thus they are normally not recommended for wells with high bending stresses.

Figure 15: Coupling connection (left) and integral connection (right)[7]

For slender well applications a more suitable connection is the integral. They have high pressure ratings, but not as high tensile efficiency as a T&C connection. In addition they have high torque rating which enables rotating while cementing or drilling. More important is the design of the connection. They are cut in non-upset pipe, called flush-joints. Both the ID and OD are the same in the tubing and connection. VAM SLIJ-II was found to be a suitable connection. It is delivered by VAM, a producer of connections for the oil and gas industry. This is the flush-jointed connection with the highest tensile efficiency found in the literature survey, ranging from 66-94% of pipe body strength [33]. It is however a semi-flush-joint, meaning the ID and OD is not 100% identical to the pipe. The drift ID is approximately 0.1" smaller than the pipe ID, and the OD is in the same range larger than the pipe OD. Technical data and torque values for a 7" connection can be found in Appendix D.

[7] www.vam-usa.com

5 Material Theory

The bulk of the following is found in the book “Theory of plasticity”, by Chakrabarty [34].

5.1 Fundamental Theory

Expansion of liner hangers involves plastic deformation of the material. Plastic deformation is a non-recoverable state induced by applied forces, here represented by the expansion mandrel. Correct modeling of the plastic deformation and subsequent residual stress field within a cylinder require attention to several physical properties [35]:

- Equilibrium and compatibility equations
- Equivalence/yield criterion
- End conditions of the tube
- Flow rule and compressibility
- Stress-strain relationship of the considered material

A typical stress-strain curve is showed in Figure 16. Elastic behavior is represented by the straight line OA. The slope of the line is of magnitude E, also known as Young’s modulus. Strain as a result of stress below point A is recoverable. Point B is called the yield point and marks the “proportional limit”, which represents the point where the linear relationship between stress and strain ceases to exist. For most metals the transition from elastic to plastic behavior is gradual. The corresponding stress at point B is the yield stress, σ_y. The two most common yield criteria are Tresca and von Mises.

Tresca’s yield criterion
The criterion states that yielding occur when the greatest of the three shear stresses reaches a critical value, when the yield stress is in pure shear *k*.

$$|\sigma_1 - \sigma_2| \vee |\sigma_2 - \sigma_3| \vee |\sigma_3 - \sigma_1| = 2k$$

Onset of yield in simple tension, $\sigma_1 = \sigma_y, \sigma_2 = \sigma_3 = 0$, hence; $\sigma_y = 2k$.

von Mises yield criterion
Yielding is predicted to occur when the shear strain energy per volume reaches a critical value.

$$(\sigma_1 - \sigma_2)^2 + (\sigma_2 - \sigma_3)^2 + (\sigma_3 - \sigma_1)^2 = 6k^2$$

Onset of yield in simple tension, $\sigma_1 = \sigma_y, \sigma_2 = \sigma_3 = 0$, hence;

$$2\sigma_y^2 = 6k^2$$
$$\sigma_y = \sqrt{3}k$$

For the relevant cylindrical case it is assumed that $\sigma_\theta > \sigma_z > \sigma_r$, thus Tresca and von Mises yield criterion gives the following result respectively:

$$\sigma_\theta - \sigma_r = \sigma_y = 2k \tag{5}$$

$$\frac{(\sigma_\theta - \sigma_r)^2}{2} + \frac{2}{3}\left(\sigma_z - \frac{\sigma_r + \sigma_\theta}{2}\right)^2 = \frac{2\sigma_y^2}{3} = 2k^2 \tag{6}$$

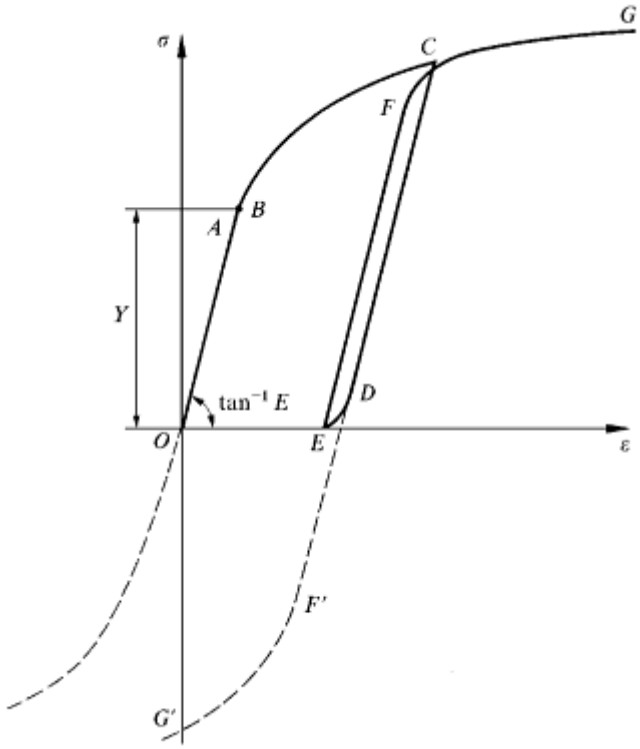

Figure 16: Stress-strain curve with effects of unloading and reversed loading [34]

Beyond the yield point the plastic strain increases with increased stress, line BC in Figure 16. The stress-strain behavior post-yield can be described as bi-linear, multi-linear or non-linear, see Figure 17

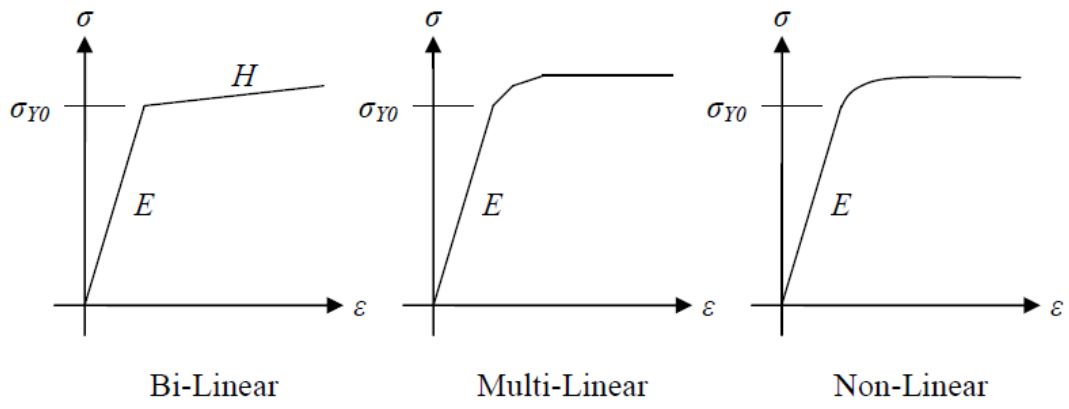

Figure 17: Post-yield stress-strain behavior [35]

The slope of the post-yield stress-strain curve represents the rate of strain hardening *H*. A bi-linear model with no strain hardening is called elastic, perfectly plastic. For bi-linear model the stress-strain relationship reduces to that of Figure 18.

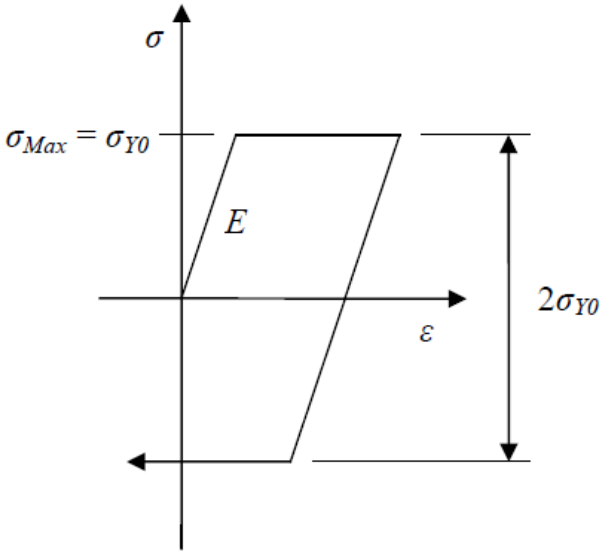

Figure 18: Stress-strain curve for elastic, perfectly plastic material [35]

If the material is stressed to a point C (Figure 16) and then released, there is an elastic recovery following a linear line CD with slope E. The permanent strain is represented by the distance OE. Assuming the material is reloaded with an equal force after recovery. The stress-strain curve now follows the line DF, with the new release point corresponding to F, where F is considerably smaller than C. This is known as the Bauschinger effect. The phenomenon arises due to residual stresses left in the specimen on a microscopic scale as a result of the different stress states in the individual crystals.

5.2 Variations in Material Behavior

Several factors affect the material behavior, such as:

- Isotropic hardening
- Kinematic hardening
- Bauschinger effect

An example of strain hardening was shown in Figure 17. However, the model only considered initial yield. The response of the yield stress to plastic strain with reversed loading must also be considered. This can be modeled in two ways, isotropic hardening or kinematic hardening. The isotropic model assumes that the stress range is twice the peak tensile stress. The kinematic model assumes that the stress range between peak tensile stress and the compressive yield stress is twice the initial yield stress, see Figure 19.

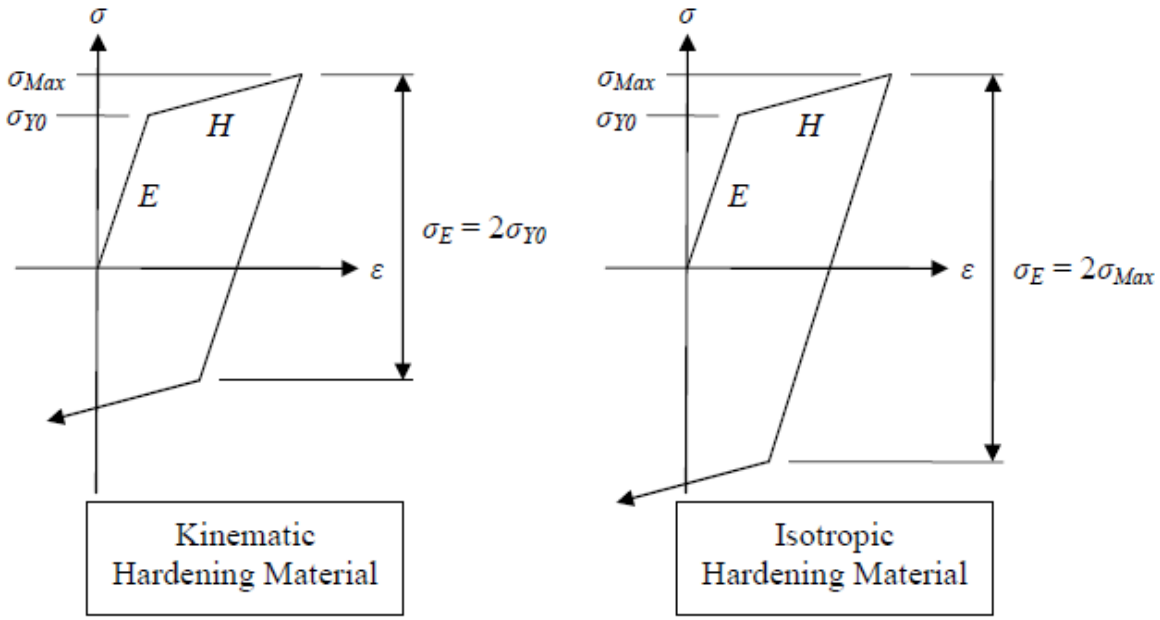

Figure 19: Difference between kinematic- and isotropic hardening [35]

With respect to expansion, strain hardening reduces the size of the plastic zone through the wall thickness for a given internal pressure. Meaning the material can take a higher pressure load than a perfectly plastic material.

Yield stress during load reversal is affected by the Bauschinger effect. For a liner hanger without internal support the Bauschinger effect would have been important to consider. Especially regarding post-expanded pressure rating. In the system considered the expansion mandrel is retained, thus the liner hanger is unaffected by reversed pressure loading.

5.3 Material Model

Total strain is expressed by the Ramberg-Osgood equation [34]:

$$\varepsilon = \frac{\sigma}{E}(1 + \alpha\left(\frac{\sigma}{\sigma_{Y0}}\right)^{m-1} \quad \textbf{(7)}$$

Where σ is the prevailing stress, α is a constant and m equals 1/n, where n is a material hardening index equal to 0,07 for casing grade Q125 [36]. For a range of materials the stress-strain curve can be reasonably fitted by Equation (7) with α equals 3/7 [34]. The stress-strain curve for API grade Q125 is found using Equation (7), see Figure 20. The tangent modulus, T, at any point of the curve is given by [34]:

$$\frac{E}{T} = 1 + \alpha m\left(\frac{\sigma}{\sigma_{Y0}}\right)^{m-1} \quad \textbf{(8)}$$

For the purpose of the analysis presented later in the thesis, a bi-linear isotropic hardening model was assumed. The tangent modulus was found from Equation (8).

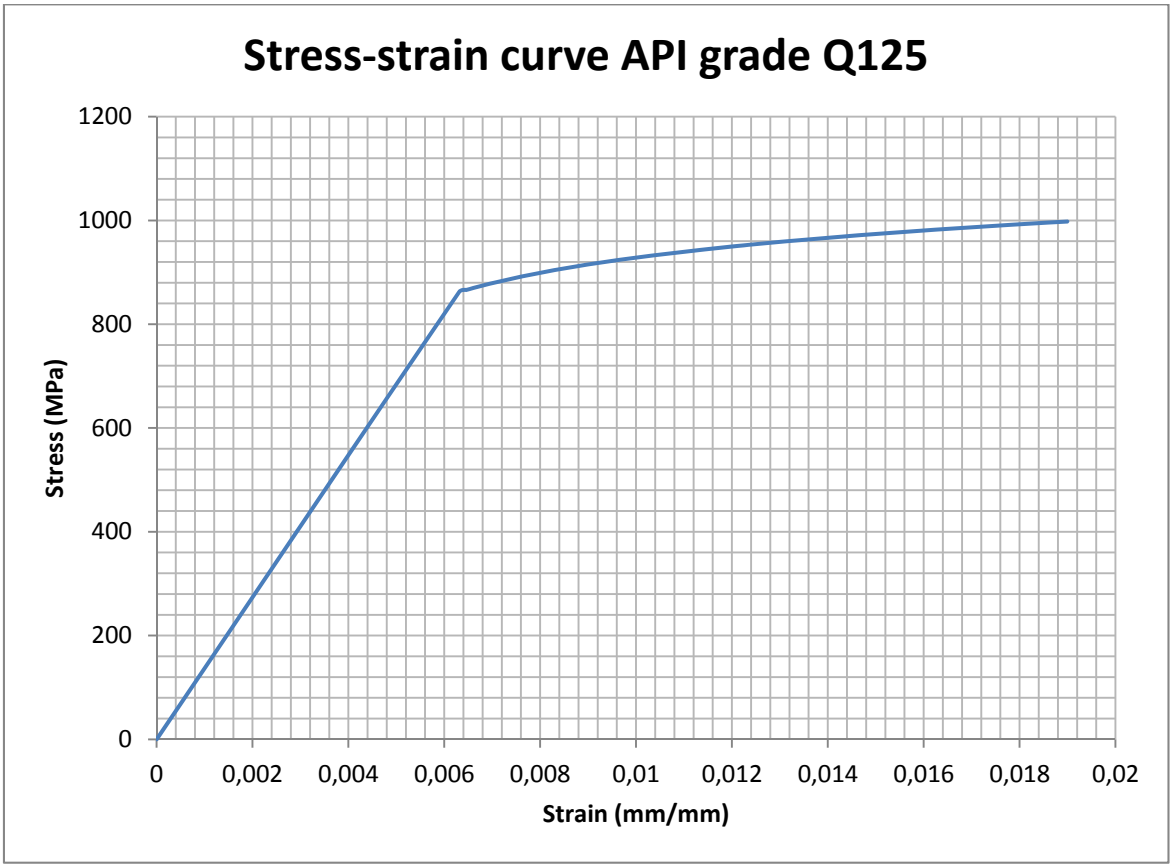

Figure 20: Stress-strain curve for API casing grade Q125

5.4 Expansion

Expansion is obtained by displacing an oversized tubular mandrel through the liner hanger by applied force. The nature of the loading induces shear stresses due to the localized loading and friction between the mandrel and the cylinder.

Correct material selection and lubrication is used to reduce the sliding friction at the contact. Nevertheless, considerable axial force is applied by the mandrel to the liner hanger that has to be constrained. Two constraint locations are illustrated in Figure 21. The axial stress may influence the residual stress pattern.

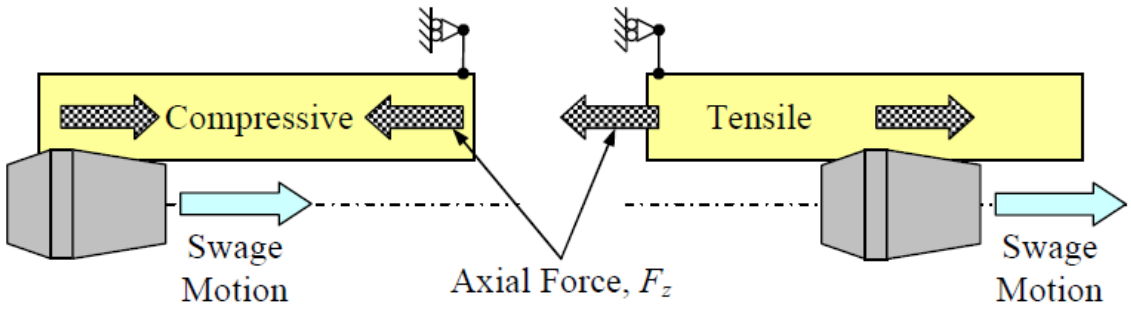

Figure 21: Cylindrical constraint during expansion [35]

The left case in Figure 21 is called mechanical expansion under compression. The liner hanger is supported from the bottom end. The support induces compressive axial stresses in the non-expanded section. In the expanded zone the axial stress is zero.

The right case in Figure 21 is called mechanical expansion under tension. The liner hanger is supported from the expanded top. The support condition cause tensile axial stresses to form in the expanded section. In the non-expanded zone the axial stress is zero.

For the relevant liner hanger system expansion under compression is the prevailing constraint. This is due to the design of the running tool, with the placement of the collet below the hanger.

When the cylinder is subjected to an increasing internal pressure, a non-recoverable plastic zone spreads from the inner radius. The elastic/plastic boundary at any stage being of radius c, see Figure 22. The elastic boundary region is:

$$c \leq r \leq r_0$$

And the plastic boundary region is:

$$r_i \leq r \leq c$$

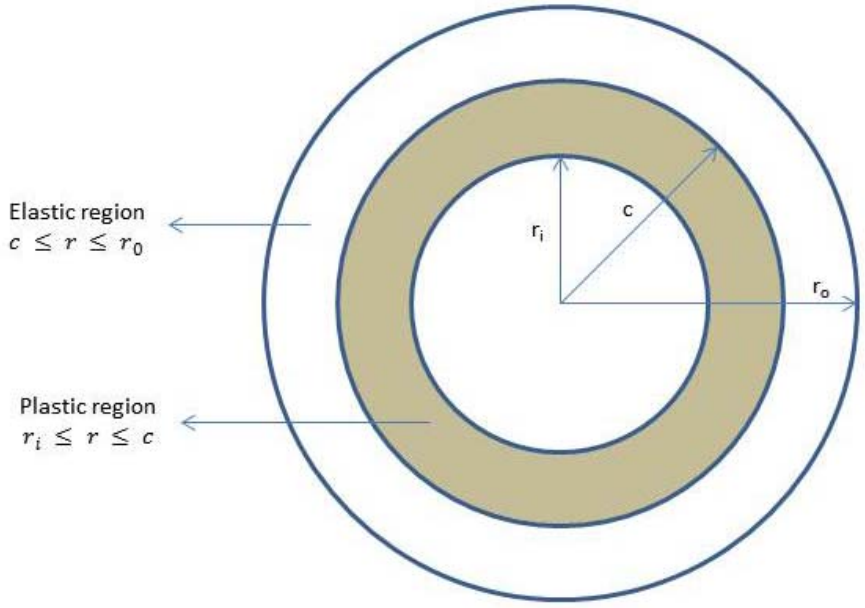

Figure 22: Elastic/plastic regions in a cylinder wall

The corresponding stresses in each of the regions are summarized in Appendix E. The minimum pressure required for yielding at the inner surface is [37]:

$$p_e = \frac{\sigma_y}{2}\left(1 - \frac{{r_i}^2}{{r_o}^2}\right) \quad \textbf{(9)}$$

According to Tresca's yield criterion plastic yielding across the whole wall thickness of a perfectly plastic material occurs at a pressure given by [37]:

$$p_p = \sigma_y ln(K) \quad \textbf{(10)}$$

Where K is defined as r_o/r_i.

5.4.1 Stress-Controlled Expansion

There are two ways to expand a liner hanger, direct hydraulic pressure or expansion mandrel. The preferred method in this thesis is an expansion mandrel, but the most obvious way may be by internal hydraulic pressure. An attempt to show why an expansion mandrel is to prefer is presented below (referred from R.B Stewart et.al. [26]).

Once the internal pressure exceeds the yield pressure in Equation (9) the liner hanger starts to expand. The expansion is similar to a burst test halted at a pressure between yield and burst rupture. F.J. Klever [38] showed that the logarithmic hoop strain at burst is:

$$\varepsilon_\theta = \frac{n}{2}$$

Where *n* is the material hardening index, which corresponds to the logarithmic uniform strain. The uniform strain ε_{UTS} is the strain at ultimate tensile stress where necking starts in a tensile specimen. *n* relates to ε_{UTS} as $n = \ln(1 + \varepsilon_{UTS})$. *n* is a good measure for achievable tubular expansion ratios. Typical formable metals and their strain-hardening index are listed in the first and second column in Table 5. The maximum achievable expansion ratio δ_{max} is defined as the engineering hoop strain at burst rupture pressure:

$$\delta_{max} = \frac{\Delta d}{d} = \left(e^{\frac{n}{2}} - 1\right) \cdot 100\ [pct] \quad \textbf{(11)}$$

The third column in Table 5 lists the maximum expansion ratios based on Equation (11). From the table it is obvious that imposing stress significantly restricts the expansion ratios. Further, it is a possibility of failure due to localization at flaws in regions of geometric imperfections.

5.4.2 Strain-Controlled Expansion

A better expansion method is to impose displacement by propelling an expansion mandrel through the liner hanger. This form of expansion is called strain-controlled. Higher expansion ratios at higher rates for a tubular with identical mechanical properties as for a stress-controlled expansion are achieved. Through experimental observations R.B. Stewart et.al. [26] have found that the maximum achievable expansion ratio δ_{max} for strain-controlled expansion can be estimated as:

$$\delta_{max} = \frac{\Delta d}{d} \approx \frac{3}{2}(e^{n} - 1) \cdot 100\ [pct] \quad \textbf{(12)}$$

The fourth column in Table 5 lists the expansion limits according to Equation (12).

Table 5: Strain hardening coefficients and maximum expansion ratios for different materials [38]

Material	Maximum n	Stress controlled radial expansion Maximum δ	Strain controlled expansion Maximum δ
Low-carbon steel	0.2	10.5	33.2
Interstitial steel	0.3	16.2	52.5
High-strength low-alloy steel	0.18	9.4	29.6
Dual-phase (TRIP) steel	0.25	13.3	42.6
Austenitic stainless steel	0.5	28.4	97.3
Ferritic stainless steel	0.23	12.2	38.7
Duplex stainless steel	0.15	7.8	24.3

5.4.3 Discussion

An important aspect with expandable liner hangers is the rate of plastic deformation in the tubular. For most expandable systems the mandrel is pulled after expansion. Thus the hanger is not supported internally, and the elastic deformation is free to recover.

Another drawback with having an unsupported hanger is the potential for reverse yielding. During expansion the liner hanger comes into contact with the casing and the casing undergoes elastic deformation. This forms a contact pressure at the hanger/casing interface. If the contact pressure is too high two things can happen. Either the casing does not support the internal pressure formed by the contact, yielding plastic deformation of the host-casing. Or the hanger does not support the collapse pressure created by the contact, initiating reverse yielding. Neither of the options is desirable.

If retaining the mandrel in the liner hanger after expansion the above mentioned problems are avoided. Reverse yielding of the hanger is prevented by internal support from the mandrel. However, it is still important to avoid plastic deformation of the host-casing as this weakens the integrity of the contact. The hanger can deform purely elastic since it is constrained from recovering. This is however unlikely since only small deformation yields plasticity.

The investigated material was API casing grade Q125. This was chosen on the basis of the desired pressure rating of the system. It can be argued that Q125 is not the most ideal with respect to expansion. It has a very low material hardening index (0.07), which yields a low maximum expansion ratio according to Equation (12). For further analysis it is recommended to test other materials to compare the results. When selecting materials it is important to consider all factors influencing the liner hanger during its service life, e.g. corrosion, H_2S and fatigue.

5.5 Analysis of Post-Expansion Burst and Collapse Pressure of Tubular

Expansion reduces the burst and collapse pressure rating of a tubular. The extent of alteration of properties depends on the strain hardening behavior of the material. Degradation in pressure rating for expanded tubular is derived in the following sections. The results of the calculations support the argument of leaving the mandrel in place post-expansion.

5.5.1 Burst Pressure

The API burst-pressure rating is based on Barlow's equation for thick cylinders [39]. API bases the calculation on an allowed wall thickness variation for casing of 12.5%. By using 87.5% of the minimum yield strength for steel, the minimum allowable wall thickness is taken into account. The liner hanger body is assumed to be accurately machined and with that be 100%. This yields the following formula for burst:

$$p_{br} = \frac{2t\sigma_y}{d_o} \tag{13}$$

Burst pressure of an expanded hanger can be calculated by using Equation (13) with the OD (d_o) and thickness (t) of the expanded hanger. If strain hardening is considered in the material model the burst pressure can be calculated based on the yield strength found in Equation (A-12) in Appendix E.

5.5.2 Collapse Pressure

Collapse of a steel pipe from external pressure is a much more complex phenomenon than burst. Application of elastic stability theory leads to the following elastic collapse formula [39]:

$$p_{cr} = \frac{2E}{(1-\nu^2)\left(\frac{d_o}{t}\right)\left(\frac{d_o}{t}-1\right)^2} \tag{14}$$

The lower limit of the elastic collapse range is calculated by:

$$\frac{d_o}{t} = \frac{2 + F_2/F_1}{3F_2/F_1} \tag{15}$$

Values of F_1, F_2, F_3, F_4 and F_5 are given in Table 6. The range of d_o/t for various collapse pressure regions when axial stress is zero is shown in Table 7. In the other end of the collapse pressure region, the prevailing collapse mode is called yield strength collapse, and is given as:

$$p_{cr} = 2\sigma_{y,e}\left[\frac{\frac{d_o}{t} - 1}{\left(\frac{d_o}{t}\right)^2}\right] \quad \textbf{(16)}$$

Where $\sigma_{y,e}$ is the effective yield strength, equal to the minimum yield strength when axial stress is zero. The upper limit of the yield-strength collapse is calculated by:

$$\frac{d_o}{t} = \frac{\sqrt{(F_1 - 2)^2 + 8\left(F_2 + \frac{F_3}{\sigma_{y,e}}\right)} + (F_1 - 2)}{2\left(F_2 + \frac{F_3}{\sigma_{y,e}}\right)} \quad \textbf{(17)}$$

The transition from one region to the other is not sharp, but covers a significant range of $\frac{d_o}{t}$ values. API has adopted two additional collapse-pressure equations to cover the transition region. Just above the yield strength collapse a plastic collapse rating is predicted according to:

$$p_{cr} = \sigma_{y,e}\left(\frac{F_1}{\frac{d_o}{t}} - F_2\right) - F_3 \quad \textbf{(18)}$$

The upper limit of the plastic collapse range is calculated by:

$$\frac{d_o}{t} = \frac{\sigma_{y,e}(F_1 - F_4)}{F_3 + \sigma_{y,e}(F_2 - F_5)} \quad \textbf{(19)}$$

Between plastic and elastic collapse a transition region is defined by:

$$p_{cr} = \sigma_{y,e}\left(\frac{F_4}{\frac{d_o}{t}} - F_5\right) \quad \textbf{(20)}$$

An important aspect of tubular expansion is the variation in thickness as a function of expansion ratio. It should be evident that when expanding a pipe the wall thickness reduces. A recent paper by O.S. Al-Abri [40] presents the relationship between thickness variation and expansion ratio as follows:

$$\int_{t_1}^{t_2} \frac{dt}{t} = \int_{r_{1i}}^{r_{2i}} \frac{(-2H_2 + H_3 \sin^2\alpha)r^3 + (2H_1 - H_4 \sin^2\alpha)r + 2H_0}{(H_2 - 2H_3 \sin^2\alpha)r^3 - (H_1 - 2H_4 \sin^2\alpha)r - H_0} \frac{dr}{r} \quad \textbf{(21)}$$

The derivation of Equation (21) is presented in Appendix F. Integration of Equation (21) was performed numerically in Matlab using the Simpson 1/3 rule.

Table 6: Empirical coefficients used for collapse-pressure determination [39]

	Empirical Coefficients				
Grade*	F_1	F_2	F_3	F_4	F_5
H-40	2.950	0.0465	754	2.063	0.0325
-50	2.976	0.0515	1,056	2.003	0.0347
J-K 55 & D	2.991	0.0541	1,206	1.989	0.0360
-60	3.005	0.0566	1,356	1.983	0.0373
-70	3.037	0.0617	1,656	1.984	0.0403
C-75 & E	3.054	0.0642	1,806	1.990	0.0418
L-80 & N-80	3.071	0.0667	1,955	1.998	0.0434
C-90	3.106	0.0718	2,254	2.017	0.0466
C-95	3.124	0.0743	2,404	2.029	0.0482
-100	3.143	0.0768	2,553	2.040	0.0499
P-105	3.162	0.0794	2,702	2.053	0.0515
P-110	3.181	0.0819	2,852	2.066	0.0532
-120	3.219	0.0870	3,151	2.092	0.0565
-125	3.239	0.0895	3,301	2.106	0.0582
-130	3.258	0.0920	3,451	2.119	0.0599
-135	3.278	0.0946	3,601	2.133	0.0615
-140	3.297	0.0971	3,751	2.146	0.0632
-150	3.336	0.1021	4,053	2.174	0.0666
-155	3.356	0.1047	4,204	2.188	0.0683
-160	3.375	0.1072	4,356	2.202	0.0700
-170	3.412	0.1123	4,660	2.231	0.0734
-180	3.449	0.1173	4,966	2.261	0.0769

Table 7: Range of d_0/t for various collapse-pressure regions [39]

	←Yield Strength→ |	←Plastic→ |	←Transition→ |	←Elastic→ |
Grade*	Collapse	Collapse	Collapse	Collapse
H-40		16.40	27.01	42.64
-50		15.24	25.63	38.83
J-K-55 & D		14.81	25.01	37.21
-60		14.44	24.42	35.73
-70		13.85	23.38	33.17
C-75 & E		13.60	22.91	32.05
L-80 & N-80		13.38	22.47	31.02
C-90		13.01	21.69	29.18
C-95		12.85	21.33	28.36
-100		12.70	21.00	27.60
P-105		12.57	20.70	26.89
P-110		12.44	20.41	26.22
-120		12.21	19.88	25.01
-125		12.11	19.63	24.46
-130		12.02	19.40	23.94
-135		11.92	19.18	23.44
-140		11.84	18.97	22.98
-150		11.67	18.57	22.11
-155		11.59	18.37	21.70
-160		11.52	18.19	21.32
-170		11.37	17.82	20.60
-180		11.23	17.47	19.93

Based on the paper from C.G. Ruan and W.C. Maurer [41] and O.S. Al-Abri [40] a model for burst and collapse performance as a function of expansion ratio was created in Excel, see Figure 23. A 7 5/8" OD tubular of grade L80 is used in the calculations. Properties and calculated data are found in Appendix G. No strain hardening is accounted for. The pressure

rating for zero expansion agrees with values found in tables of mechanical properties of casings [11], adjusted for thickness variations.

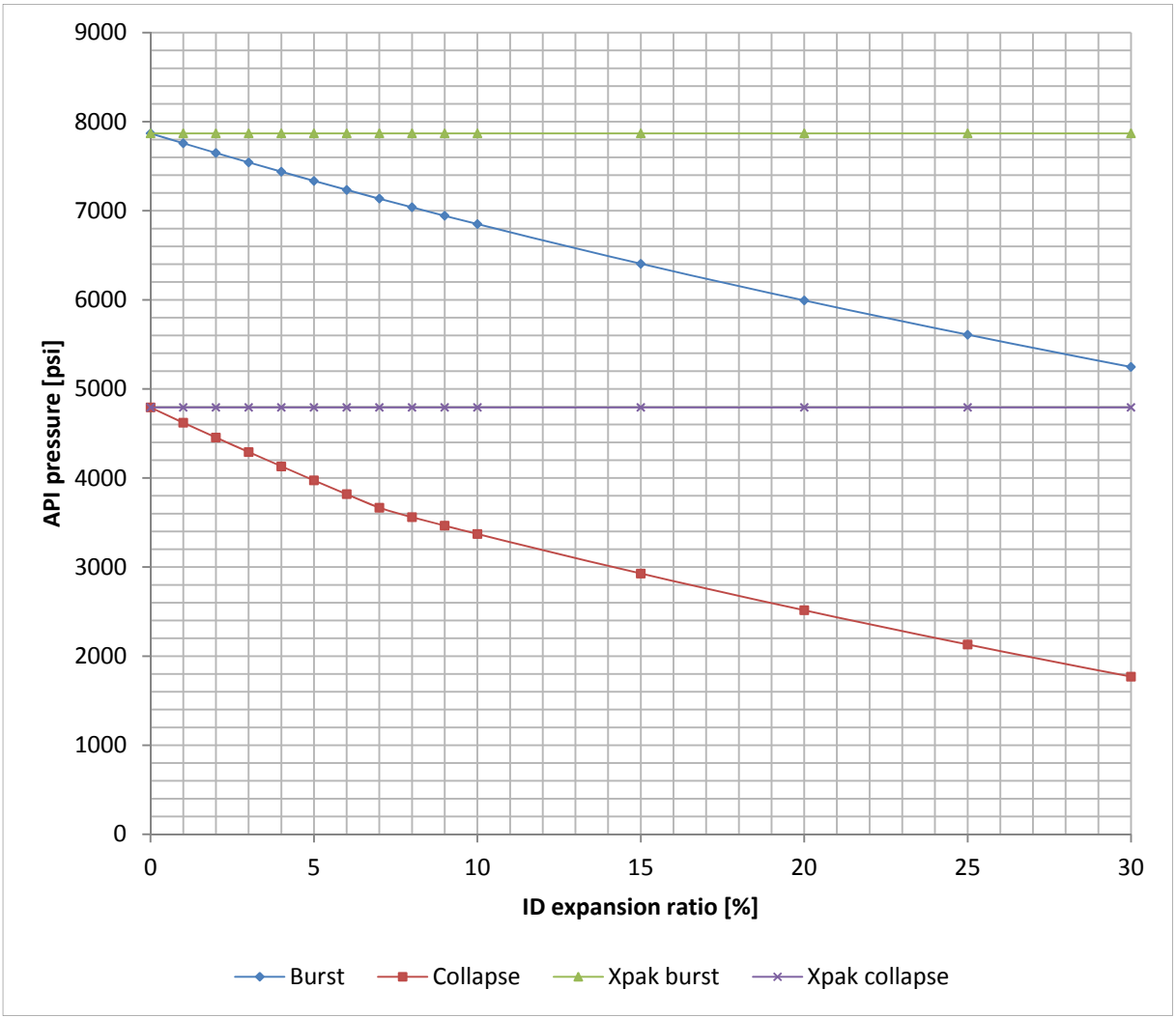

Figure 23: Burst and collapse rating of an expanded L-80 tubular

The red and blue line represents the collapse and burst pressure as a function of tubular expansion ratio respectively. The purple and green line is the collapse and burst pressure of an unexpanded casing of the same material grade and dimension. It is assumed that the combined wall thickness of the mandrel and the expanded liner hanger creates a higher pressure rating than the liner string. Thus the pressure rating of the liner string, purple and green line, becomes the design criteria for the system.

5.6 Evaluation of Wall Thickness Variation

It is assumed that the post-expanded wall thickness of the liner hanger equals the wall thickness of the liner string, see Chapter 4.2.1. Thus the pre-expanded wall thickness of the liner hanger has to be larger. Based on Equation (21) the necessary initial wall thickness of the liner hanger is calculated. A 7” liner hanger with a wall thickness of 0.453” is chosen as a benchmark. It is further assumed that the liner is to be set in a 9 5/8” casing with a wall thickness of 0.625”, leading to a required liner hanger ID expansion ratio of 22.5%. These dimensions follow directly from the suggested casing program, see Figure 2. Calculations showed that the required pre-expanded wall thickness of the liner hanger is 0.533”. Figure 24 illustrates the pre- and post-expanded dimensions of the liner hanger. The thickness t2 is 0.533” and t1 is 0.453”.

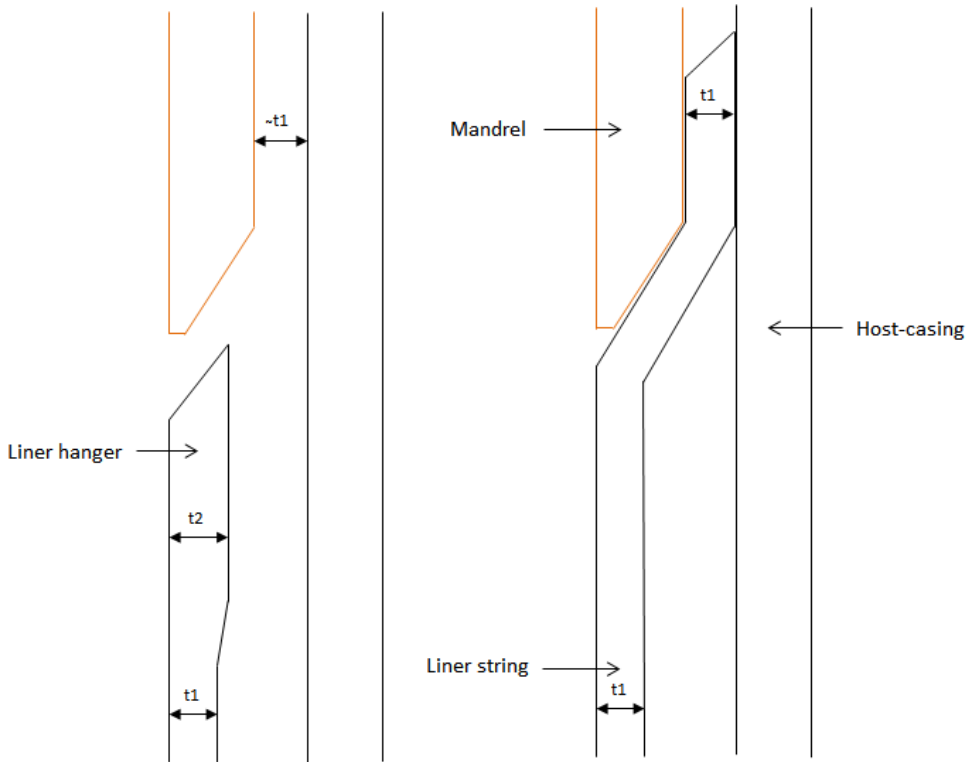

Figure 24: Pre- and post-expanded wall thickness of liner hanger

6 Finite Element Analysis

The bulk of this passage is found in the book “Finite element procedures in engineering analysis” [42]. A finite element analysis is a convergence of an actual physical problem. The analysis requires idealization of the physical problem into a mechanical description. It should be recognized that a mechanical idealization is actually implied in the finite element representation of the physical problem. Thus, a proper finite element solution should converge, as the number of elements is increased, to the analytical (exact) solution of the differential equations that govern the response of the mechanical idealization. The process of obtaining a finite element solution is summarized in Figure 25.

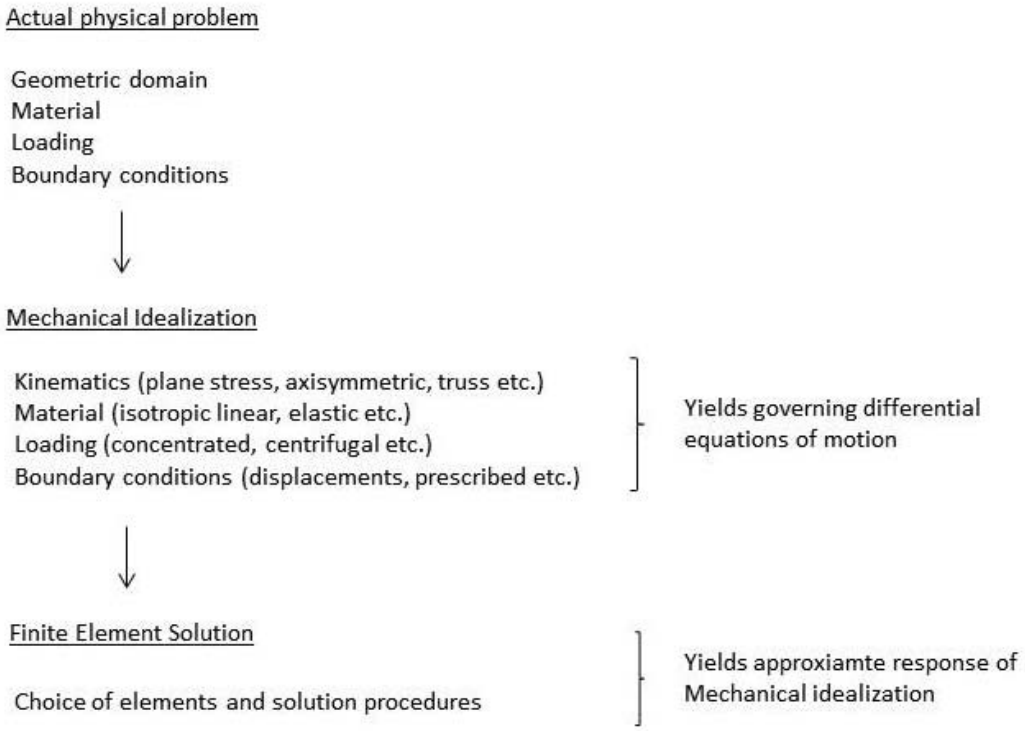

Figure 25: Finite element solution process [42].

The software used for the analysis was Ansys Workbench and Ansys Mechanical APDL. The liner hanger expansion was simulated in Ansys Workbench. The sealing capacity was analyzed using a fluid-pressure-penetration simulation in Ansys Mechanical APDL.

Actual Physical Problem

The liner hanger system is a relatively complex system, with a lot of components and contacting surfaces. However, the boundary conditions and interactions can be simplified during modeling to yield an approximate setup. The input data for the model are listed in Table 8.

Table 8: Input parameters for the finite element model

Part	Parameters	Value
Liner hanger	Inner diameter	6.094”
	Outer diameter	7.16”
	Wall thickness	0.533”
	Young’s modulus	200 000 [MPa]
	Poisson ratio	0.3
	API material grade	Q125
	Yield strength	862 [MPa]
	Ultimate strength	931 [MPa]
	Stress-strain data	See Figure 27
Mandrel	Inner diameter	6.094”
	Maximum outer diameter	7.47”
	Tip angle	20°
	Material	Tungsten
	Young’s modulus	365 000[8] [MPa]
	Poisson ratio	0.22
	Yield strength	3447 [MPa]
	Friction coefficient (lubricated)	0.06
Host casing	Inner diameter	8.375”
	Outer diameter	9.625”
	Wall thickness	0.625”
	Section length	3 feet 3 3/8”
	Young’s modulus	200 000 [MPa]
	Poisson ratio	0.3
	API material grade	Q125
	Yield strength	862 [MPa]
	Ultimate strength	931 [MPa]

During expansion the liner is held in place by the collet. Hydraulic pressure generates force to propagate the mandrel through the liner hanger. The host-casing is cemented in place. In addition it is object to external pressure from the formation and hydrostatic pressure.

Mechanical Idealization

When analyzing cylindrical objects, e.g. a liner hanger, it can be modeled as an axisymmetric element that is rotationally symmetric about the y-axis, see Figure 26. In the analysis the liner hanger was modeled as a surface body from the cross-section of the tubular. If the element is subjected to axisymmetric loads, a 2D analysis of a unit radian of the structure yields the complete stress and strain distribution. The main argument for doing a 2D axisymmetric analysis is savings in computational time, while still yielding a good convergence to the actual physical problem. 3D-modeling was performed to validate the result of the axisymmetric analysis. The results agreed well with each other, only minor differences were observed. This could be a result of mesh differences.

[8] Material data found on: http://www.hightempmetals.com/techdata/hitempTungstendata.php

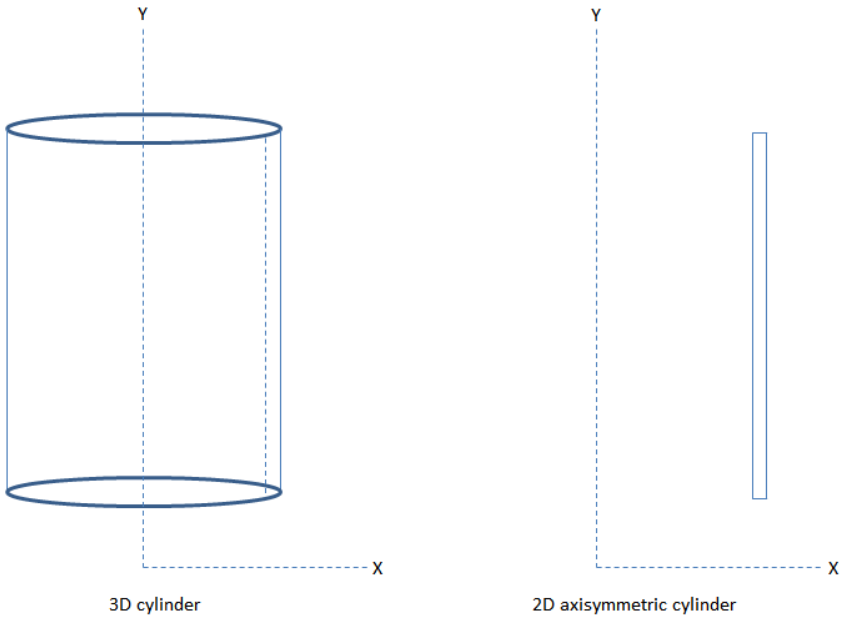

Figure 26: Axisymmetric view of tubular

The boundary conditions for the model are illustrated in Appendix H, Figure 48. The propagation force is represented by a 300 mm displacement of the mandrel in the negative y-direction. The fixed support at the bottom of the liner hanger represents the collet on the setting tool. The host-casing is fixed in the lower and upper end. This is a simplification of the actual boundary condition of the casing. As mentioned the formation and hydrostatic pressure will act on the external surface. For the relevant analysis these conditions are not considered due to increased complexity and convergence problems. Neglecting the external forces yields a more conservative result, especially concerning burst-like deformation of the casing. The casing section is only 3 ft. 3 3/8” long, as the actual casing is very long and therefore unsuitable to model.

The material model for the liner hanger and casing is set to bi-linear isotropic hardening with a tangent modulus of 11092 MPa, calculated from Equation (8). The resulting stress-strain curve, see Figure 27, is a simplification of the true stress-strain behavior of the material found in Chapter 0.

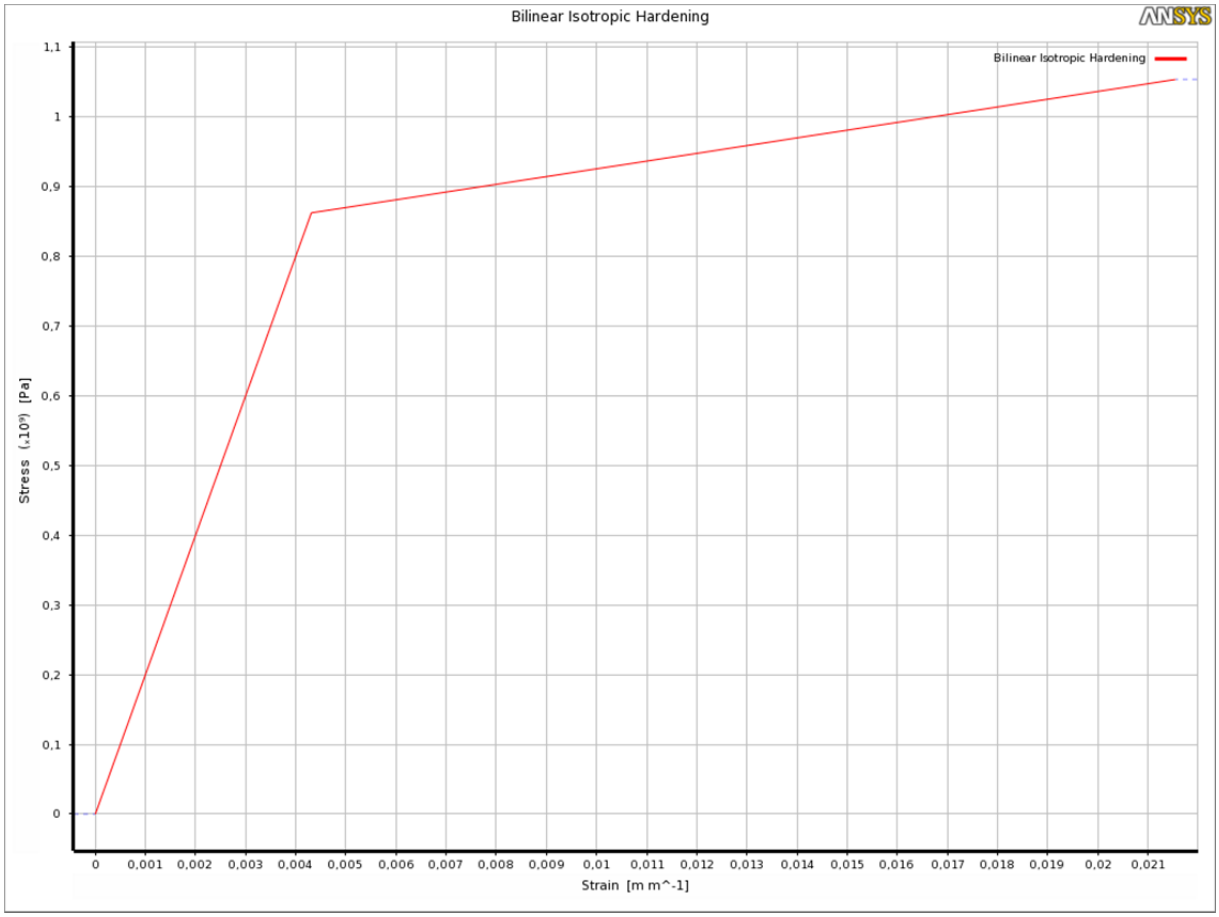

Figure 27: Bi-linear isotropic hardening model in FE-analysis

Finite Element Solution

Initial procedures involve refinement of the model to obtain consistent convergence. Since this report do not have any experimental results to compare with the model results, it is difficult to know the true answer for the stresses, strains etc. Such circumstances require convergence checking of at least two successively refined meshes for a total of three meshes. This is done in Ansys by "adaptive mesh refinement". The tool runs consecutive simulations with a refined mesh in each run. In advance the maximum allowable delta in e.g. stress from one run to the other is specified by the user. The software performs repeatedly simulations until the criteria is met, and with that convergence. G.B. Sinclair et.al. [43] have specified convergence checks for situations where the true stress is unknown. The solution is judged to have converged if:

$$|\sigma_f - \sigma_m| / |\sigma_f| < \bar{e}_s \qquad \textbf{(22)}$$

Where σ is the stress of interest and the subscript distinguish the mesh used to calculate it. Subscript m is an intermediate mesh density, f represent the finer mesh following m. $\bar{e}_s$ is the relative delta sought. A $\bar{e}_s$ value less than 0.01 (1%) is considered as an excellent level, less than 0.05 (5%) as a good level and less than 0.1 (10%) as a satisfactory level [43]. This test can also be used for parameters other than stress, e.g. strain or pressure.

Mesh
In Chapter 5.4 it was deducted that the expansion is strain-controlled. During simulations convergence was chosen to depend on strain. The adaptive mesh refinement tool registers where the peak strain occurs, and refines the mesh in these areas to get a more accurate result. This is repeated until the convergence criterion is met.

Default mesh settings was chosen, which gives a higher flexibility during the refinement loops. The resulting mesh consisted of a combination of quadratic and triangular elements. The number of nodes and elements are given under the result section.

6.1 Analysis Procedure

Expansion alters the material properties and closer modeling is required. The main focus of the simulations was stress and strain exerted on the system during expansion. Post-expansion the liner hanger has been exposed to a burst and collapse pressure of 100 MPa (15000 psi) to evaluate the pressure rating.

Analysis of the seal and host-casing interaction was performed in separate simulations. This was decided because of the complexity it introduced to the global liner hanger model. Special attention was given to the deformation of the casing from indentation of the seal wedge. Beforehand it was assumed that the metal seal would not affect the global stress picture, but rather create local deformations. Hence, the decision to leave them out of the global analysis should not affect the results noticeably.

6.2 Results

6.2.1 Liner Hanger Expansion

For the liner hanger expansion analysis a maximum change of 2% in elastic strain was defined as convergence criteria. The resulting convergence history is presented in Figure 28. From the figure it can be seen that a change of 1.9% was obtained, which is defined as a good level. The associated mesh consisted of 20588 nodes and 6401 elements for the whole model, as seen from the table in Figure 28. The results of the analysis are presented in Figure 29 and Figure 30. The stress distribution shows that the tip of the expansion mandrel is subject to a very high stress, see Figure 29. The stress results in some elastic deformation of the tip, but no plastic deformation, see Figure 30. It has not been identified whether the actual running tool supports the mandrel internally or not. A closer examination of the influence of internal support is performed in Chapter 6.2.2.

As desired the expansion of the liner hanger results in elastic deformation of the host-casing, see right picture in Figure 30.

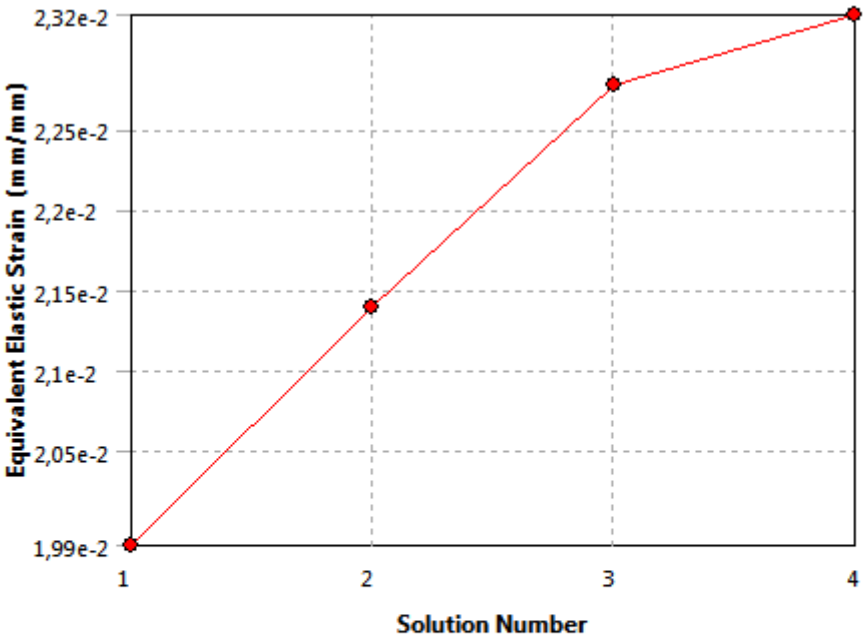

	Equivalent Elastic Strain (mm/mm)	Change (%)	Nodes	Elements
1	1,9914e-002		3569	968
2	2,139e-002	7,1471	6381	1840
3	2,2775e-002	6,2728	15060	4623
4	2,3214e-002	1,9112	20588	6401

Figure 28: Convergence history

From Figure 30 one sees that only a small portion of the total deformation is represented by elastic strain. The whole wall thickness of the liner hanger is plastically deformed after the expansion. The inner surface sees the largest plastic deformation, which corresponds to the theory in Chapter 5.4. As desired neither the mandrel or the host-casing undergoes any plastic deformation. The left picture in Figure 30 shows the deformation in the radial direction (x-direction). The liner hanger experiences a radial deformation of 17.54 mm. This value denotes an expansion ratio of 22.65%, which is approximately the same ratio found in Chapter 5.6.

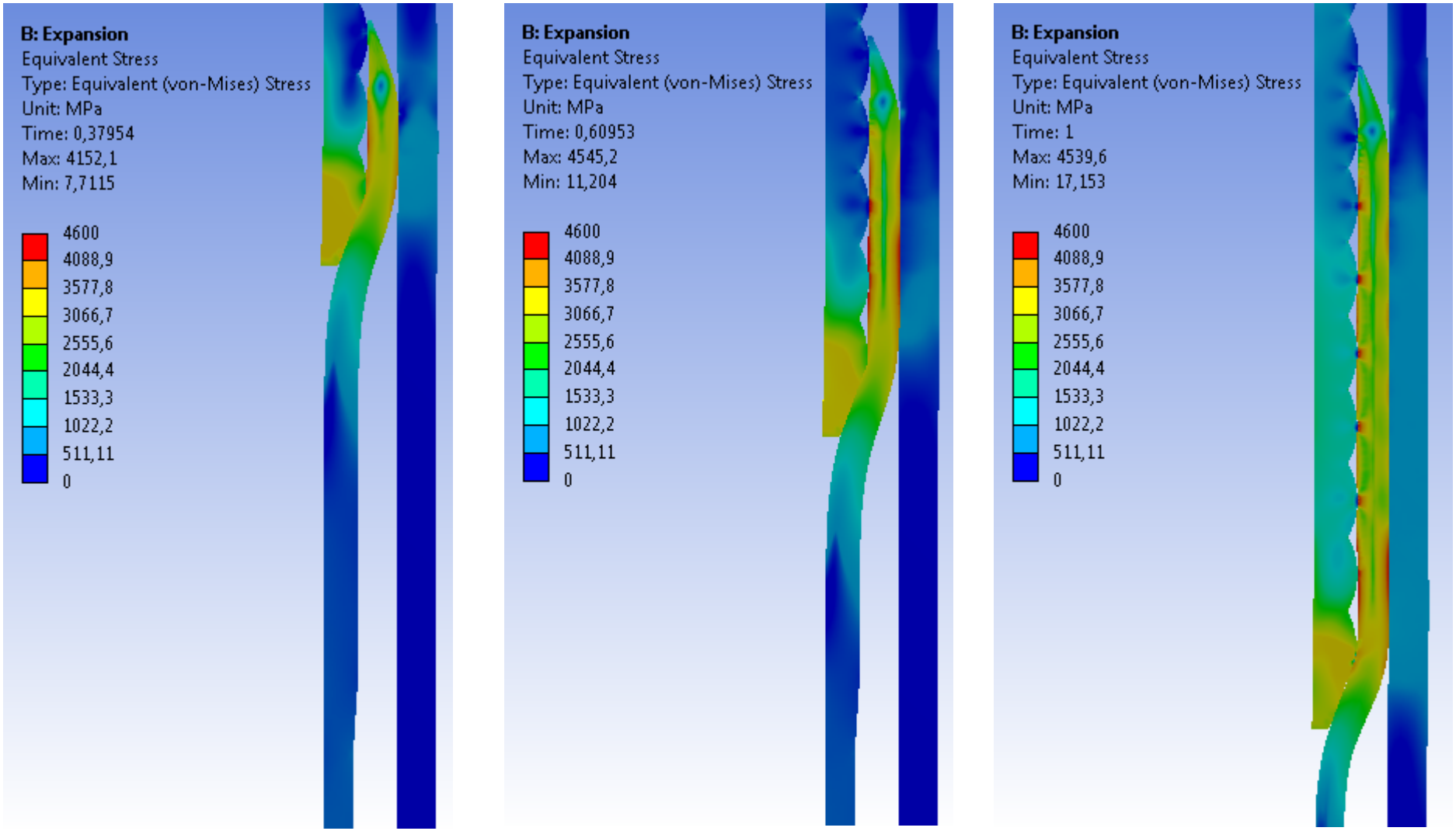

Figure 29: Equivalent stress vs. mandrel displacement

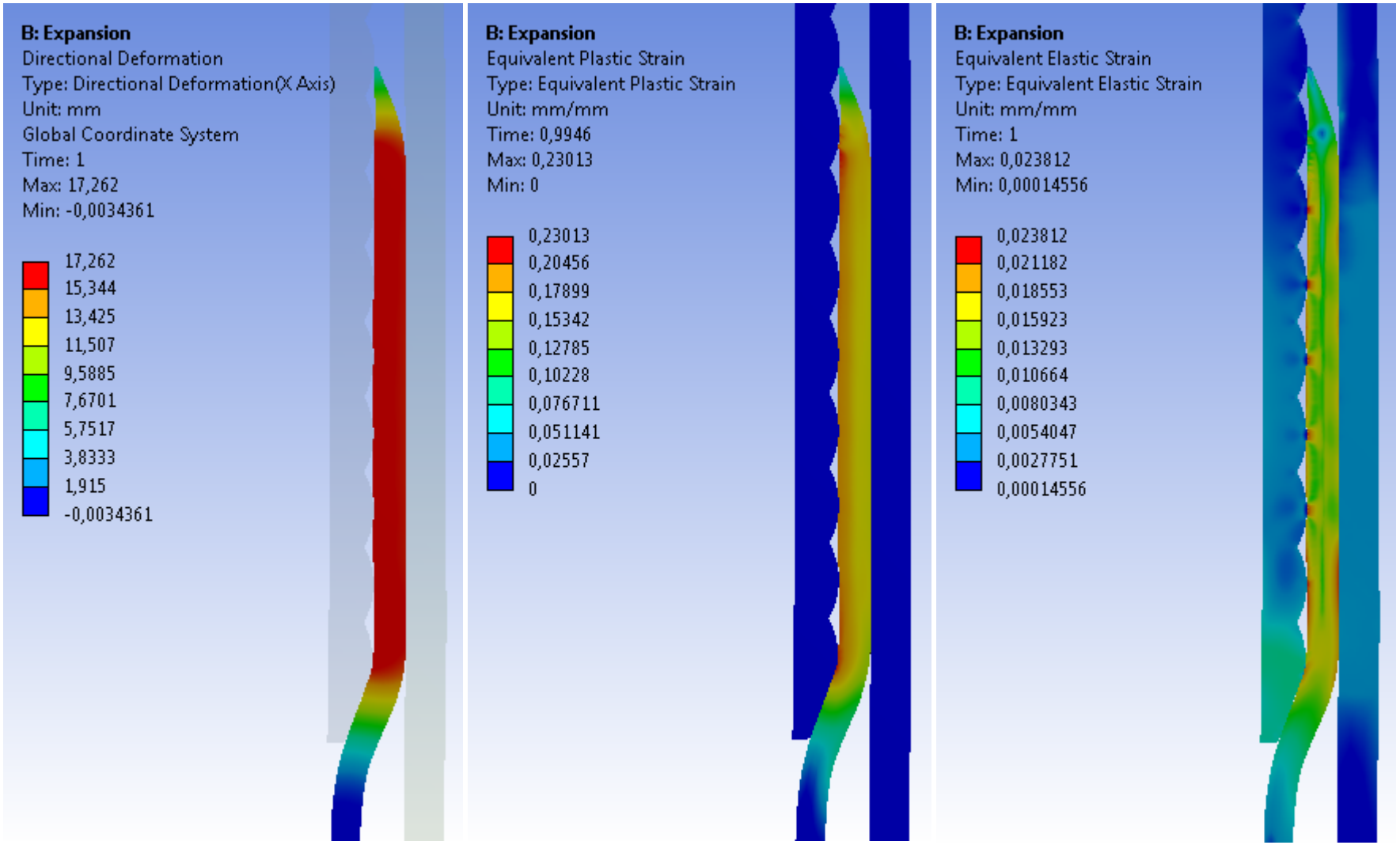

Figure 30: Directional deformation (left), plastic strain (middle) and elastic strain (right)

6.2.2 Internally Supported Mandrel

As a consequence of the stress intensity at the tip of the mandrel, a simulation with internal support was run. This drastically alters the stress distribution, see left picture in Figure 31. Considerably smaller stress intensity is observed at the tip of the mandrel. Less stress also reduces the mandrel deformation, see right picture in Figure 31. With internal support during expansion the mandrel can be fabricated from a lower strength metal, while maintaining the same wall thickness, thus reducing the cost of the system.

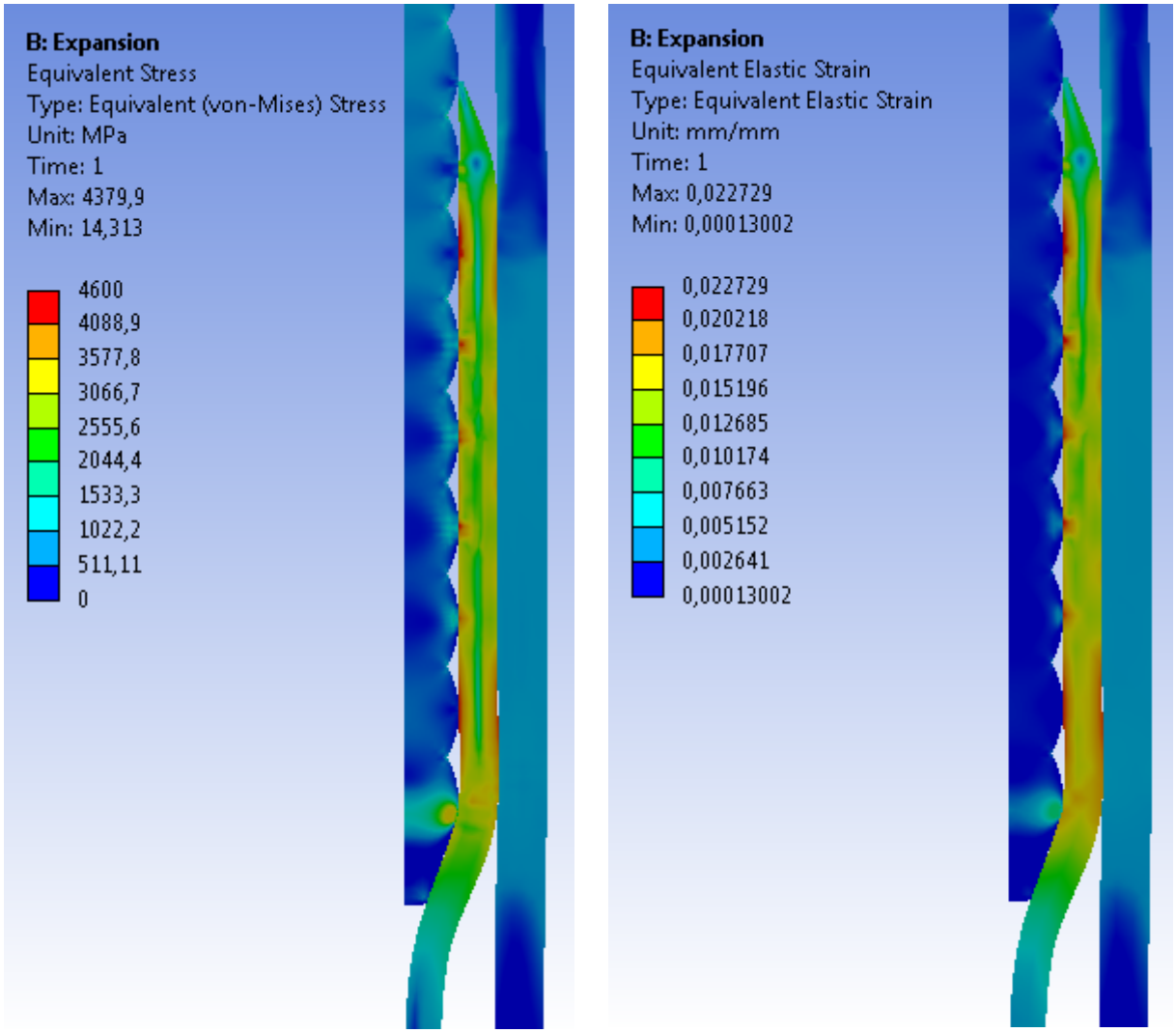

Figure 31: Equivalent stress (left) and elastic strain (right) for internally supported mandrel

A conspicuous result is the stress concentration observed in the lower ball profile of the mandrel. It is most likely a result of the design, as this is the point where the liner hanger winds around the mandrel during expansion.

6.2.3 Collapse Pressure

The liner hanger is first expanded and then subjected to a 100 MPa collapse pressure. The pressure is put on the external surface of the liner hanger. No pronounced deformation takes place as a result of the collapse pressure, see Figure 32. The critical point is again the tip of the expansion mandrel. The tip experiences high stress intensity during collapse loading. If one compares the directional deformation in the right picture to that of the directional deformation in Figure 30, it is evident that the collapse pressure deforms the liner hanger. This is however not enough to separate the liner hanger and the host-casing.

It is only relevant to test the collapse pressure during service, thus the mandrel is not internally supported at this point. Due to limitations in the software it has not been possible to simulate the expansion with internal support and pressure loading without internal support.

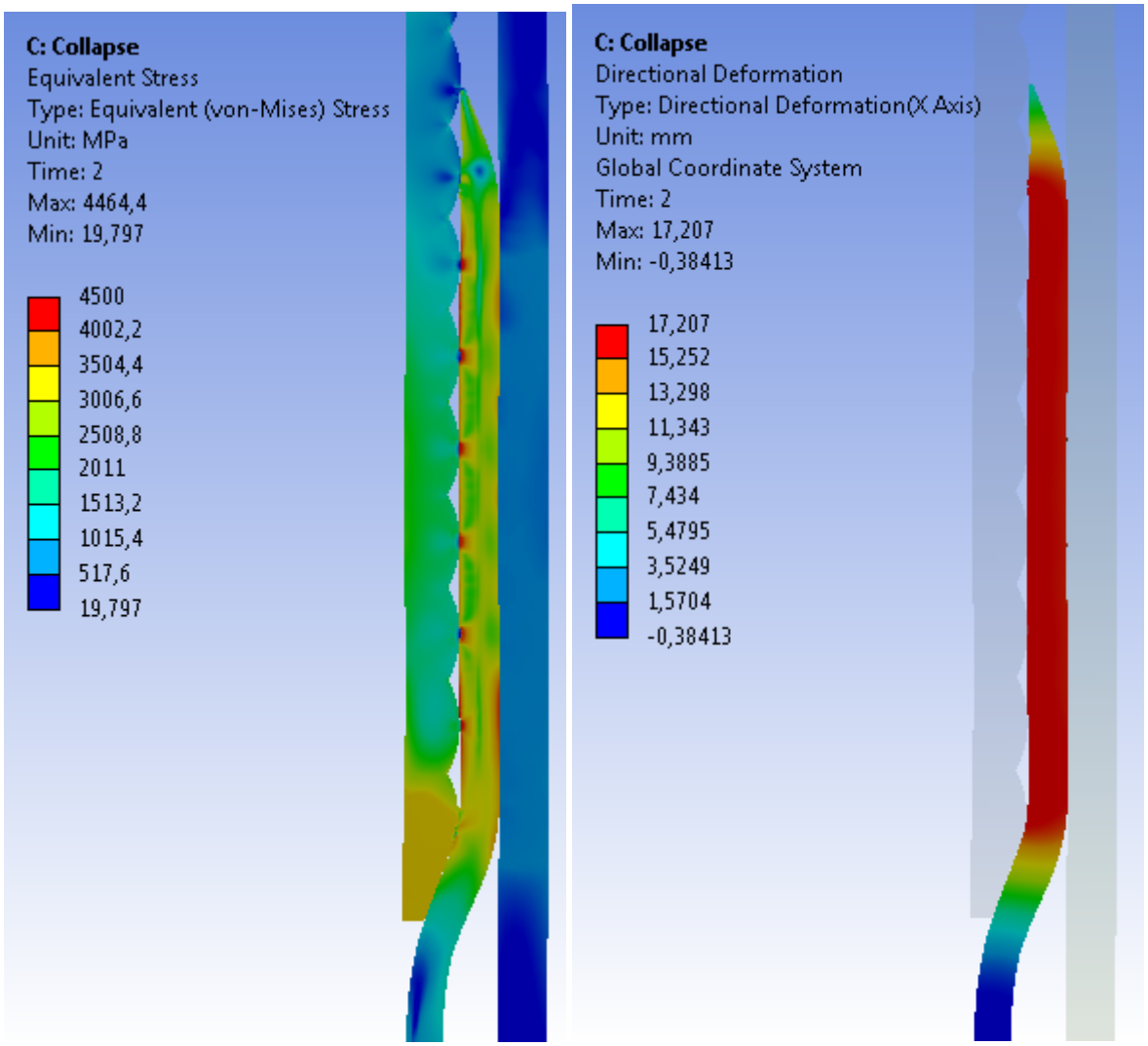

Figure 32: Equivalent stress (left) and deformation post-expansion (right) with 100 MPa collapse pressure

6.2.4 Burst Pressure

Similar to the collapse pressure analysis, burst rating was evaluated by first expanding the liner hanger and then exposing the system to an internal pressure of 100 MPa. The result is presented in Figure 33. The result show that stress on the host-casing increases. Since the external formation and hydrostatic pressure are not considered, the result are conservative with respect to burst rating, and is not considered to be of any significance.

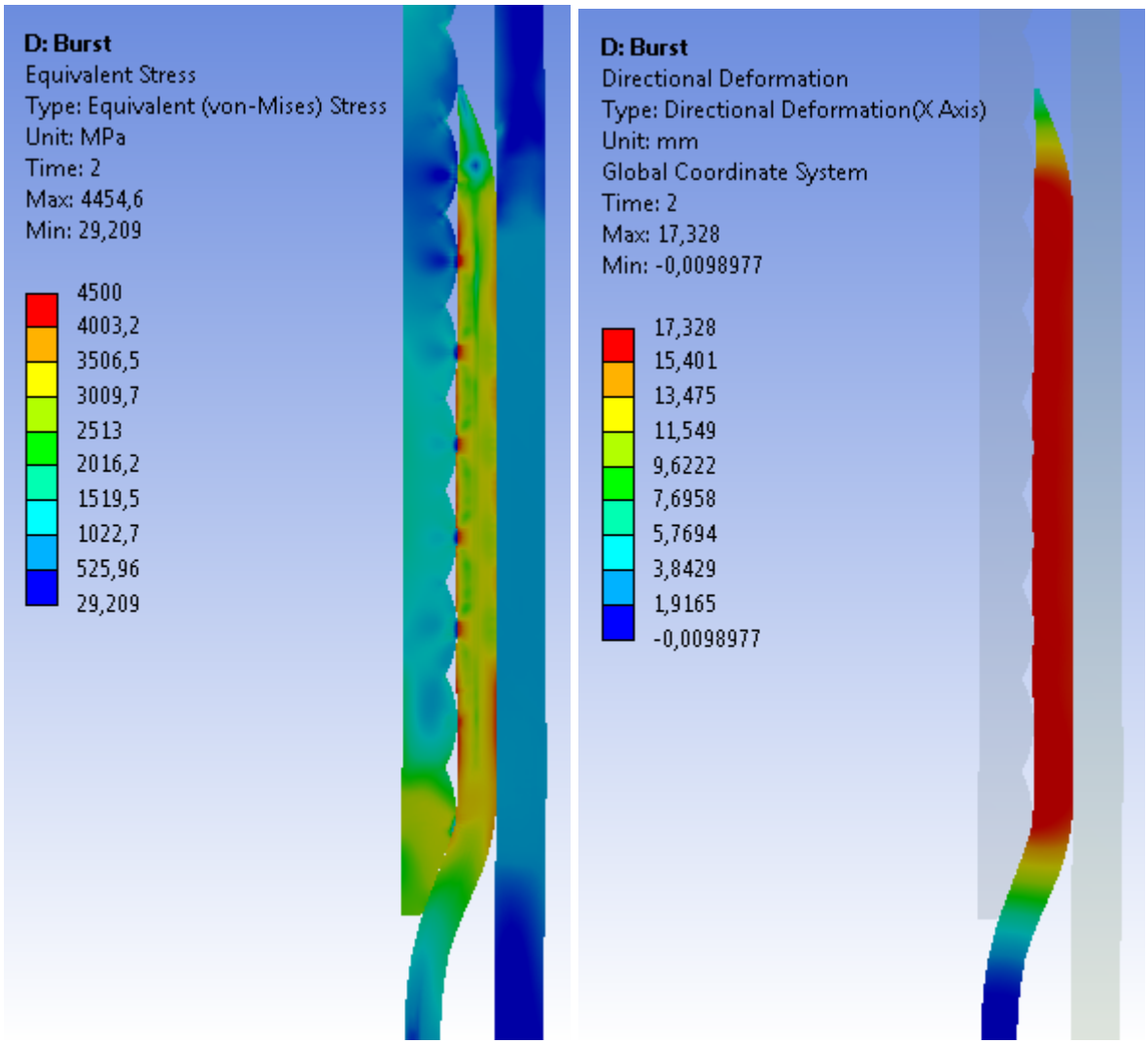

Figure 33: Equivalent stress (left) and elastic strain (right) post-expansion with 100 MPa burst pressure

6.2.5 Seal integrity

To investigate the sealing integrity of the mandrel/liner hanger-contact a fluid penetration analysis was conducted. The analysis exposes two contacting surfaces to an increasing fluid pressure, and reveals whether fluid can leak through or not. The contact was exposed to a fluid pressure of 100 MPa. At 100 MPa no fluid leaked through, see Figure 49 in Appendix H. Ansys APDL was used for this analysis. The figures produced by software are of poor quality.

6.2.6 Seal/casing deformation

For the purpose of the seal/casing deformation analysis a single seal has been modeled. The actual liner hanger is designed with a series of seals with intervening elastomeric bands. However, the metal seal wedge is considered the primary seal, thus the elastomer is not considered in the FEA. The elastomer does neither induce considerable deformations.

The indentation of the seal creates a large local stress in the host-casing, see Figure 34. The seal is suppressed in the figure to emphasize the behavior of the casing material. For the purpose of this analysis, the seal was made from tungsten. Tungsten meets the requirement of a differential hardness compared to structural steel of 10 on the Rockwell C-scale stated in Chapter 4.1.1.

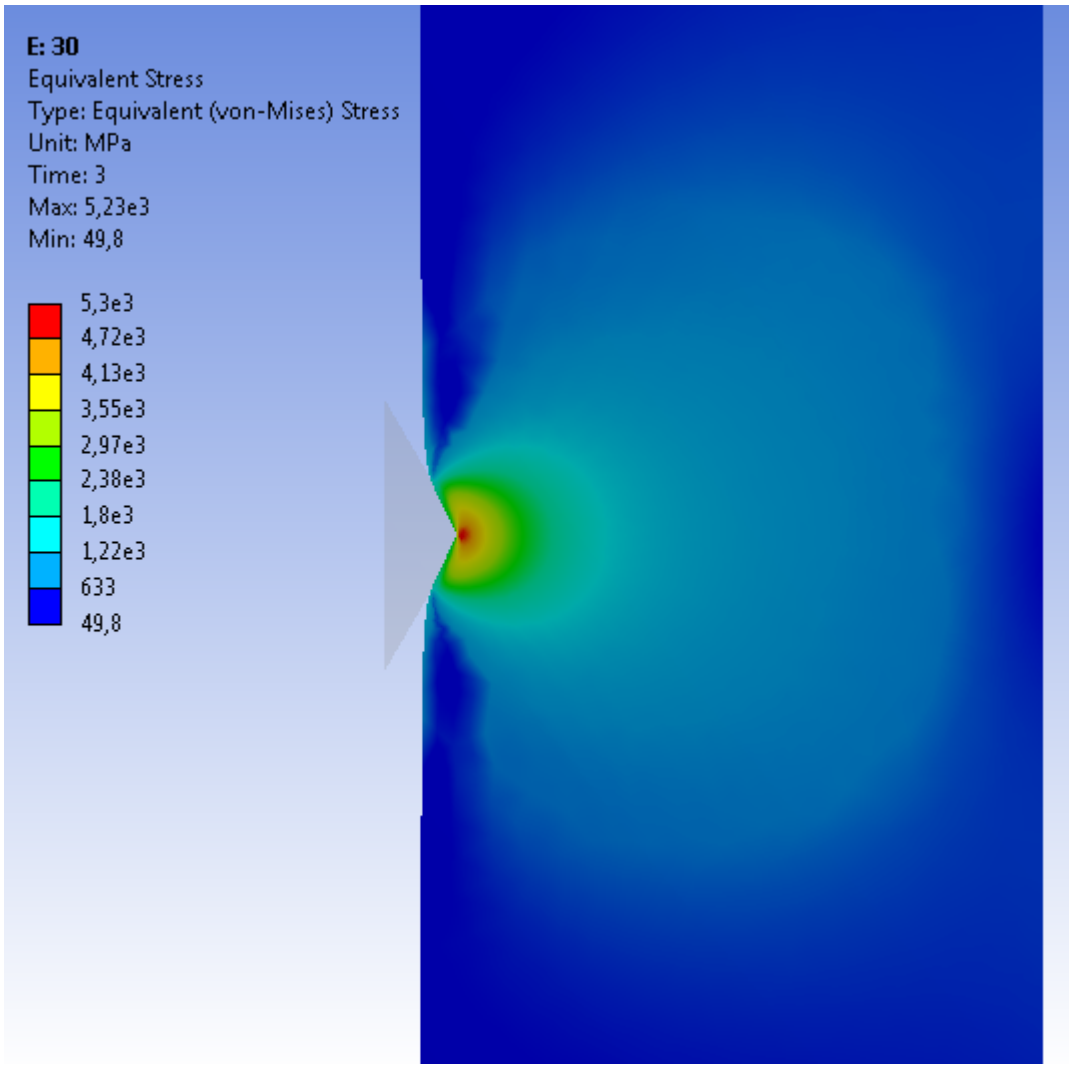

Figure 34: Stress from seal indentation

The resulting plastic deformation is illustrated in Figure 35. The elastic deformation is very similar to the stress pattern, thus it is not shown here. The plastic deformation is concentrated around a small area in front of the seal tip. From the figure one also sees that there is little to no plastic deformation of the seal, verifying that the condition in Equation (4) is met.

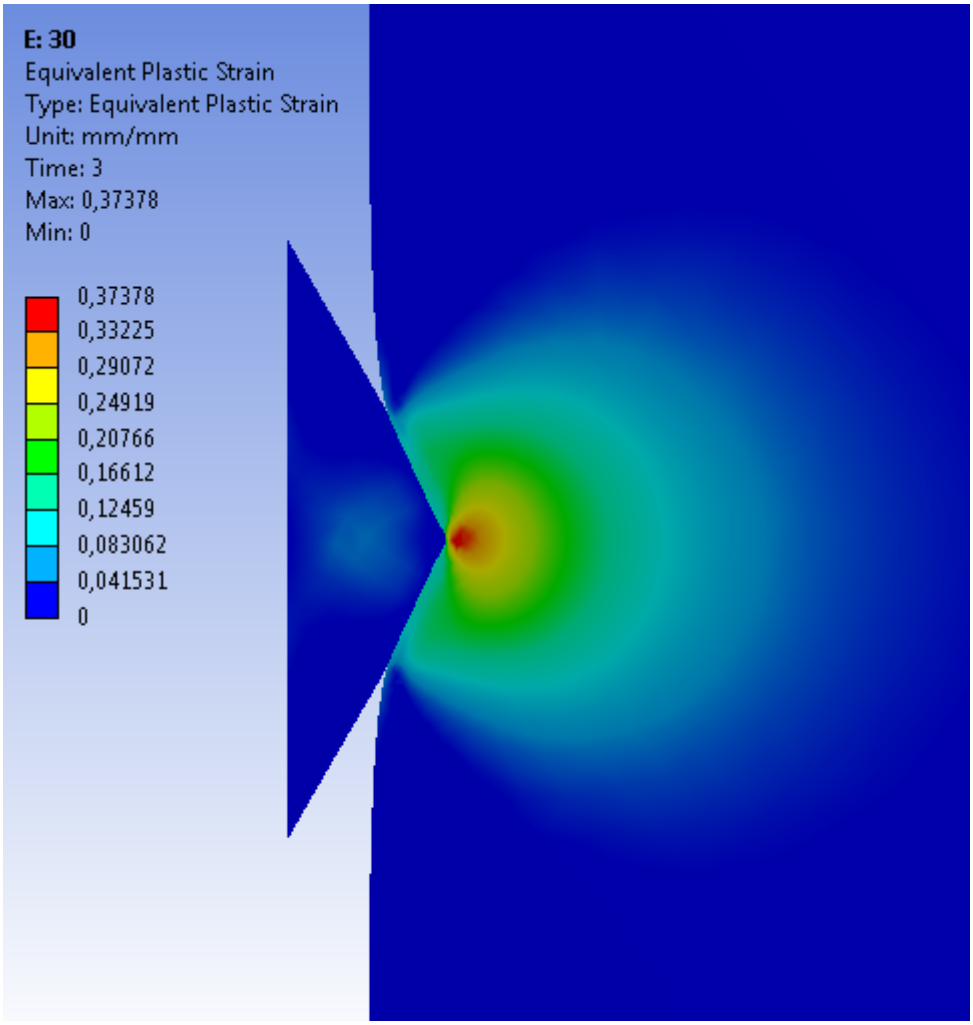

Figure 35: Plastic deformation from seal indentation

The contact pressure between the seal and the casing is approximately 6 times the yield strength of the casing metal, see Figure 36. This should provide a reliable seal against any fluids or gas entering the annulus. As indicated in Chapter 4.1 a pressure of twice the weaker materials yield strength is required to observe leakage. This is highly unlikely, and much else will fail before reaching this pressure. A fluid-penetration analysis with a 100 MPa pressure was performed on the seal. The seal showed no leakage at this pressure, see Figure 50 in Appendix H.

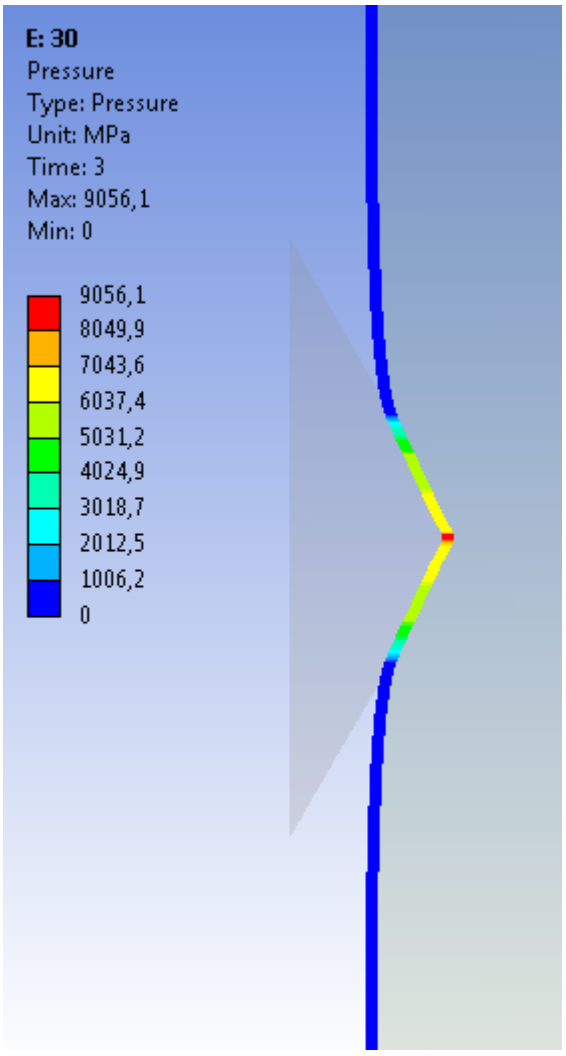

Figure 36: Contact pressure at the seal/casing interface

The seal in the above pictures is designed with a tip half-angle of 30°. A closer investigation of the seal design was performed to investigate the influence of the tip half-angle. The force required to energize the seal and equivalent plastic deformation of the seal was studied, see Figure 37. From the results it is evident that the force required to energize the seal is increasing with increasing tip half-angle. The plastic deformation of the seal works the other way around, decreasing with increasing half-angle. Increasing force means that more work is required to displace the mandrel through the liner hanger. More plastic deformation of the seal is neither desirable with respect to the seal integrity. From the analysis it was found that the contact pressure does not correlate with the force to energize the seal. Based on these findings it is believed that a larger tip half-angle yields a better seal because of the reduced plastic deformation. This is of course only relevant up to a certain value, as the seal becomes close to flat as the tip half-angle approaches 90°.

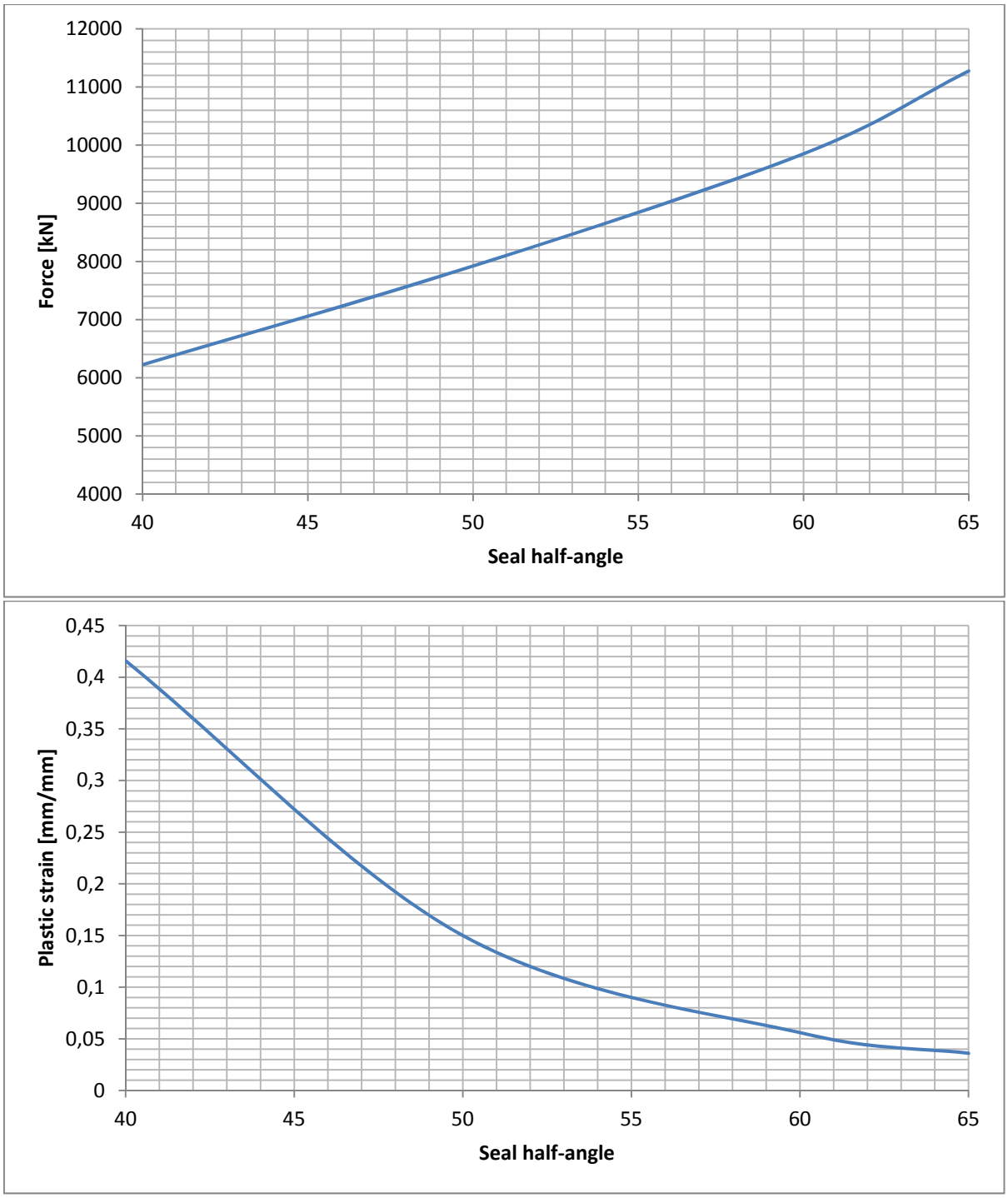

Figure 37: Force to energize seal vs. tip half angle (top). Plastic strain in seal vs. tip half angle (bottom)

6.3 Discussion

This section will evaluate the findings from the analysis and identify potential sources of error.

The starting point for the analysis was to set a 7” liner hanger in a 9 5/8” host-casing. The liner string should have an internal flush design with the expansion mandrel retained down hole. This introduces some limitations regarding the design of the mandrel. Ideally the wall thickness of the mandrel should have been larger to avoid deformations during expansion. To limit deformation the mandrel was made of tungsten carbide. Polished tungsten carbide has a low coefficient of friction, and the fact that it is very hard makes it ideal as material for the mandrel, but the cost is high. The cost is a result of the temperature required to melt and form the metal. Normally tungsten carbide is coated on a base metal, forming a hard outer surface. For the purpose of the analysis this has not been possible to recreate. Should a lower grade metal be used it is found that the mandrel needs internal support to avoid collapse-like deformation. Another solution could be to make the tip of the mandrel from harder metal than rest of the body.

The liner hanger and host-casing has the properties of API casing grade Q125. In the analysis a bilinear isotropic hardening model was chosen for the material. The isotropic model increases the material strength in all stress directions plastic deformation increases. For closer analysis of the expandable liner hanger it is recommended to evaluate the material model against real data. In addition it is necessary to try constructing the liner hanger from different materials. This can have a drastic effect on the stress and strain during and after expansion.

In case the mandrel had not been retained in the liner hanger after expansion, the elastic deformation could have recovered. This would most likely have degraded the seal integrity. The liner hanger would also have been prone to collapse like deformation from external pressure, potentially separating the two surfaces. The contact pressure between the liner hanger and host-casing also creates reloading, potentially forcing the liner hanger deformation back. By leaving the mandrel in-place this is avoided. Another advantage with retaining the mandrel is that it isolates the expanded liner hanger from the well stream, which reduces the sensitivity to H_2S. Within material theory it is well known that expansion or tension of metal reduces the sulfide stress cracking (SSC) resistance [44]. This might be irrelevant for exploration drilling, but in production wells it is a clear advantage.

No real test data are provided to compare the results from the finite element analysis. This is vital for proper evaluation and qualification of the liner hanger system. The analysis provided in this thesis can be considered as an initial investigation. The positive results reason for more thorough testing to qualify the system for 15000 psi. Full scale testing is also important to get more accurate data on friction, material behavior etc.

6.3.1 Sources of error

During the expansion analysis the liner hanger was not designed with slips and seals. This will yield some errors in the results from the expansion, but due to the increased complexity of the analysis it was chosen to perform separate simulations of the seal. The hanging capacity of the liner hanger was not possible to test without the slips. This should however be included in any further work on the topic.

A possible source of error in the analysis is the contact status between surfaces in the finite element model. During the analysis the software establish a relationship between contacting surfaces to prevent them from passing through each other. This is called enforcing contact compatibility. The contact formulation chosen was Augmented Lagrange, which is a penalty-based formulation. The contact pressure in the Augmented Lagrange formulation is calculated as:

$$F_{normal} = k_{normal} x_{penetration} + \lambda$$

Where k_n is the contact stiffness and x_p is the penetration, see Figure 38. Ideally the penetration should be zero for an infinite k_n. With penalty-based methods this is numerically impossible, but as long as x_p is small or negligible, the solution will be accurate. The term λ is a factor reducing the contact stiffness sensitivity. For the analysis performed a value of 0.1 was chosen for the contact stiffness.

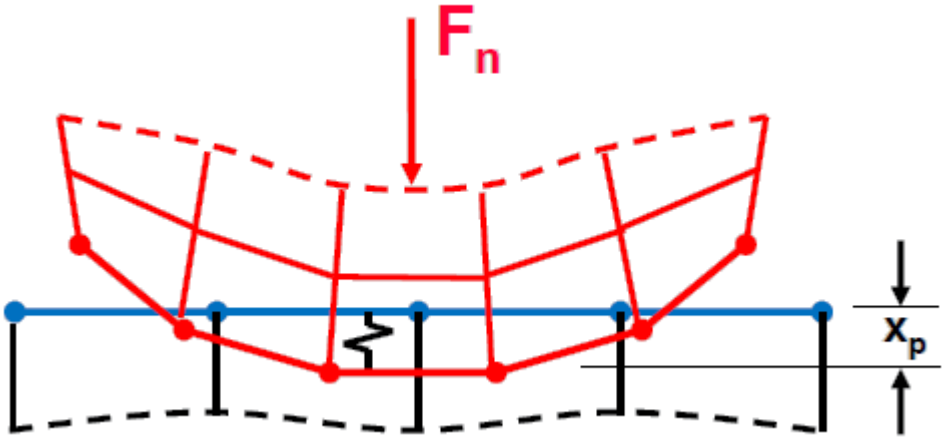

Figure 38: Finite element contact

Large stiffness values yields more accurate results, but it often raises convergence problems. Smaller stiffness allows for more penetration, but in most cases it still yields acceptable results. The factor that might see the largest deviation is the maximum contact pressure, which is directly related to the penetration. This raises an issue with the fluid penetration analysis. High contact pressure and penetration results in a sticking contact condition, rather than sliding. The phenomenon might invalidate the fluid penetration analysis. As a consequence of the latter, it was chosen not to focus too much on this in the analysis. For proper verification of the seal integrity it is recommended to do full-scale testing.

Due to the uncertainty around temperatures in the well, an ambient temperature of 25°C was used in the analysis. Temperature will affect the behavior of the material, and is recommended to evaluate in any further analysis.

7 Conclusion

This thesis has proposed a solution for a slender well concept related to offshore exploration drilling. The solution is based on literature survey, evaluation of technology enablers and finite element analysis. The objective of the slender well concept is to reduce the cost of drilling a well as compared to a conventional well design, without compromising the integrity or functionality of the well. Slender wells are associated with considerable cost savings. It includes casing steel, drilling fluids and handling of cuttings. The potentially largest saving is however related to the rig cost.

The main findings are summarized below:

- Employ modified 3rd or 4th generation semi-submersible rigs to avoid the high day-rates associated with 5th and 6th generation rigs. This is made possible by reducing the size of the marine drilling riser and BOP.
- The conductor and surface casing size is reduced without compromising the final pipe size. Optimum final pipe size is obtained by reducing the radial clearance between consecutive liner sections.
- Enabling technologies include muds, drill-bits, LWD, MWD and expandable liner hangers.
- Consumption of steel is reduced by using liners. Expandable liner hangers were identified as the best way to hang the liners in close-clearance wells. The slender well design also reduces the consumption of mud and handling of cuttings.
- By pre-installing a liner in the surface casing an additional casing section is rendered possible. The liner does not have to be run through the riser, thus the riser ID can be reduced. An 8 5/8” ID riser is suggested used. A J-slot hanging mechanism can suspend the PIL in the surface casing before running in hole.
- It is suggested to adapt a surge protection system to the proposed liner system to reduce the probability of abnormal surge pressures and damage to the formation. The protection system displaces fluid in an artificial annulus inside the liner.
- Expansion of the liner hanger is obtained by displacing an oversized tubular mandrel. After expansion the mandrel is retained in the liner hanger to avoid the reduced burst and collapse rating associated with expanded tubular. The mandrel is designed such that it creates an internal flush design with the liner string.
- Finite element analysis indicated that an expandable liner hanger with a pressure rating of 15000 psi is obtainable. From the analysis it was found that the mandrel needs to be made from a strong material to avoid deformations. Alternatively the mandrel can be internally supported during expansion. A low coefficient of friction between mandrel and liner hanger is important to avoid excessive stress and required force to displace the mandrel.
- Metal-to-metal was identified as the most reliable liner hanger seal.

7.1 Further Work

The next step in the development of the slender well concept will be to get a detailed plan, including cost picture, required technological development and potential show-stoppers. Further, field trials are necessary to validate the functionality and reliability of the concept. The petroleum industry is known to be conservative towards new technology, so thorough testing and positive results are essential to get operators “onboard”. As mentioned in the introduction, operators have often rejected slim wells due to the additional work it represents, their functionality, or they have not been convinced of the potential. The importance of trials should therefore not be underestimated.

The focus of this thesis has been on exploration drilling. A detailed assessment of slender well production drilling would also be necessary to fully exploit the potential in the slender well concept.

Further modeling and analysis are required before commencing with full-scale testing of the expandable liner hanger. It is recommended to create a complete model of the liner hanger system to get a detailed picture of the expansion. Such a model would include seals and slips for investigation of sealing and hanging capacity. Full-scale testing is important to validate the results found in analysis and simulations. As mentioned the liner hanger are being used by TIW today, but development is required to qualify it for higher pressure rating. Special attention should be given to the sealing integrity and choice of materials. Correct design of the mandrel is important to avoid unnecessary stress concentrations and residual stresses after expansion.

8 References

1. P. Head, et al., *Slimwells without the pain*, in *SPE/IADC Conference*1999, Society of Petroleum Engineers: Amsterdam, Holland.
2. P.D. Howlett, et al., *Evolutionary Well Construction Method That Challenges Convention*, in *SPE/IADC Drilling Conference,*2007, Society of Petroleum Engineers: Amsterdam, The Netherlands.
3. C. Lee Lohoefer, et al., *Expandable Liner Hanger Provides Cost-Effective Alternative Solution*, in *IADC/SPE Drilling Conference*2000, Society of Petroleum Engineers: New Orleans, Louisiana.
4. P. Smith and J. Williford, *Case histories: Liner-completion difficulties resolved with expandable liner-top technology*, in *Canadian International Petroleum Conference*2006, Society of Petroleum Engineers: Calgary, Alberta.
5. Strand, H., *Efficient Exploration*, 1994, Saga Petroleum.
6. Ikäheimonen, E., *SEB Enskilda Nordic Seminar*, 2012: Copenhagen, Denmark.
7. Barker, J.W., *Wellbore Design With Reduced Clearance Between Casing Strings*, in *SPE/IADC Drilling Conference, 4-6 March 1997*1997, Society of Petroleum Engineers: Amsterdam, Netherlands.
8. J. J. Azar and G.R. Samuel, *Drilling Engineering*2007, Tulsa, Oklahoma, USA: PennWell Corporation.
9. National Oilwell Varco, *Motor Handbook*. Seventh edition ed2011, http://www.nov.com/Downhole/Drilling_Motors.aspx.
10. Tor B. Gjersvik SPE FMC Technologies and Audun Faanes and Bjørn A. Egerdahl Statoil, *Subsea MMX, Year 2010*, in *Offshore Technology Conference*2007, Offshore Technology Conference: Houston, Texas.
11. G. Gabolde and J.P. Nguyen, *Drilling data handbook*. Eigth edition ed, ed. E. Technip2006: IFP Puplications. C37 - C81.
12. Halliburton, *VersaFlex ELH System - Simplifying Liner Installations with Reliable Expandable Solutions*, 2012: http://www.halliburton.com/public/cps/contents/Brochures/web/H05234.pdf.
13. International Organization for Standardization, *ISO 14310:2008*, in *Petroleum and natural gas industries - Downhole equipment - Packers and bridge plugs*2008, Standard Norge.
14. J. Williford and P. Smith, *Expandable Liner Hanger Resolves Sealing Problems and Improves Integrity in Liner Completion Scenarios*, in *Production and Operations Symposium*2007, Society of Petroleum Engineers: Oklahoma City, Oklahoma, U.S.A.
15. TIW, *Expandable liner hanger technology*.
16. J.W. Agnew and R.S. Klein, *The leaking liner top*, in *SPE Deep Drilling and Production Symposium*1984, Society of Petroleum Engineers: Amarillo, Texas.
17. L.J. Milberger and A. Radi, *Evolution of metal seal principles and their application in subsea drilling and production*, in *Offshore Technology Conference*1992, Offshore Technology Conference: Houston, Texas.
18. C.F. Boehm and S. Hosie, *Metal annulus seals for subsea wellheads: Important systems considerations*, in *Offshore Technology Conference*1990, Offshore Technology Conference: Houston, Texas.
19. J. Grunzweig, I.M. Longman, and N.J. Petch, *Calculations and measurements on wedge-indentation.* journal of the Mechanics and Physics of Solids, 1954. **Volume 2**: p. 81-86.
20. Buchter, H.H., *Industrial sealing technology*1979, New York: Wiley. xxiii, 441 s.
21. TIW, *Development of XPak expandable liner hanger system*, 2011.
22. G. Mackenzie and G. Garfield, *Wellbore Isolation Intervention Devices Utilizing a Metal-to-Metal Rather Than an Elastomeric Sealing Methodology*, in *SPE Annual Technical Conference and Exhibition*2007, Society of Petroleum Engineers: Anaheim, California, U.S.A.
23. Institute, A.P., *Specification for Wellhead and Christmas Tree Equipment*, in *ANSI/API SPECIFICATION 6A*2011, API Publishing Services.
24. Lunde, L., *Friction and contact*, 2011, NTNU: It's learning.
25. W. Johnson, F.U. Mahtab, and J.B. Haddow, *The indentation of a semi intfinite block bu a wedge of comparable hardness-Theoretical.* International Journal of Mechanical Science, 1964. **Volume 6**: p. 329-336.
26. R.B. Stewart, et al., *Expandable Wellbore Tubulars*, in *SPE Technical Symposium*1999, Society of Petroleum Engineers: Dhahran, Saudi Arabia.
27. TIW *TIW XPak drill down liner system*. 2010.
28. P. Head, P. Gullett, and P. Wilmott, *System for controlling the flow of fluid in an oil well*, in *http://ip.com/patent/US56737511992*, Stirling Design International Limited US.
29. TIW-Tools, *TIW X-Pak*, Wellbore A/S: Unpublished work.
30. Institute, A.P., *Specification of casing and tubing*, in *API Specification 5CT*2012, IHS: http://specs4.ihserc.com/DocViewFrame.aspx?sess=671681717&prod=SPECS4&docid=WNFPMEAAAAAAAAAA.
31. C.A. Bollfrass, S., Thread Technology Intl., *Sealing Tubular Connections.* Journal of Petroleum Technology, 1985. **Volume 37, Number 6**.
32. Byrom, T.G., *Casing and Liners for Drilling and Completion - Design and Application*, 2007, Gulf Publishing Company: http://www.knovel.com/web/portal/browse/display?_EXT_KNOVEL_DISPLAY_bookid=2157&VerticalID=0.
33. VAM, *VAM Book*, 2011, VAM: www.vam-usa.com. p. 334.

34. Chakrabarty, J., *Theory of plasticity*. Third edition ed2006: Elsevier Butterworth-Heinemann. 333-352.
35. Gibson, M.C., *Determination of residual stress distributions in autofrettaged thick-walled cylinders*, in *Department of engineering systems and management*2008, Cranfield University.
36. Renpu, W., *Advanced well completion engineering*2011, Britain: Petroleum Industry Press.
37. F. Liu, et al., *Forming mechanism of double-layered tubes by internal hydraulic expansion.* International Journal of Pressure Vessels and Piping, 2004. **81**.
38. F.J. Klever and G. Stewart, *Analytical burst strength prediction of OCTG with and without defects*, in *SPE Applied technology workshop on risk based design of well casing and tubing*1998, Society of Petroleum Engineers: The Woodlands, Texas, USA.
39. A.T. Bourgoyne, et al., *Applied drilling engineering*, ed. J.F. Evers and D.S. Pye1997, USA: Society of Petroleum Engineers. 307-325.
40. Al-Abri, O.S., *Analytical and Numerical Solution for Large Plastic Deformation of Solid Expandable Tubular*, in *SPE Annual Technical Conference and Exhibition*2011, Society of Petroleum Engineers: Denver, Colorado, USA.
41. C.G. Ruan and W.C. Maurer, *Analytical model for casing expansion*, in *SPE/IADC Drilling Conference*2005, Society of Petroleum Engineers: Amsterdam, The Netherlands.
42. Bathe, K.J., *Finite element procedures in engineering analysis*1982: Prentice-Hall Inc., Englewood Cliffs, New Jersey 07632. 114-165,.
43. G.B. Sinclair, J.R. Beisheim, and S. Sezer, *Practical Convergence-Divergence Checks for Stresses from FEA*, in *ANSYS Conference*2006.
44. R.D. Mack, et al., *In-Situ Expansion of Casing and Tubing: Effect on Mechanical Properties and Resistance to Sulfide Stress Cracking*, in *CORROSION 2000*2000, NACE International: Orlando, Florida.

Appendix

Appendix A

Comparison of casing/liner string length in slender well vs. conventional well

Exploration drilling						
Slender well	**OD [in]**	**Length [m]**	**Conventional well**	**OD [in]**	**Length [m]**	**Depth from RKB [m]**
Riser	8 5/8	260	Riser	19 1/5	260	260
BOP	11	10	BOP	18 ¾	10	270
Conductor	20	60	Conductor	30	60	330
Surface Casing	11 3/4	745	Surface Casing	20	745	1015
Liner	9 5/8	745	Casing 1	13 3/8	1490	1760
Liner	7	2180	Casing 2	9 5/8	3650	3920
Liner	5	550	Casing 3	7 5/8	4200	4470
OH	4 3/8	120	OH	6	120	4590

Appendix B

Expandable liner hanger systems

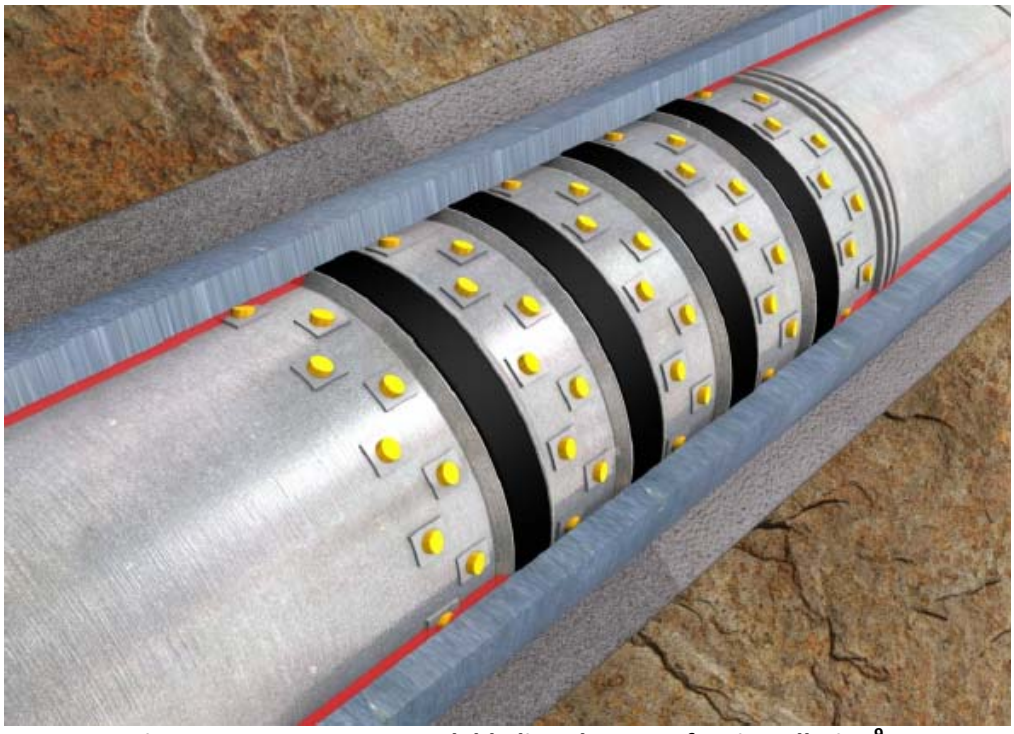

Figure 39: TruForm expandable liner hanger after installation[9]

Figure 40: TORXS expandable liner hanger during expansion[10]

[9] Ref. www.weatherford.com
[10] Ref. www.bakerhughes.com

Figure 41: Expandable liner hanger body, tieback receptacle (TBR) and running sleeve [14].

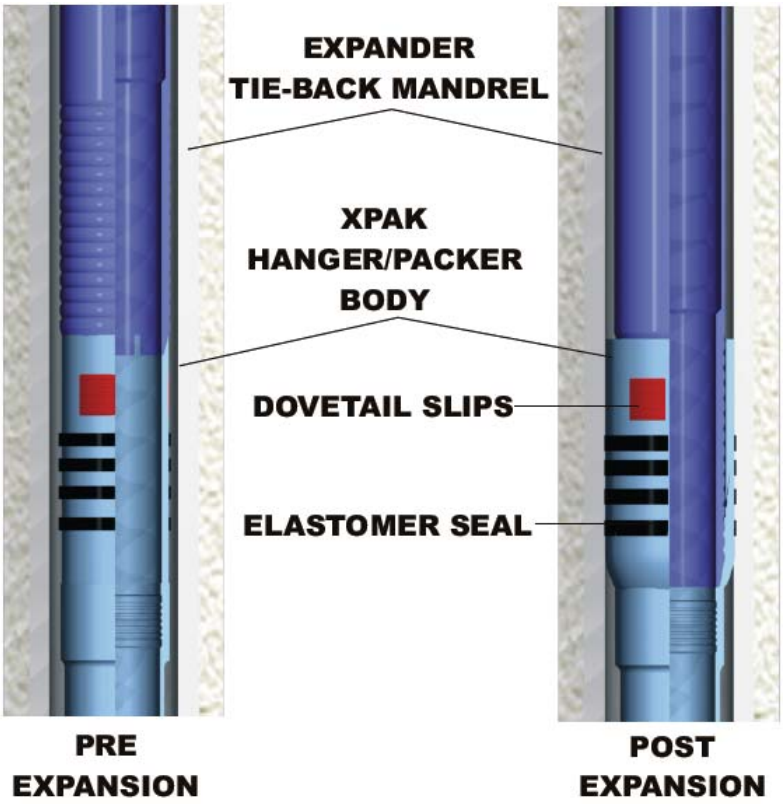

Figure 42: Components comprised in the XPak-liner hanger [27]

Figure 43: HETS expandable liner hanger with Downhole Hydraulics Module[11]

[11] Ref. http://www.readwellservices.com

Appendix C

XPak setting tool
Circulation modes with artificial inner annulus

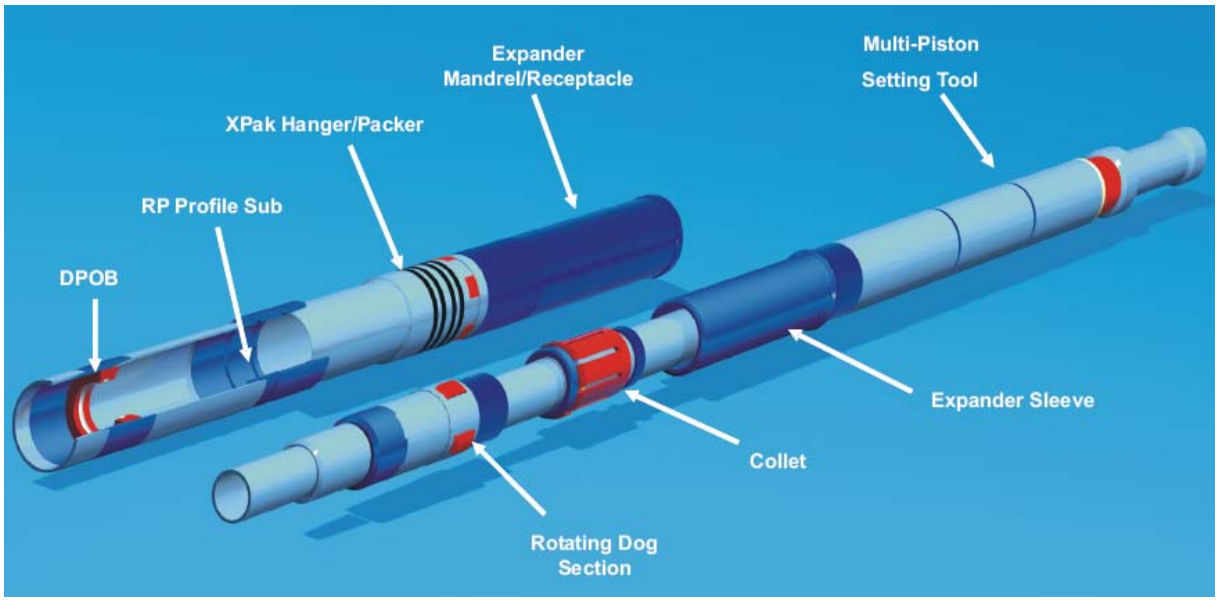

Figure 44: XPak setting tool [21]

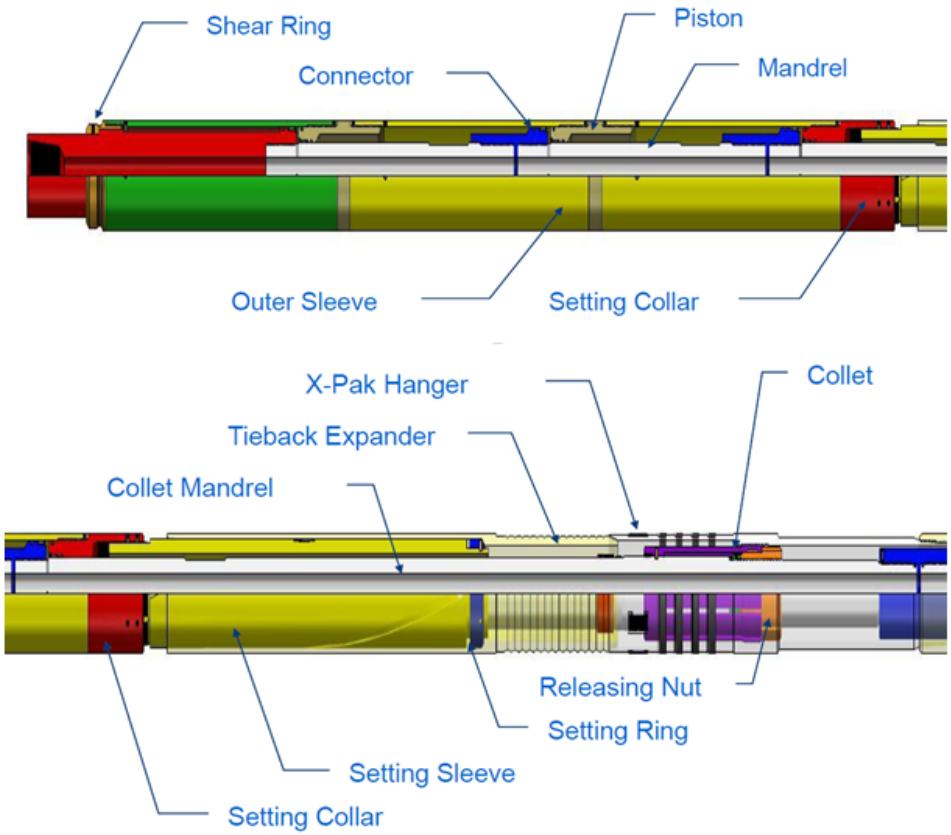

Figure 45: Detailed view of components in setting tool [15]

Description of the setting tool, Figure 45:

- Hydraulic pressure from surface breaks the shear ring to activate the setting tool.
- The inner mandrel moves down and pulls the setting sleeve with it.
- The setting sleeve displaces the tieback expander (mandrel) through the liner hanger.

- After setting the inner mandrel is pushed down by drill string slack off. This pushes out the retainer nut that locks the collet in place.
- The setting tool is free to be pulled.
- Alternatively the collet can be released by right hand rotation.

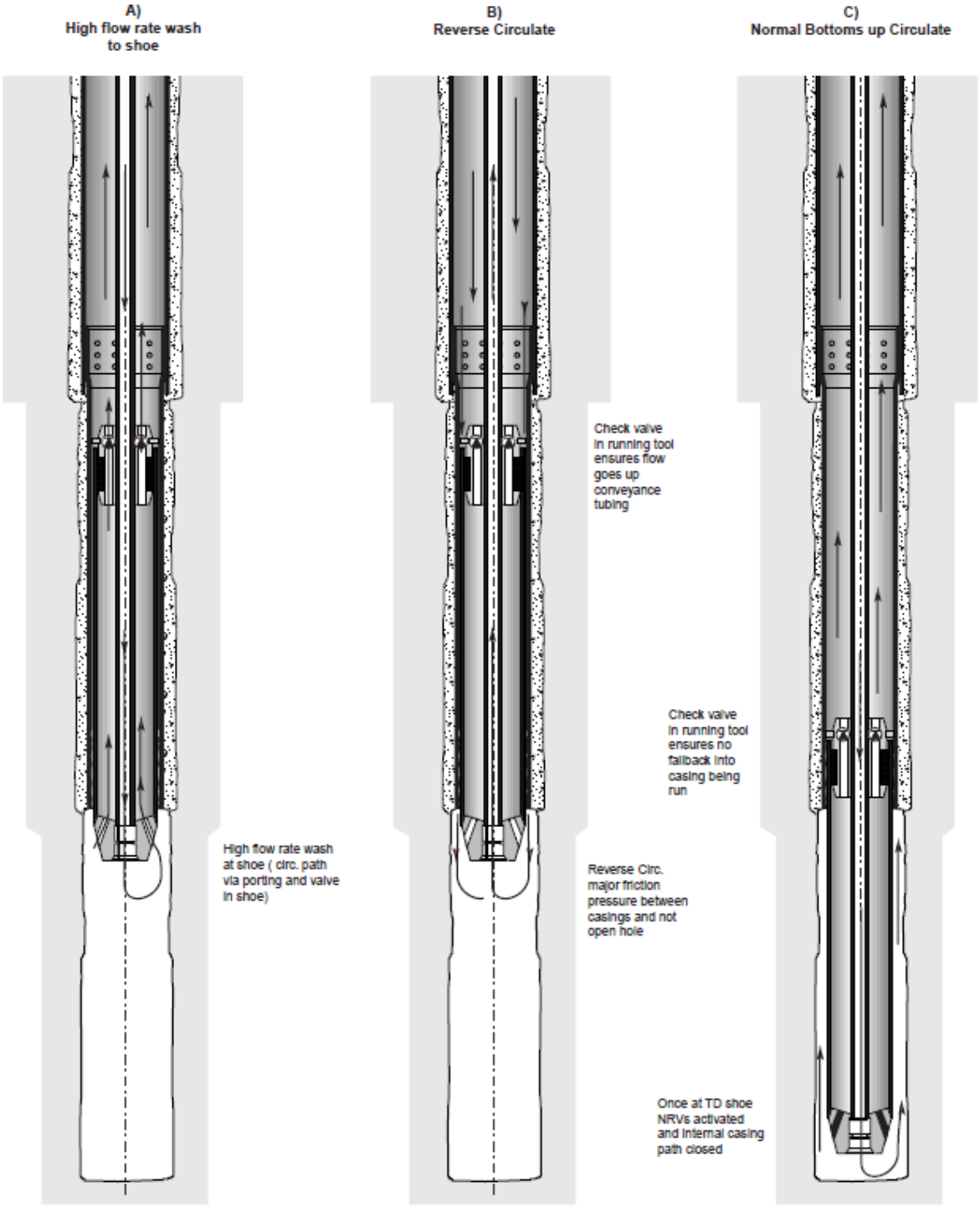

Figure 46: Circulation modes while conveying liner into well [1]

Appendix D

VAM SLIJ-II connection data

VAM SLIJ-II TECHNICAL DATA

Size (OD)	Nominal Weight	Wall Thickness		Inside Diameter	Drift Diameter	Pipe body section	Box O.D.	Pin I.D.	Make up Loss	Threads per inch	Joint Efficiency %	Joint Yield Strength (1000 lb)				
inch mm		inch	mm									L80 N80	C90	C95 T95	C110 P110	Q125
	lb./ft.			inch.	inch.	sq.in.	inch.	inch.	inch.							
7"	26.00	0.362	9.19	6.276	6.151	7.549	7.084	6.220	4.580	7	68.9	416	468	494	572	650
177.80	29.00	0.408	10.36	6.184	6.059	8.449	7.119	6.128	5.050	7	72.6	491	552	583	675	767
	32.00	0.453	11.51	6.094	5.969	9.317	7.162	6.053	5.176	6	74.2	553	622	657	761	864
	35.00	0.498	12.65	6.004	5.879	10.172	7.198	5.948	5.473	6	76.8	625	703	742	860	977
	38.00	0.540	13.72	5.920	5.795	10.959	7.231	5.864	5.776	6	79.0	692	779	822	952	1082
	41.00	0.590	14.99	5.820	5.695	11.881	7.264	5.764	5.917	6	80.0	761	856	903	1046	1188
	42.70	0.625	15.88	5.750	5.625	12.517	7.299	5.694	6.128	5	80.6	807	908	958	1110	1261
	44.00	0.640	16.26	5.720	5.595	12.788	7.309	5.664	6.157	5	80.8	827	930	982	1137	1292
	45.40	0.670	17.02	5.660	5.535	13.324	7.318	5.604	6.428	5	81.0	863	971	1025	1186	1348
	46.40	0.687	17.45	5.626	5.501	13.625	7.323	5.570	6.472	5	80.9	882	993	1048	1213	1378
	49.50	0.730	18.54	5.540	5.415	14.379	7.333	5.484	6.562	5	80.9	931	1047	1105	1280	1454
7 5/8"	29.70	0.375	9.53	6.875	6.750	8.541	7.711	6.820	4.822	7	69.2	473	532	562	650	739
193.68	33.70	0.430	10.92	6.765	6.640	9.720	7.754	6.711	5.169	7	73.2	569	641	676	783	890
	39.00	0.500	12.70	6.625	6.500	11.192	7.818	6.570	5.525	6	76.2	682	767	810	938	1065
	42.80	0.562	14.27	6.501	6.376	12.470	7.866	6.446	5.887	6	79.0	788	887	936	1084	1232
	45.30	0.595	15.11	6.435	6.310	13.141	7.889	6.380	6.157	6	80.1	842	948	1000	1158	1316
	47.10	0.625	15.88	6.375	6.250	13.744	7.920	6.320	6.168	5	80.1	881	991	1046	1211	1376
	51.20	0.687	17.45	6.251	6.126	14.974	7.962	6.196	6.539	5	81.4	975	1097	1158	1341	1524
	52.10	0.700	17.78	6.225	6.100	15.229	7.967	6.170	6.770	5	81.6	994	1118	1180	1366	1553
	52.80	0.712	18.08	6.201	6.076	15.463	7.976	6.146	6.802	5	82.0	1014	1141	1204	1394	1584
	55.30	0.750	19.05	6.125	6.000	16.199	7.989	6.070	6.899	5	82.4	1068	1201	1268	1468	1668
	59.20	0.812	20.62	6.001	5.876	17.380	7.991	5.946	7.214	5	81.3	1130	1271	1342	1554	1766
7 3/4"	46.10	0.595	15.11	6.560	6.435	13.374	8.019	6.555	6.128	5	78.8	843	948	1001	1159	1317
196.85	46.90	0.615	15.62	6.520	6.395	13.785	8.036	6.465	6.154	5	79.5	877	987	1041	1206	1370
	47.60	0.625	15.88	6.500	6.375	13.990	8.045	6.446	6.167	5	80.0	895	1007	1063	1230	1398
	48.60	0.640	16.26	6.470	6.345	14.296	8.056	6.415	6.413	5	80.5	921	1036	1094	1266	1439
8 5/8"	36.00	0.400	10.16	7.825	7.700	10.336	8.721	7.772	5.083	7	70.0	579	651	687	796	904
219.08	40.00	0.450	11.43	7.725	7.600	11.557	8.767	7.681	5.424	6	72.1	667	750	792	917	1042
	44.00	0.500	12.70	7.625	7.500	12.763	8.809	7.572	5.535	6	75.0	766	862	910	1053	1197
	49.00	0.557	14.15	7.511	7.386	14.118	8.855	7.457	5.880	6	77.8	879	989	1044	1209	1374

VAM SLIJ-II TORQUE VALUES

SIZE	NOMINAL	WALL	75-80-85 ksi			90-95-100 ksi			105-110-115 ksi			120-125-130 ksi			135-140-145 ksi		
(OD)	WEIGHT	THICKNESS	min.	opti.	max.	min.	opti.	max.	min.	opti.	max.	min.	opti.	max.	min.	opti.	max.
in. mm	ft.lb.	in. mm.	ft.lb. N.m.												ft.lb. N.m.		
6 7/8"	32.70	0.478	10700	11900	13100	11400	12700	14000	12100	13500	14900	13000	14400	15800	-	-	-
174.63		*12.13*	*14490*	*16100*	*17710*	*15600*	*17300*	*19000*	*16500*	*18300*	*20100*	*17500*	*19500*	*21500*	-	-	-
7"	26.00	0.362	8700	9700	10700	9100	10100	11100	9500	10600	11700	9900	11000	12100	-	-	-
177.80		*9.19*	*11800*	*13100*	*14400*	*12300*	*13700*	*15100*	*12900*	*14300*	*15700*	*13500*	*15000*	*16500*	-	-	-
	29.00	0.408	10400	11600	12800	10900	12100	13300	11400	12700	14000	12000	13300	14600	-	-	-
		10.36	*14100*	*15700*	*17300*	*14800*	*16500*	*18200*	*15500*	*17200*	*18900*	*16200*	*18000*	*19800*	-	-	-
	32.00	0.453	11900	13200	14500	12600	14000	15400	13400	14900	16400	14100	15700	17300	-	-	-
		11.51	*16100*	*17900*	*19700*	*17100*	*19000*	*20900*	*18200*	*20200*	*22200*	*19200*	*21300*	*23400*	-	-	-
	35.00	0.498	13600	15100	16600	14600	16200	17800	15500	17200	18900	16400	18200	20000	-	-	-
		12.65	*18400*	*20500*	*22600*	*19700*	*21900*	*24100*	*21000*	*23300*	*25600*	*22100*	*24600*	*27100*	-	-	-
	38.00	0.540	15300	17000	18700	16300	18100	19900	17400	19300	21200	18400	20400	22400	-	-	-
		13.72	*20700*	*23000*	*25300*	*22100*	*24600*	*27100*	*23600*	*26200*	*28800*	*24900*	*27700*	*30500*	-	-	-
	41.00	0.590	17100	19000	20900	18400	20400	22400	19600	21800	24000	20800	23100	25400	-	-	-
		14.99	*23200*	*25800*	*28400*	*24900*	*27700*	*30500*	*26500*	*29500*	*32500*	*28300*	*31400*	*34500*	-	-	-
	42.70	0.625	18500	20600	22700	19800	22000	24200	21100	23500	25900	22800	25300	27800	-	-	-
		15.88	*25200*	*28000*	*30800*	*26900*	*29900*	*32900*	*28700*	*31900*	*35100*	*30900*	*34300*	*37700*	-	-	-
	44.00	0.640	19100	21200	23300	20400	22700	25000	21100	23500	25900	22800	25300	27800	-	-	-
		16.26	*25900*	*28800*	*31700*	*27700*	*30800*	*33900*	*28700*	*31900*	*35100*	*30900*	*34300*	*37700*	-	-	-
	45.40	0.670	20200	22400	24600	21100	23500	25900	22800	25300	27800	24400	27100	29800	-	-	-
		17.02	*27300*	*30300*	*33300*	*28700*	*31900*	*35100*	*30900*	*34300*	*37700*	*33100*	*36800*	*40500*	-	-	-
	46.40	0.687	20800	23100	25400	22800	25300	27800	24400	27100	29800	26000	28900	31800	-	-	-
		17.45	*28200*	*31300*	*34400*	*30900*	*34300*	*37700*	*33100*	*36800*	*40500*	*35300*	*39200*	*43100*	-	-	-
	49.50	0.730	22800	25300	27800	24400	27100	29800	26000	28900	31800	27600	30700	33800	-	-	-
		18.54	*30900*	*34300*	*37700*	*33100*	*36800*	*40500*	*35300*	*39200*	*43100*	*37500*	*41700*	*45900*	-	-	-
7 5/8"	29.70	0.375	10300	11400	12500	10800	12000	13200	11300	12600	13900	11900	13200	14500	-	-	-
193.68		*9.53*	*13900*	*15500*	*17100*	*14700*	*16300*	*17900*	*15400*	*17100*	*18800*	*16100*	*17900*	*19700*	-	-	-
	33.70	0.430	12600	14000	15400	13200	14700	16200	13900	15500	17100	14700	16300	17900	-	-	-
		10.92	*17000*	*18900*	*20800*	*18000*	*20000*	*22000*	*18900*	*21000*	*23100*	*19900*	*22100*	*24300*	-	-	-

Appendix E

Expansion stress
Strain
Strain hardening
Bauschinger effect

Expansion stresses

$$r_i \le r \le c$$

$$\sigma_r = -\frac{\sigma_y}{2}\left(1 - \frac{c^2}{{r_0}^2} + ln\frac{c^2}{r^2}\right)$$
$$\sigma_\theta = \frac{\sigma_y}{2}\left(1 + \frac{c^2}{{r_0}^2} + ln\frac{c^2}{r^2}\right) \quad \textbf{(A-1)}$$
$$\sigma_z = E\varepsilon_z + v\sigma_y\left(\frac{c^2}{r_0^2} - ln\frac{c^2}{r_0^2}\right)$$

$$c \le r \le r_0$$

$$\sigma_r = -\frac{\sigma_y c^2}{2{r_0}^2}\left(\frac{{r_0}^2}{r^2} - 1\right)$$
$$\sigma_\theta = \frac{\sigma_y c^2}{2{r_0}^2}\left(\frac{{r_0}^2}{r^2} + 1\right) \quad \textbf{(A-2)}$$
$$\sigma_z = E\varepsilon_z + v\sigma_y\left(\frac{c^2}{r_0^2}\right)$$

Strains

The radial deflections observed during axisymmetric expansion of a cylinder are illustrated in Figure 47.

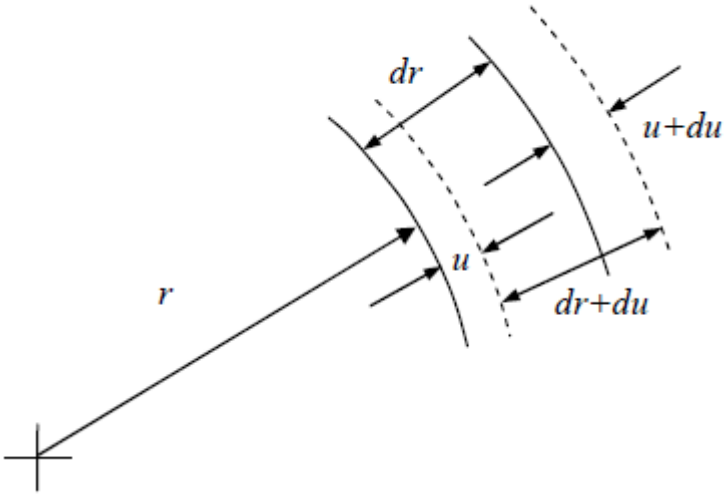

Figure 47: Deflection diagram [35]

From the figure radial and hoop strain may be defined as follows:

$$\varepsilon_r = \frac{du}{dr} \quad \textbf{(A-3)}$$

$$\varepsilon_\theta = \frac{2\pi(r+u) - 2\pi r}{2\pi r} = \frac{u}{r} \quad \textbf{(A-4)}$$

The following constitutive relations apply [35]:

$$E\varepsilon_r = \sigma_r - v(\sigma_\theta + \sigma_z) \quad \textbf{(A-5)}$$

$$E\varepsilon_\theta = \sigma_\theta - v(\sigma_r + \sigma_z) \quad \textbf{(A-6)}$$

$$E\varepsilon_z = \sigma_z - v(\sigma_r + \sigma_\theta) \quad \textbf{(A-7)}$$

Equations (A-5)-(A-7) can only assess elastic strain. To calculate plastic strain the elastic strain are subtracted from the total values. Axial strain is assumed elastic, making equation (A-7) true for the whole cylinder. Plane strain conditions ($\varepsilon_z = 0$) are applied to equation (A-7) and substituted into equation (A-5) and (A-6), giving:

$$\varepsilon_r = \frac{du}{dr} = -v\varepsilon_z + \frac{1+v}{E}[(1-v)\sigma_r - v\sigma_\theta] \quad \textbf{(A-8)}$$

$$\varepsilon_\theta = \frac{u}{r} = -v\varepsilon_z + \frac{1+v}{E}[(1-v)\sigma_\theta - v\sigma_r] \quad \textbf{(A-9)}$$

Strain hardening

Both strain hardening and the Baushinger effect are dependent on plastic strain. Plastic radial and hoop strains are given by Equations A-12 and A-13 respectively. These equations may be combined into the Tresca equivalent plastic strain using the following [35]:

$$\varepsilon_{Tr}^p = \varepsilon_\theta^p - \varepsilon_r^p = 2\varepsilon_\theta^p \quad \textbf{(A-10)}$$

It is further assumed that strain hardening is proportional to the Tresca equivalent plastic strain. σ is the same function of ε_θ^p as the stress is of the plastic strain in uniaxial tension, the yield criterion becoming [34]:

$$r_i \le r \le c \qquad \sigma_\theta - \sigma_r = \sigma = F(\varepsilon_{Tr}^p) \quad \textbf{(A-11)}$$

Assuming linear isotropic hardening, the yield stress of the strain-hardened material becomes:

$$F\left(\varepsilon_{Tr}^p\right) = \sigma = \sigma_y + H\varepsilon_{Tr}^p \quad \textbf{(A-12)}$$

The Tresca yield criterion for a linearly strain hardened cylinder can be found by substituting for Tresca equivalent plastic strain (equation A-9) and rearranging:

$$\sigma_\theta - \sigma_r = \sigma = \frac{\sigma_y\left[1 + 2(1-v^2)\frac{Hc^2}{Er^2}\right]}{\left[1 + 2(1-v^2)\frac{H}{E}\right]} \quad \textbf{(A-13)}$$

Bauschinger effect

F_{SU} is dependent on the Bauschinger Effect Factor, a ratio of reverse yield strength to initial yield strength, as given below:

$$0 \leq \beta \leq 1 \qquad F_{SU} = \frac{1+\beta}{2} \qquad \textbf{(A-14)}$$

For the purpose of this study scaling of the decrease in yield stress is taken from Gibson [35]:

$$\beta = 1 - F_{S\beta}\varepsilon_{Tr}^{p} \qquad \textbf{(A-15)}$$

Where $F_{S\beta}$ is a positive scaling factor. To find $F_{S\beta}$ end constraints are applied, $\beta = \beta_0$ at $r = r_i$, then:

$$F_{S\beta} = \frac{1-\beta_0}{\varepsilon_{Tr}^{p}\big|_{r=r_i}} \qquad \textbf{(A-16)}$$

Appendix F

Derivation of relationship between thickness variation and expansion ratio

H_0, H_1, H_2, H_3 and H_4 in Equation (21) are given as:

$$H_0 = -(r_{1o}^2 - r_{1i}^2)^2 r_{1o} r_{1i} \sin^2 \alpha$$

$$H_1 = (r_{1o}^2 - r_{1i}^2) r_{1i} \sin^2 \alpha \left[(r_{1o} r_{1i} - r_{1i}^2)(1 + cot\beta) + (r_{1o}^2 - r_{1i}^2)\right]$$

$$H_2 = (r_{1o} - r_{1i})(r_{1o}^2 - r_{1i}^2)(1 + cot\beta) \sin^2 \alpha \quad \textbf{(A-17)}$$

$$H_3 = (r_{1o} - r_{1i})(r_{1o}^2 - r_{1i}^2)(1 + cot\beta)$$

$$H_4 = (r_{1o} - r_{1i})(r_{1o}^2 - r_{1i}^2)(1 + cot\beta) r_{1i}^2 + (r_{1o}^2 - r_{1i}^2)^2 r_{1i} \sin^2 \alpha$$

Equation (21) is itself a combination of equations for longitudinal stress (σ_z), contact pressure between mandrel and tubular (P_c), radial stress (σ_r) and equivalent plastic strain increment (d_t/r). Equations for the above mentioned variables are given below, for a more detailed derivation see the paper of O.S. Al-Abri [40].

$$\sigma_z = -\frac{\pi(r^2 - r_{1i}^2)(1 + \mu cot\beta) P_c}{\pi(r_{1o}^2 - r_{1i}^2)} \quad \textbf{(A-18)}$$

$$P_c = \frac{m\sigma_y (r_{1o} - r_{1i})(r_{1o}^2 - r_{1i}^2)}{(\sin^2 \alpha)(r_{1o}^2 - r_{1i}^2) r_{1i} - (r^2 - r_{1i}^2)(1 + \mu cot\beta)(r_{1o} - r_{1i})} \quad \textbf{(A-19)}$$

$$\sigma_r = P_c \left(\frac{r_{1i}}{r}\right) + \frac{(\sigma_z - m\sigma_y)}{\sin^2 \alpha} \left[1 - \left(\frac{r_{1i}}{r}\right)\right] \quad \textbf{(A-20)}$$

$$\frac{dt}{t} = \frac{-2(\sigma_z - \sigma_r) + m\sigma_y}{(\sigma_z - \sigma_r) - 2m\sigma_y} \frac{dr}{r} \quad \textbf{(A-21)}$$

Appendix G

Tubular performance properties

OD (in.)	Weight (lb./ft.)	Grade	ID (in.)	Min Yield (psi)	Min Tensile (psi)
7.625	29.7	L80	6.875	80000	95000

OD exp (in.)	ID exp (in.)	t (in.)	d0/t	ID Exp (%)	Burst (psi)	Collapse (psi)	Collapse pressure region
7.63	6.88	0.375	20.33	0	6885	4792	Plastic
7.69	6.94	0.373	20.62	1	6788	4621	"
7.75	7.01	0.371	20.92	2	6693	4455	"
7.82	7.08	0.369	21.21	3	6600	4291	"
7.88	7.15	0.366	21.51	4	6508	4130	"
7.95	7.22	0.364	21.81	5	6419	3973	"
8.01	7.29	0.362	22.11	6	6331	3818	"
8.08	7.36	0.360	22.42	7	6244	3667	"
8.14	7.43	0.358	22.73	8	6159	3560	Transition
8.21	7.49	0.356	23.04	9	6076	3465	"
8.27	7.56	0.354	23.36	10	5994	3371	"
8.59	7.91	0.344	24.98	15	5604	2926	"
8.92	8.25	0.334	26.70	20	5244	2515	"
9.24	8.59	0.324	28.53	25	4907	2131	"
9.56	8.94	0.314	30.49	30	4591	1770	"

Appendix H

Finite element analysis boundary conditions
Fluid pressure penetration results

Finite element analysis boundary conditions

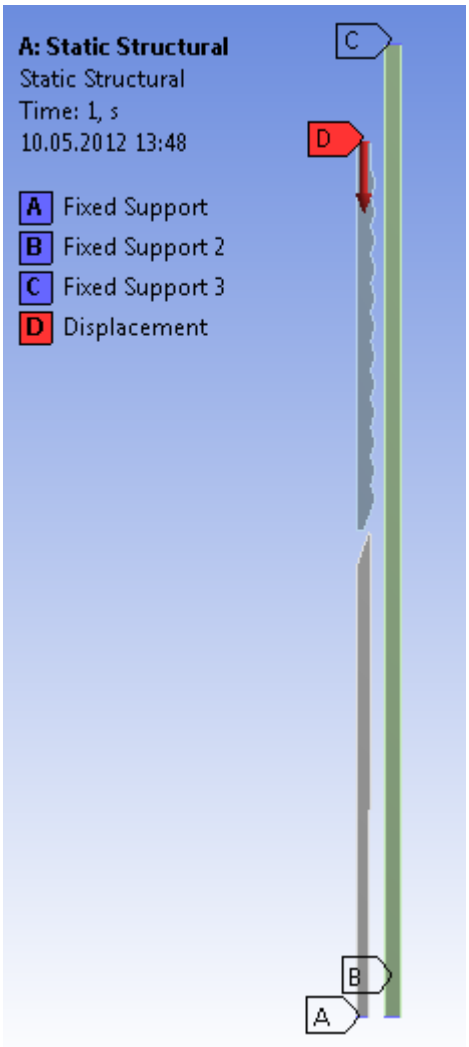

Figure 48: Finite Element Analysis boundary conditions

Fluid pressure penetration analysis

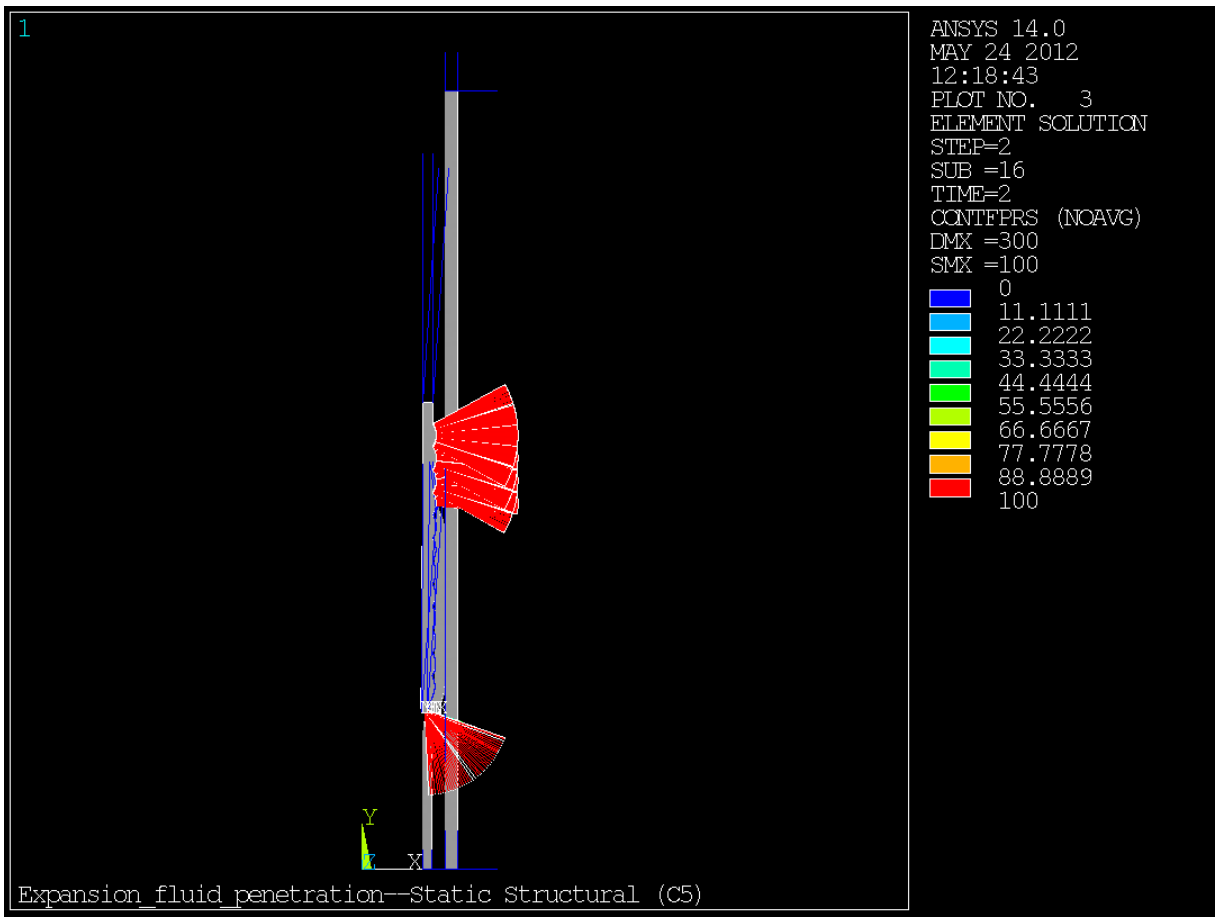

Figure 49: Fluid pressure penetration at mandrel/liner hanger contact

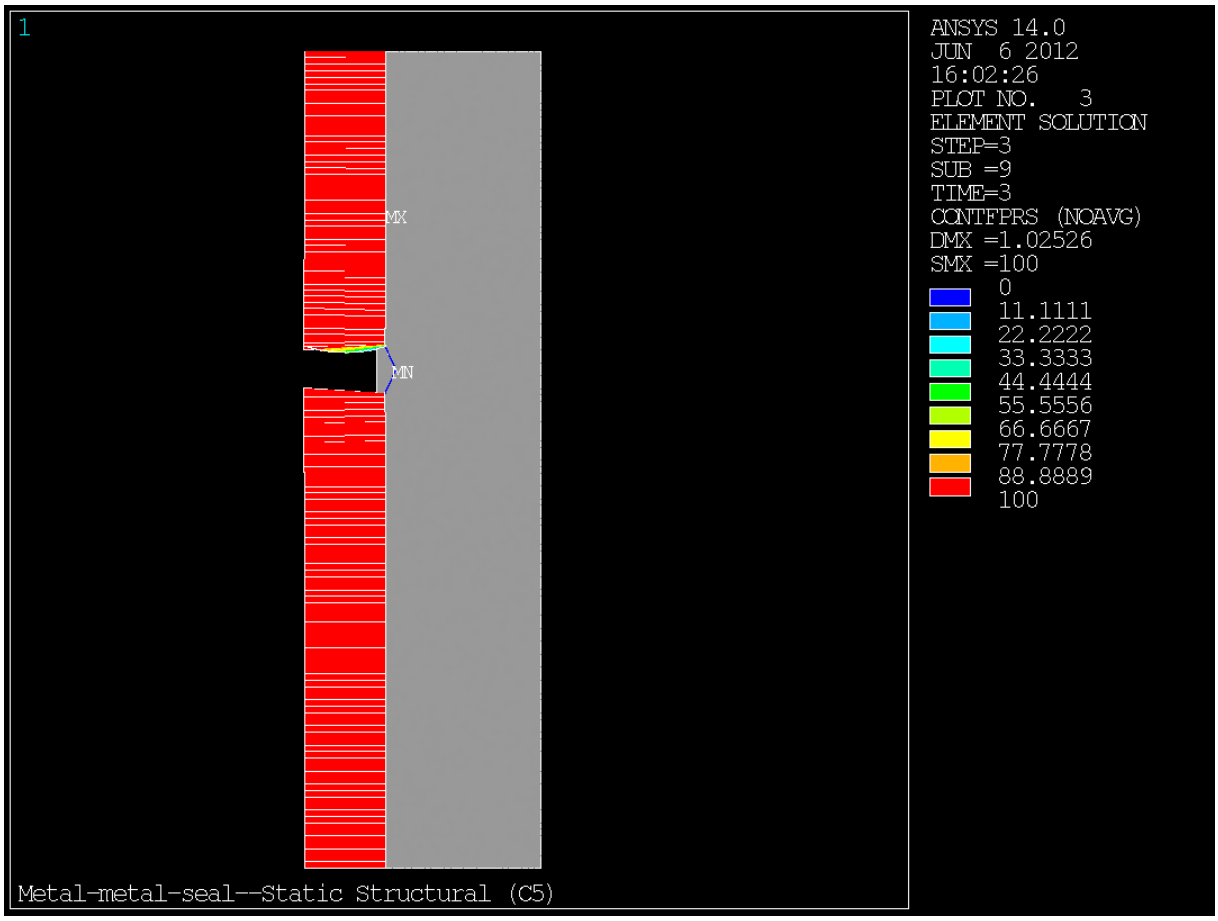

Figure 50: Fluid pressure penetration at seal/casing contact